

UNIVERSITY OF BELGRADE  
FACULTY OF TECHNOLOGY AND METALLURGY

Mohamed Mohamed Abudabbus

**ELECTROCHEMICAL SYNTHESIS AND  
CHARACTERIZATION OF POLY(VINYL  
ALCOHOL) NANOCOMPOSITES WITH  
SILVER NANOPARTICLES**

Doctoral Dissertation

Belgrade, 2018.

UNIVERZITET U BEOGRADU  
TEHNOLOŠKO-METALURŠKI FAKULTET

Mohamed Mohamed Abudabbus

**ELEKTROHEMIJSKA SINTEZA I  
KARAKTERIZACIJA NANOKOMPOZITA  
POLIVINIL-ALKOHOLA I NANOČESTICA  
SREBRA**

Doktorska disertacija

Beograd, 2018.

**Supervisor:** \_\_\_\_\_  
Prof.dr. Vesna Mišković-Stanković,  
University of Belgrade, Faculty of Technology and  
Metallurgy.

**Committee Members:** \_\_\_\_\_  
Prof.dr. Bojana Obradović,  
University of Belgrade, Faculty of Technology and  
Metallurgy.

\_\_\_\_\_  
Prof.dr. Jelena Bajat,  
University of Belgrade, Faculty of Technology and  
Metallurgy.

\_\_\_\_\_  
Dr. Ana Janković,  
Research Associate, Innovation center, Faculty of  
Technology and Metallurg, Belgrade.

**Date of defense:** \_\_\_\_\_ **2018.**

### *Thanks and appreciativeness*

*I extend my sincerely great thanks and highly sincere appreciates to my supervisor Professor dr. Vesna Mišković - Stanković for all her efforts to follow directly and continuously all the stages of my PhD studies. My great thanks go to Prof. dr. Bojana Obradović and Prof. dr. Jelena Bajat and dr. Ana Janković for their valuable comments and suggestions. Also, I extend great thanks and high appreciates for all the assistance provided by dr. Ana Janković, dr. Ivana Jevremović, and Katarina Nešović, PhD student in the experimental work and in writing the scientific papers. My gratitude goes to Professor dr. Aleksandra Perić - Grujić and Professor dr. Maja Vukašinović - Sekulić at the Faculty of Technology and Metallurgy for their great assistance in atomic absorption experiments and microbiology experiments. I am very thankful to dr. Ivana Matić at the institute of Oncology and Radiology of Serbia for her valuable assistance in cytotoxicity tests. Great thanks to all my professors who taught theoretical courses. Great thanks to Professor dr. Nenad Radović*

*(the corresponding of Libyan students at the Faculty of Technology and Metallurgy) and Professor dr. Djordje Janacković (Dean of the Faculty of Technology and Metallurgy). All thanks to University of Belgrade and the Libyan embassy in Serbia. Great thanks to the Republic of Serbia for the invitation and acceptance for PhD studies in their nice country. My deepest gratitude goes to my country Libya for giving me a chance and support to complete my PhD program. Thanks to everybody who helped me along this path.*

## *Dedication*

*To my generous family, my wife who tolerated my parting patiently a lot of months, my daughter and sons who missed their father for a time, to the pure and timeless souls of my father and mother who always invocated me to succeed , to my beloved country Líbya.*

**Belgrade, 2017**

## **Electrochemical synthesis and characterization of poly(vinyl alcohol) nanocomposites with silver nanoparticles**

### **Summary**

In this doctoral dissertation, a composite hydrogel consisting of poly(vinyl alcohol), graphene and silver nanoparticles, (Ag/PVA/Gr), was prepared by the immobilization of silver nanoparticles (AgNPs) in poly(vinyl alcohol)/graphene (PVA/Gr) hydrogel matrix in two steps. The first step was cross linking of the PVA/Gr colloid solution by the freezing/thawing method, while in the second step, *in situ* electrochemical method was used to incorporate AgNPs inside the PVA/Gr hydrogel matrix. The main aim of this study was to produce the nanocomposite graphene-based biomaterial with incorporated silver nanoparticles using *in situ* electrochemical method, aimed for soft tissue implants, wound dressings and drug delivery. The electrochemical route of nanoparticles synthesis is especially attractive for biomedical applications due to high purity and precise size control of metal particles and the absence of chemical cross linking agents and undesired products.

Repeated cyclic freezing/thawing method was used to prepare poly(vinyl alcohol) PVA and poly(vinyl alcohol)/graphene (PVA/Gr) hydrogel discs, followed by electrochemical reduction method of different concentrations of Ag<sup>+</sup> ions (0.25, 0.5, 1.0 and 3.9 mM AgNO<sub>3</sub> swelling solution) inside the hydrogel polymer matrices at a constant voltage that enables the silver particle size control, in a specially designed electrochemical cell.

Silver/poly(vinyl alcohol) (Ag/PVA) and silver/poly(vinyl alcohol)/graphene (Ag/PVA/Gr) nanocomposites were characterized by UV–visible spectroscopy. The absorption spectra at about 405-420 nm proved existence of AgNPs in both Ag/PVA and Ag/PVA/Gr nanocomposites. Cyclic voltammetry revealed some oxidation and reduction peaks suggesting the presence of AgNPs between polymer chains. Raman spectroscopy analysis confirmed the graphene structure in its pure form, X-ray diffraction was used to reveal the additional interactions established between the PVA molecules and graphene sheets and the AgNPs situated between the polymer chains in

the Ag/PVA/Gr nanocomposite. The calculated interspacing (d-spacing) value for (002) lattice plane of the PVA and Ag/PVA hydrogels was 0.457 nm, while the obtained value changed slightly with the introduction of graphene sheets (0.449 nm for Ag/PVA/Gr nanocomposite). Fourier transform infrared spectroscopy (FTIR) results for both Ag/PVA and Ag/PVA/Gr nanocomposites suggested the interaction between AgNPs and hydroxyl groups of the PVA molecules through decoupling between the corresponding vibrations. Thermogravimetric analysis and corresponding differential thermal analysis were done to investigate the role of graphene sheets in the thermal stability of thus prepared nanocomposite samples, and the results showed higher stability of Ag/PVA/Gr than Ag/PVA nanocomposites. Morphology of the prepared PVA, PVA/Gr, Ag/PVA and Ag/PVA/Gr samples were examined by field-emission scanning electron microscopy (FE-SEM) technique and the microphotographs showed sphere-shaped AgNPs at nanoscale levels which were around 36 nm in the Ag/PVA and around 17 nm in the Ag/PVA/Gr nanocomposites.

Also, the incorporation of graphene into the PVA matrix and bonding between AgNPs and PVA molecules and graphene sheets led to improved thermal stability of Ag/PVA/Gr and prevented the further growth and aggregation of AgNPs as observed by FTIR and FE-SEM.

Ag/PVA and Ag/PVA/Gr hydrogel discs with the lowest AgNP concentration (0.25 mM) classified as non-cytotoxic towards peripheral blood mononuclear cells (PBMC) according to 3-(4,5-dimethylthiazol-2-yl)-2,5-diphenyltetrazolium bromide (MTT) cytotoxicity test, while exhibited antibacterial activity against *Staphylococcus aureus* and *Escherichia coli*.

The slow silver release and high remaining silver content of ~ 67- 68 wt. % after 28 day immersion in phosphate buffer (PB) confirmed that both Ag/PVA and Ag/PVA/Gr composites can preserve their sterility over time. Sorption characterization experiments were done by immersing dry PVA, PVA/Gr, Ag/PVA and Ag/PVA/Gr discs in simulated body fluid (SBF) for 72 h at 37±1 °C. The results indicated higher swelling degree in SBF of PVA/Gr hydrogels than PVA hydrogels, also on the other hand Ag/PVA/Gr nanocomposites had slightly higher sorption rates as compared with

Ag/PVA nanocomposites. These results of sorption studies it could indicate that graphene sheets expand the PVA hydrogel networks.

All obtained results contribute in to fulfilling the aim of this dissertation concerning the *in situ* electrochemical synthesis of nanocomposite hydrogels based on poly(vinyl alcohol) with silver nanoparticles. The synthesized nanocomposites are non-toxic, with antibacterial activity, and can be considered for potential use in medicine as wound dressings and soft tissue implants.

The experiments were performed at the Department of Physical chemistry and Electrochemistry, Faculty of Technology and Metallurgy, University of Belgrade, while the antibacterial activity experiments were performed in the microbiology laboratory at the Department of Biochemical Engineering and Biotechnology. Cytotoxicity tests were performed in the Institute of Oncology and Radiology, Belgrade, Serbia.

**Keywords:** polymer-matrix composites (PMCs), poly(vinyl alcohol), silver nanoparticles, scanning electron microscopy, thermal analysis, cytotoxicity, antibacterial activity, silver release.

**Scientific field:** Chemical sciences.

**UDC number:**

# Elektrohemijska sinteza i karakterizacija nanokompozita polivinil-alkohola i nanočestica srebra

## Rezime

Ova doktorska disertacija se bavi sintezom hidrogelova polivinil-alkohola, grafena i nanočestica srebra (Ag/PVA/Gr), imobilizacijom nanočestica srebra u matrici hidrogela polivinil-alkohol/grafen (PVA/Gr) u dva koraka. Prvi korak je umrežavanje koloidnog rastvora PVA/Gr metodom zamrzavanja i odmrzavanja, dok je u drugom koraku primenjena *in situ* elektrohemijska metoda za inkorporaciju nanočestica srebra u matrici PVA/Gr hidrogela. Glavni cilj ovog istraživanja je bila priprema nanokompozitnih biomaterijala na bazi grafena sa inkorporisanim nanočesticama srebra, sa mogućom primenom u vidu implantata mekog tkiva, obloga za rane i nosača za lekove. Elektrohemijski postupak sinteze nanočestica je posebno atraktivan za primene u medicini, zbog velike čistoće i mogućnosti precizne kontrole dobijenih nanočestica, kao i zbog odsustva hemijskih agenasa i neželjenih produkata.

Metoda umrežavanja cikličnim zamrzavanjem i odmrzavanjem je korišćena u cilju dobijanja polivinil-alkohol (PVA) i polivinil-alkohol/grafen (PVA/Gr) hidrogelova u obliku diskova, a zatim je izvršena elektrohemijska redukcija  $\text{Ag}^+$  jona različitih koncentracija (0,25, 0,5, 1,0 i 3,9 mM  $\text{AgNO}_3$  swelling solution) u polimernoj matrici hidrogela, na konstantnom naponu, što omogućava kontrolu dimenzija čestica srebra, u posebno dizajniranoj elektrohemijskoj ćeliji.

Srebro/polivinil-alkohol (Ag/PVA) i srebro/polivinil-alkohol/grafen (Ag/PVA/Gr) nanokompoziti su karakterisani UV-vidljivom spektroskopijom. Apsorpcioni spektri sa maksimumom na oko 405-420 nm su dokazali prisustvo nanočestica srebra u Ag/PVA i Ag/PVA/Gr nanokompozitima. Cikličnom voltametrijom su pokazani pikovi oksidacije i redukcije koji ukazuju na prisustvo nanočestica srebra u polimernoj matrici. Ramanova spektroskopija je potvrdila čistu grafensku strukturu, dok je rendgenska difrakcija korišćena za ispitivanje interakcija između PVA molekula sa grafenom i nanočesticama srebra, smeštenim između polimernih lanaca Ag/PVA/Gr nanokompozita. Izračunato rastojanje između kristalnih

ravni za (002) ravan u PVA i Ag/PVA hidrogelovima je iznosilo 0.457 nm, dok se ova vrednost promenila nakon inkorporacije grafena (0.449 nm za Ag/PVA/Gr nanokompozit). Rezultati analize infracrvenom spektroskopijom sa Furijeovom transformacijom (FTIR) za Ag/PVA i Ag/PVA/Gr nanokompozite su ukazali na interakcije između nanočestica srebra i hidroksilnih grupa na PVA molekulima, na osnovu razdvajanja odgovarajućih vibracionih traka. Termogravimetrijska analiza i diferencijalna termogravimetrijska analiza su korišćene radi ispitivanja termičke stabilnosti dobijenih uzoraka hidrogelova, a rezultati su pokazali povećanu stabilnost Ag/PVA/Gr u odnosu na Ag/PVA nanokompozite. Morfologija dobijenih uzoraka PVA, PVA/Gr, Ag/PVA i Ag/PVA/Gr je ispitana tehnikom skenirajuće elektronske mikroskopije (FE-SEM), a na mikrografijama su uočene čestice srebra sfernog oblika i nanometarskih dimenzija oko 36 nm u Ag/PVA i oko 17 nm u Ag/PVA/Gr nanokompozitu.

Takođe, inkorporacija grafena u matrici PVA i formiranje veza između nanočestica srebra, PVA molekula i grafena su doveli do poboljšanja termičke stabilnosti Ag/PVA/Gr i do sprečavanja rasta i agregacije nanočestica srebra, što je potvrđeno infracrvenom spektroskopijom sa Furijeovom transformacijom i skenirajućom elektronskom mikroskopijom.

Diskovi Ag/PVA i Ag/PVA/Gr hidrogelova sa najmanjom koncentracijom nanočestica srebra (0,25 mM) su klasifikovani kao necitotoksični prema mononuklearnim ćelijama periferne krvi (PBMC) prema 3-(4,5-dimetil tiazol-2-il)-2,5-difenil tetrazolium-bromid (MTT) testu citotoksičnosti, dok su, s druge strane, pokazali antibakterijsku aktivnost prema *Staphylococcus aureus* i *Escherichia coli*.

Sporo otpuštanje srebra i visok sadržaj srebra od ~ 67- 68 mas. % koji ostaje u hidrogelu nakon 28 dana potapanja u fosfatnom puferu (PB) su potvrdili da Ag/PVA i Ag/PVA/Gr kompoziti zadržavaju sterilnost tokom dužeg vremena. Ispitivanja sorpcionih svojstava su vršena potapanjem osušenih diskova PVA, PVA/Gr, Ag/PVA i Ag/PVA/Gr u simuliranoj telesnoj tečnosti (SBF) tokom 72 h na  $37 \pm 1$  °C. Rezultati su ukazali na veći stepen bubrenja PVA/Gr hidrogela u SBF-u u odnosu na PVA hidrogel, dok su Ag/PVA/Gr nanokompoziti pokazali nešto veću brzinu sorpcije u odnosu na

Ag/PVA nanokompozite. Ovi rezultati ukazuju na proširenje hidrogelne mreže PVA pod uticajem inkorporisanog grafena.

Svi dobijeni rezultati doprinose ispunjenju cilja ove disertacije, koji se tiče *in situ* elektrohemijske sinteze nanokompozitnih hidrogelova na bazi polivinil-alkohola sa nanočesticama srebra. Sintetisani nanokompoziti su netoksični, poseduju antibakterijsku aktivnost i imaju potencijal za primenu u medicinske svrhe u obliku obloga za rane i implantata mekog tkiva.

Eksperimenti su obavljani na Katedri za fizičku hemiju i elektrohemiju Tehnološko-metalurškog fakulteta, Univerziteta u Beogradu, dok su antibakterijska ispitivanja vršena u laboratoriji za mikrobiologiju na Katedri za biohemijsko inženjerstvo i biotehnologiju. Testovi citotoksičnosti su obavljani na Institutu za onkologiju i radiologiju, Beograd, Srbija.

**Ključne reči:** kompoziti sa polimernom matricom, polivinil-alkohol, nanočestice srebra, skenirajuća elektronska mikroskopija, termička analiza, citotoksičnost, antibakterijska aktivnost, otpuštanje srebra.

**Naučna oblast:** Hemijske nauke.

**UDK broj:**

# CONTENTS

1. INTRODUCTION.....	1
2. THEORETICAL PART .....	4
2.1. POLYMERS .....	4
2.1.1. HYDROGELS.....	5
2.1.2. POLY(VINYL ALCOHOL) HYDROGELS.....	6
2.2. SILVER NANOPARTICLES .....	8
2.2.1. Ag/PVA NANOCOMPOSITES .....	8
2.3. GRAPHENE .....	16
2.3.1. PVA/GRAPHENE COMPOSITES.....	17
2.4. FREEZING/THAWING METHOD .....	18
2.5. CHARACTERIZATION OF Ag/HYDROGEL NANOCOMPOSITES .....	21
2.5.1. ANTIMICROBIAL ACTIVITY .....	21
2.5.2. CYTOTOXICITY.....	22
2.5.3. SILVER RELEASE INVESTIGATIONS.....	22
2.5.4. SORPTION STUDIES .....	23
2.6. HYDROGEL MECHANICAL PROPERTIES .....	24
3. AIMS OF RESEARCH.....	26
4. EXPERIMENTAL PART .....	27
4.1. MATERIALS .....	27
4.2. PREPARATION OF Ag/PVA AND Ag/PVA/Gr COMPOSITE HYDROGEL DISCS.	27
4.3. METHODS OF CHARACTERIZATION .....	28
4.3.1. UV-VISIBLE SPECTROSCOPY.....	28
4.3.2. RAMAN SPECTROSCOPY .....	28
4.3.3. CYCLIC VOLTAMMETRY (CV) .....	28
4.3.4. FIELD EMISSION SCANNING ELECTRON MICROSCOPY (FE-SEM).....	29
4.3.5. FOURIER TRANSFORM INFRARED SPECTROSCOPY (FT-IR).....	29
4.3.6. X-RAY DIFFRACTION (XRD).....	29
4.3.7. THERMAL ANALYSIS.....	29
4.3.8. CYTOTOXICITY.....	30
4.3.9. ANTIBACTERIAL ACTIVITY.....	31
4.3.10. SILVER RELEASE INVESTIGATION.....	32

4.3.11. SORPTION CHARACTERISTICS.....	32
5. RESULTS AND DISCUSSION .....	33
5.1. ELECTROCHEMICAL SYNTHESIS OF SILVER NANOPARTICLES INSIDE PVA AND PVA/Gr HYDROGELS.....	33
5.2. UV-VIS ANALYSIS.....	34
5.3. RAMAN SPECTROSCOPY.....	37
5.4. CYCLIC VOLTAMMETRY .....	38
5.5. FIELD EMISSION SCANNING ELECTRON MICROSCOPY (FE-SEM) .....	45
5.6. FOURIER TRANSFORM INFRARED SPECTROSCOPY (FT-IR) .....	46
5.7. X-RAY DIFFRACTION (XRD).....	48
5.8. THERMAL ANALYSIS.....	50
5.9. CYTOTOXICITY .....	53
5.10. ANTIBACTERIAL ACTIVITY .....	57
5.11. SILVER RELEASE INVESTIGATIONS .....	61
5.11.1. SILVER RELEASE FROM HYDROGELS WITH $0.25 \times 10^{-3}$ M $AgNO_3$ .....	61
5.11.2. SILVER RELEASE FROM HYDROGELS WITH $0.5 \times 10^{-3}$ M $AgNO_3$ .....	63
5.11.3. SILVER RELEASE FROM HYDROGELS WITH $1 \times 10^{-3}$ M $AgNO_3$ .....	65
5.11.4. SILVER RELEASE FROM HYDROGELS WITH $3.9 \times 10^{-3}$ M $AgNO_3$ .....	67
5.12. SORPTION CHARACTERISTICS .....	69
6. CONCLUSION .....	72
7. REFERENCES.....	74
8. APPENDIX .....	98
9. BIOGRAPHY .....	100

# 1.INTRODUCTION

Considering an importance of hydrogels and their metal/hydrogel nanocomposites for different applications in recent years, silver/poly(vinyl alcohol) (Ag/PVA) nanocomposites became favorite subject of research studies. Poly(vinyl alcohol) itself is considered a self-healing hydrogel when treated with freezing/thawing method and used in biomedical applications [1-6]. PVA hydrogel, linear polymer with three dimensional cross-linking structure possesses important properties such as aqueous solubility, non-toxicity and being a color-less material [6,7-11]. In the freezing-thawing technique, gels are formed by dissolving polymers in a suitable solvent and freezing the solution in several cycles; the properties of hydrogels are highly dependent on the molecular weight, concentration, time, and temperature of freezing as well as the number of freeze-thaw cycles. Upon freezing, the solvent crystals grow until they meet the facets of other crystals, creating a porous system upon thawing [6,7].

The study and preparation of metal particles in the nanometer scale have attracted considerable interest in both fundamental and applied research. Nanosized structures of silver particles ranging from 1 to 100 nm have been the focus of investigations over past decades. Maximization of the total nanoparticle surface area leads to the highest ratio of the activity vis weight. Therefore the properties of silver nanoparticles (AgNPs) are significantly different from those of the bulk metal [8]. Differences are especially prominent for physical and mechanical properties of metal nanosized particles compared to macroscopic materials. Silver nanoparticles AgNPs were incorporated into polymer hydrogels for many purposes, e.g. resulting in especially excellent antimicrobial or active catalytic material [12]. For example in medical fields, AgNPs were added to poly(vinyl alcohol) PVA [7,13-18] chitosan [19], hydroxyapatite [20], Na-alginate [21,22] and poly(N-vinyl-2-pyrrolidone) PVP [23-27]. To create more useful properties such as high stability, AgNPs were introduced into mixture of PVA with other polymers such as PVP [28], poly(L-lactic acid) PLLA [29], silk fibroin SF [30], chitosan CS [31,32] and cellulose [33].

AgNPs exhibit enhanced antibacterial properties compared to bulk silver due to high surface area and high fraction of surface atoms in contact with bacteria or fungi [13,34,35]. However, lack of sufficient chemical and physical stability limits to some extent the application of AgNPs [14,16,36].

Silver/poly(vinyl alcohol) nanocomposites with /or without co-polymers have many applications in the medical field as wound dressings [12,14,18,28,37,38], antibacterial materials [8,13-16,18,30,37,39-44], for tissue engineering [29,45], for blood compatibility [7], in optical application fields [46-51], as well as in electrical [48,49,52-57] and environmental fields [47].

Morphology of PVA hydrogels loaded with silver nanoparticles was studied to evaluate formation of AgNPs inside the hydrogel networks using SEM and TEM characterization techniques [7,28,37]. According to previously reported work, loading of silver nanoparticles inside the hydrogel did not affect its morphology and structural integrity, but it was inferred that the presence of intermolecular forces between PVA units facilitated formation of an extensive physical network of hydrogen bonds, which provided “nano” sites for growth of the nanoparticles as well as ensured their protection within the network [7].

Regarding the antimicrobial activity, the size and the rate of leaching of AgNPs can play a major role, especially for wound dressing applications. In such applications, a hydrophilic environment is necessary, to facilitate the release of silver from the polymer matrix, and also to maintain a hydrated surrounding of the wound bed, which is essential for optimal wound healing [39]. Release of silver from the Ag/PVA and Ag/PVA/Gr hydrogel discs was studied in phosphate buffer (PB) solution [10].

Graphene is a single layer carbon nanomaterial with two dimensional (2D) morphological structure and  $sp^2$  hybridized carbon atoms [9,55-75]. Recently, research has focused on composites of PVA and graphene, especially due to their improved mechanical strength [59-62,76-78]. Graphene/poly (vinyl alcohol) hydrogels could be employed as wound dressing [9], articular cartilage [79], in biomedical fields [70,79], for electrical applications [56], industrial and environmental applications [55,59,71,79].

Considering the methods of silver nanoparticles synthesis, several of them are based on physical processes such as thermal decomposition, and chemical methods employing chemical reduction of  $\text{Ag}^+$  ions. These syntheses techniques are carried out in organic or aqueous solvents using reducing agents such as sodium borohydride, citrate, ascorbate and some carbohydrates [80].

Acquiring highly pure metal nanoparticle as well as the possibility of precise control of particle size could be achieved using electrochemical synthesis by adjusting several parameters, such as applied potential, current density, reaction temperature, and swelling solution [8,81,82]. Further more, absence of undesired products is especially important for future applications in synthesis of metal nanoparticles at a large scale. Also, chemical methods for synthesis of nanoparticles involve the usage of reducing agents, which can be toxic to living organisms, whereas the electrochemical route of nanoparticle synthesis engages the use of mild reaction conditions and non-toxic reaction precursors and is therefore especially attractive for biomedical applications. Different electrochemical methods like potentiostatic [83-85], galvanostatic [86], pulsed sonoelectrochemical technique [87,88], single and double pulse [89] deposition methods were found to be very promising in the preparation of a variety of nanometer dimension materials.

## **2.THEORETICAL PART**

### **2.1.POLYMERS**

The first synthetic polymer was guncotton (cellulose nitrate) made by Christian F. Schönbein in 1845. Bakelite, a strong and very durable synthetic polymer based on phenol and formaldehyde, was invented in 1872. Polycondensation-based polymeric products such as Bakelite and those based on phenoxy, epoxy, acrylic, and ketone resins were developed and used as cheap substitutes for auto parts and in the electronic industry. Other synthetic polymers such as polyethylene, poly(vinyl chloride) and polystyrene were invented in 1933, polyamide in 1935, teflon in 1938, and different synthetic rubbers in 1942. Polyethylene was used to make radar equipment for airplanes. Nylon was used to make parachutes, replacing silk, that was otherwise imported from Japan [90].

Advanced pharmaceutical dosage forms utilize polymers for drug protection, taste masking, controlled release of a given drug, targeted delivery, increase drug bioavailability, and many other applications. Polymers have found relevance in liquid dosage forms as rheology modifiers. They are employed to control the viscosity of an aqueous solution or to stabilize suspensions or even for the granulation step in the preparation of solid dosage forms. Major application of polymers in the current pharmaceutical field is for the controlled drug delivery. In the biomedical area, polymers are generally used as implants and are expected to perform longterm service. This requires polymers with unique properties that are not offered by polymers intended for general applications [90].

Desirable polymer properties regarding pharmaceutical applications are film forming (coating), thickening (rheology modifier), gelling (controlled release), adhesion (binding), pH-dependent solubility (controlled release), solubility in organic solvents (taste masking), and barrier properties (protection and packaging). According to the solubility characteristics, pharmaceutical polymers can be classified as water-soluble and water-insoluble (organic soluble). The synthetic water-soluble polymers have found extensive applications in pharmaceutical industries, among them polyethylene glycol, poly(vinyl alcohol), polyethylene oxide, poly(vinyl pyrrolidone), and polyacrylate or

poly(methacrylate esters) containing anionic and cationic functionalities are well-established [90]. Water soluble polymers have a wide range of industrial applications like food, pharmaceuticals, paint, textiles, paper, constructions, adhesives, coatings, water treatment, *etc.* [91]. Production of new polymers has resulted in development of polymers with unique properties. Initially polymers were used as solubilizers, stabilizers and mechanical supports for sustained release of drugs. However, over a period of time, the functionalities of polymers have changed and they were synthesized to suit specific needs or rather solve specific problems associated with development of drug delivery systems. Therefore the roles of polymers are expanding [90].

### **2.1.1.HYDROGELS**

Hydrogels are a class of polymers in which their structure represents a three dimensional cross-linked network. This unique structure gives them important characteristics such as very high swelling ratios in water and soft elastic properties well suited for applications as biomedical substances that mimic human tissues or for drug delivery and tissue-engineering [2,4]. Other important properties of hydrogels for biomedical applications are good biocompatibility and nontoxicity and some times also that self-healing ability [1].

Recently a new kind of nanocomposite hydrogels or hybrid hydrogels, with inorganic metal nanoparticles attached to polymeric cross-linked network structure, were synthesized and used for biomedical applications [75].

Figure 2.1 shows some types of nanoparticles and polymers mixed together to produce nanocomposite hydrogels for biomedical applications.

## Nanocomposite Hydrogels for Biomedical Applications

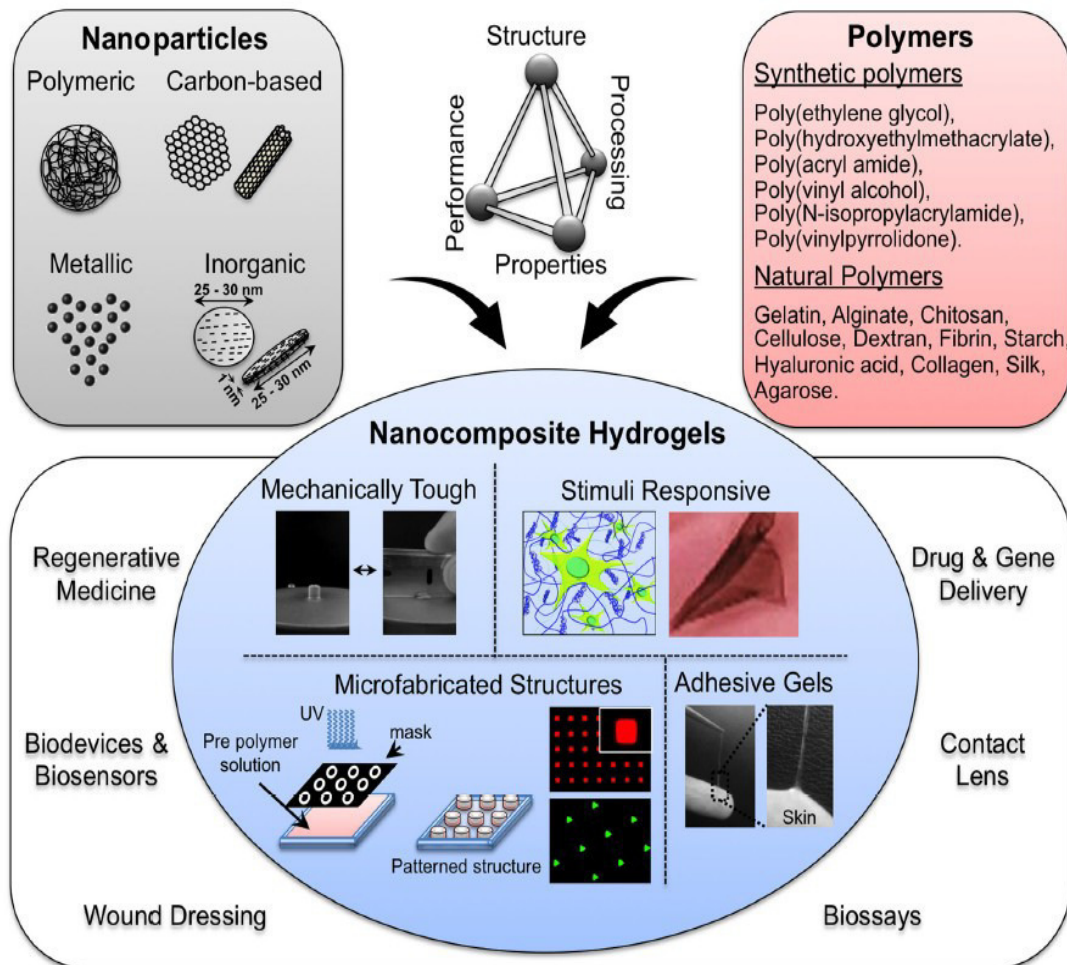


Figure 2.1. Nanocomposite hydrogels and their biomedical applications[75].

### 2.1.2. POLY(VINYL ALCOHOL) HYDROGELS

Poly(vinyl alcohol) (PVA) is a soluble polymer that has hydroxyl groups in its structure. It is synthesized by polymerization of vinyl acetate to polyvinyl acetate (PVAc) which is then hydrolyzed to gain PVA. Crystallinity and solubility of poly(vinyl alcohol) are effected by the extent of hydrolysis and content of acetate groups in PVA. Figure 2.2. shows the molecular structure of poly(vinyl alcohol) [91].

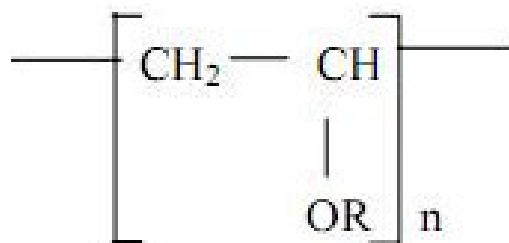


Figure 2.2. Molecular structure of poly(vinyl alcohol), where  $R = H$ [91].

PVA has a linear structure and high degree of swelling in aqueous solutions and therefore PVA can be easily soluble in highly polar and hydrophilic solvents, such as water, dimethyl sulfoxide (DMSO), ethylene glycol (EG), and N-methyl pyrrolidone (NMP); still, water is the most important solvent for PVA. The solubility of PVA in water depends on the degree of polymerization (DP), hydrolysis, and solution temperature. Any change in these three factors affects the degree and character of hydrogen bonding in aqueous solutions, and hence the solubility of PVA. It has been reported that PVA grades with high degrees of hydrolysis have low solubility in water. The solubility, viscosity, and surface tension of PVA depend on temperature, concentration, degree of hydrolysis and molecular weight [91].

Poly(vinyl alcohol) hydrogels are non-toxic, non-carcinogenic, with desirable physical properties [11], and because of their characteristics, PVA hydrogels have been used for various biomedical and pharmaceutical applications. Recently, this type of hydrogels is utilized in wide medical and pharmaceutical applications such as drug delivery [11] and tissue engineering [3]. PVA hydrogels have certain advantages which make them ideal candidates for biomaterials such as non-toxicity, non-carcinogenicity, and bioadhesiveness. PVA also shows a high degree of swelling in water (or biological fluids) and a rubbery and elastic nature and therefore closely simulates natural tissue and can be readily accepted into the body. PVA hydrogels have been used for contact lenses, the artificial hearts lining, and drug- delivery applications. PVA is mainly used in topical pharmaceutical and ophthalmic formulations. It was widely used as a stabilizer in emulsions. PVA is used as a viscosity increasing agent for viscous formulations such as ophthalmic products. It is used as a lubricant for contact lens solutions, in sustained release oral formulations and transdermal patches [91].

## **2.2.SILVER NANOPARTICLES**

Nanosized inorganic materials can be added to polymers in order to enhance their characteristics such as high chemical and heat resistance, tensile strength, glass transition temperature and viscoelastic properties. These classes of materials had attracted significant interest [44]. Silver nanoparticles (AgNPs) have been widely used because of their physical, chemical and biological properties [44]. These nanoparticles are found to be highly antimicrobial, catalytically active and exhibit good conductivity so these materials could be identified as good antibiotics [18,44]. The nanoparticles were reported to be more effective antibacterial materials than silver in ionic form, when these particles are doped inside a hydrogel network [18]. AgNPs can be synthesized in different shapes in different sizes and are characterized by TEM or SEM techniques [92].

### **2.2.1.Ag/PVA NANOCOMPOSITES**

Ag/PVA nanocomposites could be produced in the cross-linked network of poly(vinyl alcohol) (PVA) chains by reduction of silver in ionic salt solutions such as silver nitrate ( $\text{AgNO}_3$ ) by suitable methods [17]. Biofriendly characteristics of poly(vinyl alcohol) hydrogels such as non-toxicity and water-solubility, when combined with silver nanoparticles identified as high antimicrobial substances resulted in biomedical applications of these nanocomposites, like wound dressings, drug delivery and bioengineering utilizations [17]. PVA has other attractive properties e.g. being colorless, having high clarity and high transmission, and when its network fibers attach to nanosized spheres of AgNPs, thus formed nanocomposites might have other optical and electrical applications [51].

#### **2.2.1.1.Synthesis of Ag/PVA nanocomposites**

There are many different methods of production of metal polymer nanocomposites depending on the purpose of the application, such as Gamma ( $\gamma$ )-irradiation method [12,93-96], photochemical/UV-irradiation method [32,41,97,98], chemical reduction method [48,99-115] or the electrochemical method [8,21,22] to name a few. If nanocomposites are to be used for medical applications than the cleanest

possible method should be chosen. Two main routes could be applied for cross-linking of PVA polymer chains to obtain hydrogels: (i) chemical routes and (ii) physical routes. The chemical route uses cross-linking agents, i.e. chemicals are added such as glutaraldehyde or formaldehyde to react with PVA covalent bonds. However the residual chemicals remain within the polymer lattices and could be hazardous to the body if applied for biomedical purposes [18]. On the other hand, in the physical cross-linking route, i.e. irradiation, and electrochemical methods, there is no need to use any chemicals.

- **Gamma ( $\gamma$ ) –Irradiation method**

Gamma ( $\gamma$ ) irradiation technique was applied to produce controlled number and diameter of nanosized nanoparticles inside thin layer walls of hydrogels [12]. Water-soluble hydrogels were cross-linked by irradiation in dilute solutions for incorporation of nano-silver in their networks [12]. Oliveira et al. [18] synthesized Ag/PVA nanocomposites by dissolving PVA powder in deionized water at 90 °C under stirring, followed by addition of AgNO<sub>3</sub> solutions at different concentrations, and subsequently by irradiation by a Co-60  $\gamma$ -source metal at the dose rate of 1.5kGy h<sup>-1</sup> for 10 h [18].

In another approach, specified concentration of AgNO<sub>3</sub> solution was mixed with the dissolved PVA polymer matrix solution to form metal/polymer films with well defined structures in which metal centers are embedded directly in the polymer network [96]. Using gamma-irradiation, nucleation sites were initiated for growth of AgNPs directly inside the polymer fiber network. The irradiation method has many advantages for preparation of metal nanoparticles. The hydrated electrons which resulted from the gamma radiolysis of aqueous solutions, can reduce metal ions to zero-valent metal particles, avoiding the use of additional reducing agents and the consequent side reactions. The amount of zerovalent nuclei can be controlled by varying the irradiation dose [96]. Figure 2.3 shows the scheme diagram of  $\gamma$ -irradiation method [96].

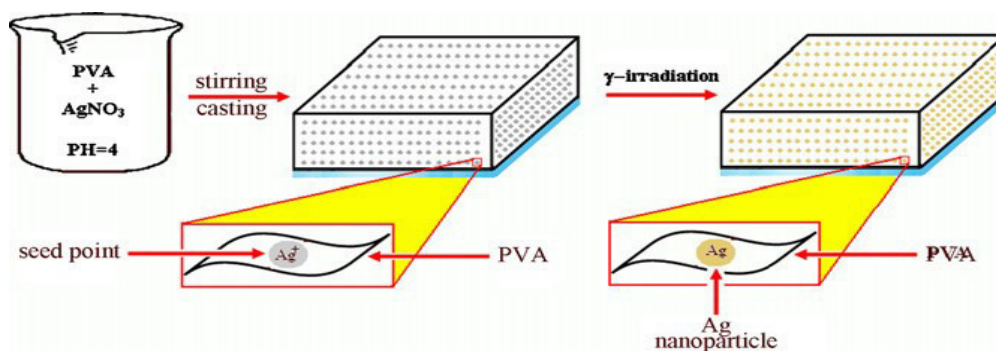


Figure 2.3. The scheme of  $\gamma$ -irradiation method of Ag/PVA nanocomposite synthesis [96].

In another study 1 mM  $\text{AgNO}_3$  solution was added to four different colloidal hydrogel stabilizer solutions (0.5% w/v) of PVA, PVP, alginate and sericin to produce Ag/polymer nanocomposites using  $\gamma$ -irradiation method. The applied dose of irradiation for AgNP synthesis was  $1.2 \text{ kGy h}^{-1}$  carried by Co-60 irradiator [16].

- **Photochemical/UV-irradiation method**

PVA nanocomposites can be produced also by UV-irradiation processes, the simple low cost and effective method in respect to other methods as  $\gamma$  or electron rays. Kim et al. [41] prepared PVA/Ag-Zeolite nanocomposites using UV-irradiation method. They varied mixtures of Ag-Zeolite with different concentrations of PVA solutions, and exposed samples to UV irradiation for several periods of time.

*In-situ* photochemical synthesis is one of the most powerful approaches to realize silver/polymer nanocomposites. A silver-acrylate nanocomposite was prepared using a photoinduced reduction and free radical polymerization processes [98].

Depending on the principle of green synthesis, the production of nontoxic chemicals, environmentally friendly materials should be considered in the preparation of AgNPs. Recently, a series of photocrosslinked thin films such as poly(vinyl alcohol) (PVA), chitosan (CS) [32], with acrylic acid (AA) monomer as a crosslinker, were investigated. Figure 2.4 shows the photocrosslinking method for preparation of PVA/CS thin films.

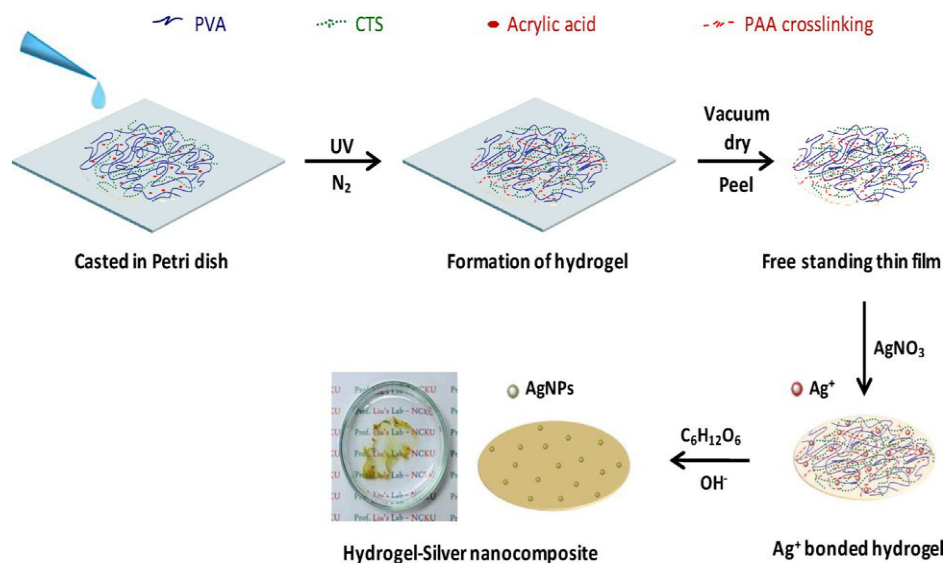


Figure 2.4. Photocrosslinking method for preparation of PVA/CS hydrogel thin films[32].

- **Electrochemical method**

Electrochemical methods are superior over chemical ones in synthesis of small metal particles due to high purity and the possibility of a precise particle size control. According to previous reports, nanosized transition metal particles could be prepared electrochemically using tetraalkylammonium salts as stabilizers for the metal clusters in nonaqueous medium [116]. Pulsed sonoelectrochemical synthesis, that involves alternating sonic and electric pulses, has been employed to obtain shape controlled synthesis of nanostructured materials [116]. Well-defined nanowires and nanorods of metals or compounds were prepared by means of electrodeposition in membrane templates [116], Gold nanorods were also synthesized via this electrochemical method by introducing a shape-inducing cosurfactant [116]. However, in aqueous medium noble metal ions can be coated on the cathode more easily, so there could be some difficulties when noble metal nanoparticles are produced by the electrochemical method in this phase [21,116]. An easier and more convenient electrochemical method to prepare large numbers of well-dispersed silver nanoparticles in aqueous phase was under the protection of poly(*N*-vinyl pyrrolidone) (PVP) and demonstrated that the particle size distribution might be further improved by adding anionic surfactants of appropriate

concentration to the electrolyte [116]. PVP is found to accelerate the silver particle formation and lowered the silver deposition on cathode [116]. Therefore, an external excitation system such as ultrasonication is no longer required, which significantly simplifies the synthesis procedure. The electrochemical method should make possible large-scale preparation of the size-controlled metal nanoparticles, especially noble metals, such as gold, platinum, and silver just by simple adjustments of current density or applied potential [116].

Another necessary condition to prepare well-dispersed particles is to accelerate the transfer of formed silver clusters from the cathodic vicinity to the bulk solution. The use of  $\text{KNO}_3$  as the primary supporting agent effectively avoids agglomeration of silver particles after depletion of silver existing in pulse sonoelectrochemical methods. The present method may be extended to synthesizing other metal nanoparticles such as gold, platinum, and copper [116].

An original electrochemical procedure was developed for production of alginate hydrogel microbeads incorporated with silver nanoparticles. It was found that increase in  $\text{AgNO}_3$  concentration in the initial alginate solution, applied current density and implementation time increased the concentration and decreased the size of electrochemically synthesized AgNPs [21].

Dobre et al. [117] used the electrochemical synthesis for doping AgNPs into PVP network hydrogel with addition of sodium lauryl sulfate (Na-LS) as a costabilizer in order to ensure wrapping and electrostatic stability of AgNPs in solutions. The use of PVP stabilizer associated with Na-lauryl sulphate costabilizer facilitated adequate dispersion of the formed silver nanoparticles and hindered their agglomeration [117]. Obradović et al [118] produced successfully Ag/alginate/PVA and Ag/alginate/PVA/PVP using electrochemical synthesis method. Stojkowska et al. [22] obtained alginate nanocomposites with silver nanoparticles using controlled production facilitated by electrochemical synthesis method. This method is attractive to use for biomedical applications without need to add any chemical agents. Surudžić et al. [8] applied this method to synthesis of Ag/PVA in colloid solutions.

- **Chemical reduction method**

Nanoparticles of different shapes and sizes can be prepared by chemical reduction and by controlling the reaction conditions. The color of metal nanoparticles depends on the shape and size of the nanoparticles and dielectric constant of the surrounding medium. The influence of different parameters such as, type of silver precursor, reducing agent and protecting agent on stability and optical properties of silver nanoparticles was investigated [100]. It was found that the silver precursor had an important effect on the crystallinity of the obtained AgNPs. When silver citrate was used as a precursor of AgNPs in aqueous solutions, all of the obtained colloids were stable in the investigated time range. When silver nitrate or silver acetate were used as precursors under investigated conditions, AgNPs aggregated and precipitated from the solution. AgNPs prepared using different reducing agents had different morphologies and sizes. For the same concentration of silver in solution smaller silver particles were obtained by using ascorbic acid as a reducing agent than by strong reducing agents such as hydrazine or sodium borohydride. Also it was found that the size of AgNPs obtained in aqueous solutions using PVA as a stabilizer did not depend on the concentration of silver in the range from 250 to 1000 mg/dm<sup>3</sup> Ag. The particle sizes in the colloids were around 44 nm. AgNPs obtained in the aqueous solution using PVP as the protecting agent increased in size with the increase in silver concentration from 36 nm for 250 mg/dm<sup>3</sup> Ag to 82 nm for 1000 mg/dm<sup>3</sup> Ag.[100].

Reduction of silver nitrate by sodium borohydride was performed in the absence and presence of two stabilizers, namely starch and PVA [105]. Upon mixing, all of the ionic silver is reduced immediately to form a differently colored silver sol. Under the experimental conditions, important parameters for obtaining stable silver nanocomposites were aging of NaBH<sub>4</sub> solution, order of reactant addition, dropwise addition of silver nitrate solution into NaBH<sub>4</sub> solution and presence of stabilizers [17]. In the presence of starch and PVA, the particles grew to a stable size nearly 20-52 nm and, during this growth process, resulting solutions changed color to golden and yellowish-green. Ag/PVA nanocomposites have been synthesized by an eco-friendly green method, where non toxic amino acid tyrosine was used as the reducing agent, in aqueous media. Biomolecule, tyrosine reduced silver ions

efficiently through a cyclic process. The advantage of the system was that it required a catalytic amount of tyrosine for the whole conversion of silver ions to silver nanoparticles and thus minimized the use of conventional chemical reductants. Ultra-sound increased the reaction rate and improved the quality of AgNPs (regular size distribution, spherical and symmetrical shape) [17]. General chemical reduction routes fall into two broadly defined categories [44]. The first one involves the use of relatively strong reducing agents, such as sodium borohydride. The second route involves heating the solution of silver salt with a weak reducing agent, such as glucose, sodium citrate, and ascorbic acid [44]. Recently, the use of toxic reducing and stabilizing agents for the synthesis of AgNPs was replaced with so-called “green” substances such as PVA is used as a safer reducing as well as stabilizing agent to synthesize the AgNPs. Synthesis method of the reactions also plays an important role in green chemistry. Sonochemistry is one of the novel, and simple methods for synthesis of nanoparticles since it is nonhazardous, increases the reaction rate and changes the selectivity of the reaction. Therefore, the ultrasonic irradiation provides a clean media to prepare different nanomaterials. For preparation of AgNPs, tyrosine is an excellent reducing agent compared to sodium borohydride. The use of tyrosine not only reduced the amount of chemical additives (milligram level to microgram) but also increased the nanoparticle production rate in contrast to sodium borohydride. Ag/PVA was synthesized by irradiation of ultrasound in the presence of catalytic amount of tyrosine in aqueous solutions. The appearance of a deep orange color in the mixture indicated the formation of AgNPs. Figure 2.5 shows the synthesis of Ag/PVA nanocomposites using chemical reduction under ultrasound application [44].

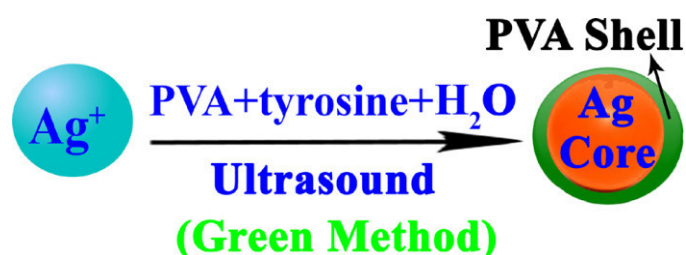


*Figure 2.5. Synthesis of Ag/PVA nanocomposites by using a chemical reduction method under sonification process [44].*

### 2.2.1.2.Applications of Ag/PVA nanocomposites

Ag/PVA nanocomposites have a lot of applications in several fields due to their attractive properties. In the medical field these composites can be applied as wound dressings [7,10,12,18], and antimicrobial agents [8,13-16,18]. The developed Ag/PVA porous hydrogel nanocomposites exhibited superior antibacterial and good mechanical properties, suggesting that they can be applied for wound dressings and other biomedical applications [28]. The antibacterial ability could be significantly enhanced by increasing the AgNP content. *In vitro* bacterial adhesion study indicated a significant difference between neat and nanocomposite gel which showed higher inhibition. It was concluded that antibacterial silver based hydrogels are suitable for many different medical applications such as wound healing [12]. PVA and Ag/PVA hydrogel samples were studied [18] to assess their potential in wound dressing applications. The presence of silver in PVA gels caused slight microstructural differences, such as lower crystallinity. In addition, all samples were effective barriers to microbial penetration and the samples containing silver presented antimicrobial activity against *E. coli*, *S. aureus* and *C. albicans*. All samples were non-toxic to mouse fibroblasts [18]. To improve properties of Ag/PVA nanocomposites, some other components were added, such as graphene nanosheets [9,10]. The PVA/Gr hydrogel was classified as non-cytotoxic against healthy peripheral blood mononuclear cells (PBMC) in a MTT assay, and exhibited strong antibacterial activity against *S. aureus*. Therefore, the evidence demonstrated that a nanosized PVA/Gr composite is an excellent candidate for biomedical applications as soft tissue implants and wound dressings [9]. The amount of silver released, as well as high remaining silver content (76%) after 28 days in simulated body fluid confirmed that both Ag/PVA/ Gr and Ag/PVA hydrogels could preserve sterility over time. This characteristic, together with their strong antibacterial activity, indicated that Ag/PVA/Gr and Ag/PVA hydrogels are excellent candidates for soft tissue implants and wound dressings [10]. On the other hand these nanocomposites can be used in electrical applications [54], or even mixed with other materials [52,56,119,120]. Electrical conductivity investigation of the PVA-PAA-glycerol polymer membrane which was consisting of Ag and Cu nanoparticles confirmed its suitability to replace the p-type semiconductor used previously in hybrid memory devices [121].

### 2.3. GRAPHENE

Graphene, as a single layer of carbon atoms in a two-dimensional honeycomb crystal lattice, has been attracting tremendous interest in the fields of electronics and composite materials because of its fascinating properties [73-75]. Theoretical and experimental results show that single-layered graphene sheets are the strongest materials developed ever. Since graphene nanosheets exhibit also high thermal conductivity and high specific surface area, graphene is an excellent additive to significantly enhance mechanical, thermal, and electrical properties of polymer materials. Efforts have been made in the use graphene materials for highly conducting composite, transparent electrode and photovoltaic device applications [73]. Graphene is composed of several planar sheets of  $sp^2$ -bonded carbon atoms. Since experimentally discovered in 2004, graphene with such unique properties has become one of the most exciting materials today [74]. However, Gr is under constant re-evaluation of researchers, companies and regulatory committees and FDA has approved it for medical devices and soft tissue implants [122,123]. Figure 2.6 shows the hexagonal monolayer structure of graphene and Figure 2.7 shows the difference between graphene and graphite [124].

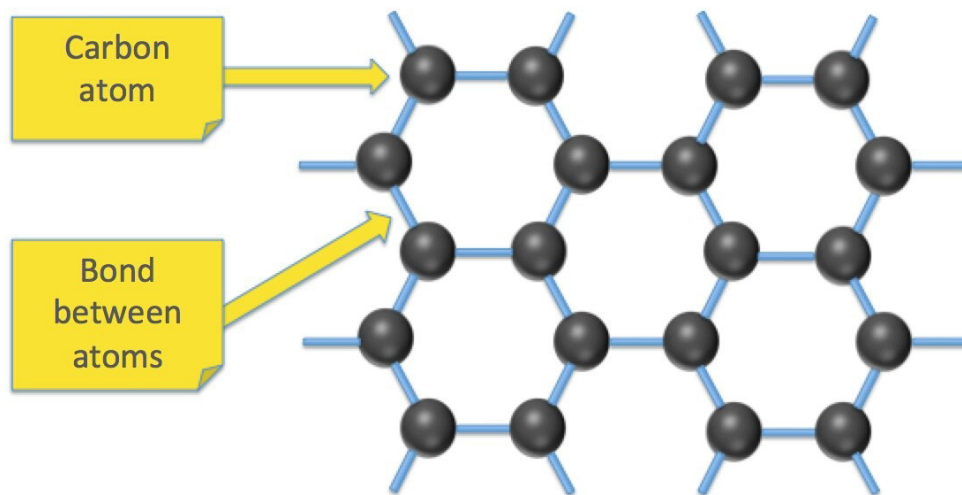


*Figure 2.6. Structure of graphene [124].*

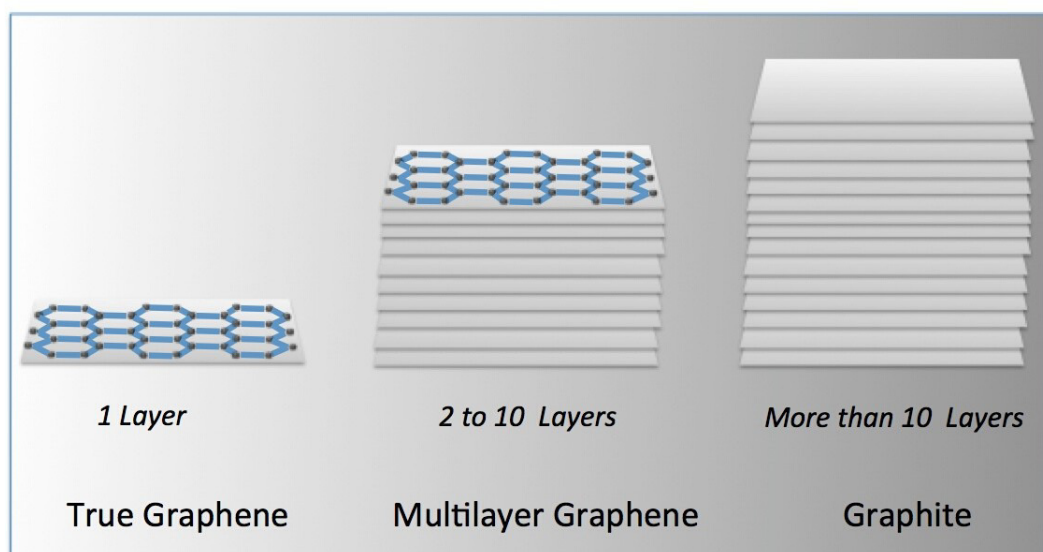


Figure 2.7. Difference between graphene, multilayer graphene and graphite [124].

### 2.3.1. PVA/GRAPHENE COMPOSITES

Graphene plays leading role among the newly discovered carbon nanomaterials on the laboratory bench. Confinement of graphene, combined with enhanced exchange properties within aqueous environment, is the key for the development of biosensors, biomedical devices, and water remediation applications. Such confinement is possible when using hydrogels as the soft matrixes. Many entrapment methods focused on the modification of the graphene structure [69]. A stable suspension containing the surfactant wrapped graphene sheets (SWGSSs) was successfully synthesized via a facile electrochemical route in the sodium dodecyl sulfate media [68]. The prepared SWGSSs, which contained monolayer as well as multilayer sheets, were then dispersed in the poly(vinyl alcohol) matrix through a liquid blending method [68]. A robust hybrid PVA-graphene construct was obtained starting from a surfactant assisted sonication of an aqueous dispersion of graphite. Stable graphene sheets suspension was photopolymerized in a methacryloyl-grafted PVA, using the vinyl moiety present on the surfactant scaffold [69]. This method can allow the incorporation in the polymer network of oligomers of N-(isopropylacrylamide). The stable inclusion of graphene in a highly hydrated matrix facilitates biomedical applications, where graphene confinement is mandatory in order to decrease, as much as possible, the contact on tissues or cells [69]. Methylated melamine grafted poly(vinyl benzyl chloride) (mm-g-

PvBCI) was prepared and used as an additive in poly(vinyl alcohol) along with graphene nanosheets (GNs) that were utilized to enhance the mechanical strength. Using a casting method, antimicrobial nanocomposite films were prepared with the polymeric biocide loading levels of 1 wt%, 5 wt%, and 10 wt%. This feasibility study demonstrated a simple route to prepare graphene reinforced nanocomposite materials and the facile way of introduction of polymeric biocide into the resultant nanocomposite materials. Further more, this biocide based graphene nanocomposite thin films demonstrated high effective antibacterial activity against both Gram negative and Gram positive bacteria at a relatively low level load. This graphene nanocomposite thin film was reported to be a promising material for food and drink packaging applications and hygiene products industry [71].

Layer-aligned PVA/graphene nanocomposites are usually prepared by reduction of graphene oxide in the presence of PVA and subsequent casting from the aqueous solution. Though the addition of graphene significantly decreases the crystallinity of PVA, the film of the PVA/graphene nanocomposite was reported to be strong and ductile [73]. The influence on the thermal and mechanical properties of the nanocomposites was ascribed mainly to homogeneous dispersion and alignment of graphene in PVA matrix and the interactions between those two components [73]. It was demonstrated that graphene could be utilized effectively as thin two-dimensional nanosheets within a polymer matrix for potential large-scale applications of polymer/graphene nanocomposites [73]. Advancements regarding graphene applicability along with improved synthesis and high yield, resulted in emerging practical the preparations of polymer nanocomposites with this exciting material. The PVA/Gr hydrogels were classified as non-cytotoxic materials against healthy peripheral blood mononuclear cells (PBMC) in a MTT assay, and exhibited strong antibacterial activity against *S. aureus* [9].

## **2.4.FREEZING/THAWING METHOD**

PVA is a biocompatible polymer which forms a hydrogel by strong non-covalent cross-linking. PVA gels prepared by freezing and thawing techniques show increased mechanical strength over most hydrogels due to the presence of crystalline regions that

serve as the physical crosslinks [125]. The physical crosslinking phenomenon by the freeze-thaw method is based on the existence of regular pendant hydroxyl groups on PVA that are able to form crystallites by strong interchain hydrogen bonding. Advantages of physically crosslinked hydrogels include their nontoxicity, noncarcinogenicity, high elasticity, and the good biocompatibility of the resulting polymer. The internal structure of a hydrogel matrix depends on the number of crosslinkages present in the network [7]. To increase the mechanical strength, repeated freezing/thawing cycles are performed [125]. Prepared gels by freezing and thawing techniques were characterized in terms of their swelling and dissolution behavior, degrees of crystallinity, and crystal size distributions [6]. In addition, the long-term stability was addressed in order to consider the appropriateness of such materials for long-term biomedical or pharmaceutical applications. The parameters of particular interest were the number of freezing/thawing cycles, PVA molecular weight, and the concentration of aqueous solution. Variation of these parameters significantly impacted the resulting behavior of the ensuing materials, and their potential pharmaceutical applications. The stability can be significantly enhanced by increasing the number of freezing and thawing cycles. In addition, it was concluded that it is actually desirable to use a low to intermediate PVA molecular weight in order to prevent the possible rearrangement of the structure over long time periods [6]. In another study, PVA cryogel-silver nanocomposites have been produced by 5 to 11 freeze-thaw cycles [7]. It was clearly indicated that the extent of swelling decreased with an increasing number of freezing/thawing cycles. The observed results may be attributed to the fact that with increasing number of freezing/thawing cycles, the gel acquired increasing crystallinity of the network, which restricts the mobility of PVA chains and consequently, results in suppressed value of the swelling ratio. Another reason for the observed lower water sorption capacity of the cryogel may be that increased number of freeze-thaw cycles results in greater intermolecular forces between PVA chains. The enhanced binding forces between the network chains reduced pore sizes of the cryogel and therefore, the water sorption capacity decreased. The prepared nanocomposites did not exhibit cytotoxicity and were blood compatible in a fair degree as evident from cytotoxicity and *in vitro* protein adsorption and hemolysis tests [7]. It was found that on increasing the

concentration of PVA, the biocompatibility of the nanocomposite increased and with increasing number of freeze thaw cycles blood compatibility decreased [7].

In another study, effects of PVA content on the crystalline structure, self-healability and water stability of PVA hydrogels obtained by freezing/thawing cycles were explored. The self-healing ability depended on the PVA content and starts at the PVA content of 25 wt%. The PVA content also significantly affected the crystalline structure of PVA and hence affected the tensile strength and water stability of the hydrogels. It was reported that increasing the crystallite size or crystallinity of PVA can enhance the water stability of PVA hydrogels [126]. Figure 2.8 shows preparation of self-healing PVA hydrogels using freezing/thawing method as proposed in literature [126].

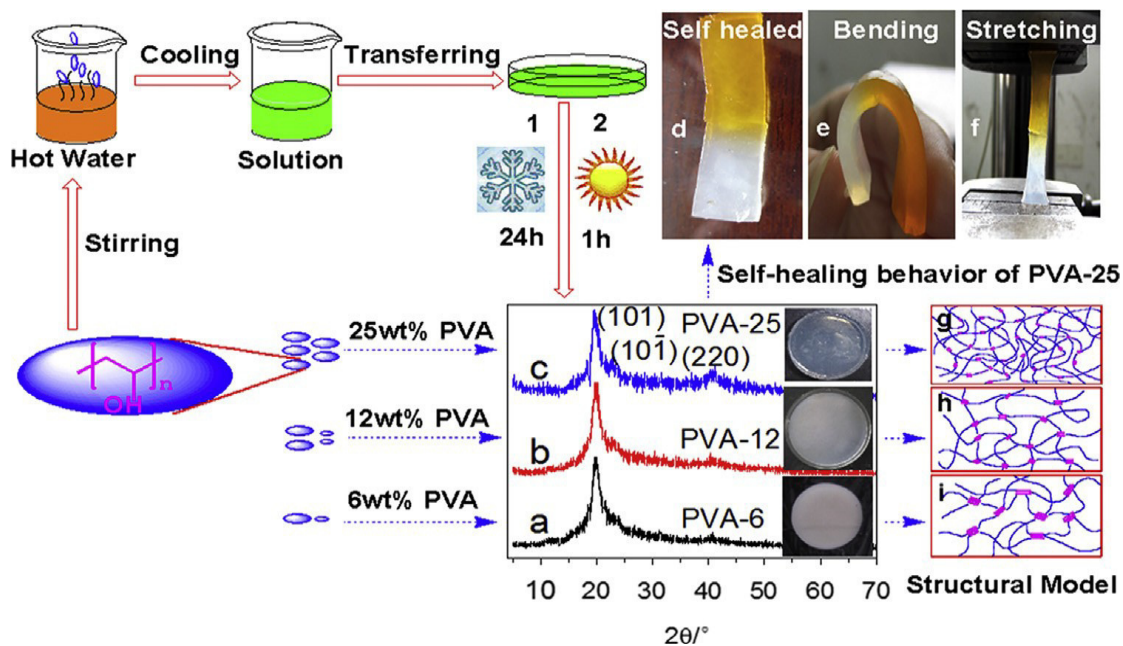


Figure 2.8. Schematic representation of self-healing PVA hydrogel samples with (6, 12, 25 wt % PVA concentrations) prepared by freezing/thawing method [126].

## **2.5.CHARACTERIZATION OF Ag/HYDROGEL NANOCOMPOSITES**

### **2.5.1.ANTIMICROBIAL ACTIVITY**

One of the main functions of poly(vinyl alcohol)/silver nanocomposites is antimicrobial activity, it was reported that Ag/PVA nanocomposite hydrogels induced inhibition zones in cultures of Gram positive bacteria (*S. aureus*, *B. subtilis*), Gram negative bacteria (*E. coli*, *P. aeruginosa*) and fungi (*A. niger* *Ferm*) [127]. It was also observed that pure PVA exhibited antibacterial activity only against *B. subtilis* and showed no activity towards other microorganisms [127]. It was reported that the activity of PVA may arise from hydroxyl groups. The antibacterial activity of silver is dependent on  $\text{Ag}^+$  that binds strongly to electron donor groups on biological molecules like sulfur, oxygen or nitrogen. The concentration of nanoparticles plays an important role in the antibacterial activity, as the interaction of particles with the cell wall of bacteria is small at low concentrations. On the other hand, at high concentrations of the particles, the aggregation probability of particles increases, and as a result, the effective surface to volume ratio of particles as well as the resulting interaction between particles and the cell wall of bacteria decrease. There are various proposed mechanisms of AgNPs action on the bacterial cell. Some of these mechanisms were summarized as follows: (i) silver nanoparticles might anchor to the bacterial cell wall and then penetrate it, (ii) formation of free radicals by the AgNPs could damage the cell membrane, (iii) release of silver ions by nanoparticles, which can interact with the thiol groups of many vital enzymes and thus inactivate them, and (iv) nanoparticles could modulate the signal transduction in bacteria which stops their growth [127]. Silver-loaded PVA nanocomposites exhibited broad activity against pathogenic organisms such as *E. coli*, *S. aureus*, *V. cholera*, Gram positive *Bacilli*, *P. aeruginosa*, and the zone of inhibition increased with the increase in the amount of silver loaded in the cryogel nanocomposites. Presence of the pores in the cryogel facilitated diffusion of liquid media within the hydrogel, which could enhance the release of AgNPs. Therefore, it was reported that porous hydrogel-silver nanocomposites exhibited good antimicrobial activity and displayed enhanced biocidal effects [7]. Antibacterial activity of Ag/PVA and Ag/PVA/Gr hydrogels was investigated quantitatively by monitoring

changes in the number of viable bacterial cells in suspension against *S. aureus* TL and *E. coli* [10]. Both hydrogels significantly reduced bacterial cell counts. But higher antibacterial activity was found for Ag/PVA/Gr than for Ag/PVA. This finding was attributed to smaller dimensions of AgNPs embedded in the former hydrogel [10].

### **2.5.2. CYTOTOXICITY**

Cytotoxicity testing is employed to reveal the effects of prepared nanocomposites on mammalian cells [9,24,128,129]. The concentration of AgNPs which are doped into hydrogel network should be controlled, otherwise the action of these nanoparticles could occur against blood cells or eukaryotic cells in addition to the action against bacteria [18]. The main difference between the two actions is the dosage amount, because bacterial or microbial cells are sensitive to a smaller amount than eukaryotic cells, so the concentration of AgNPs loaded into hydrogel must be in the range which enables antibacterial action without reaching toxicity levels for human cells [18]. Chatuvedi et al. [7] determined *in vitro* the cytotoxicity of their prepared Ag/PVA cryogels by direct contact method. They found that, the cryogels did not induce cytotoxicity towards mouse fibroblast cells. Jovanović et al. [24] prepared different concentrations of AgNO<sub>3</sub> solution for Ag/poly(N-vinyl-2-pyrrolidone) nanocomposites synthesis and they determined the cytotoxicity of their samples using peripheral blood mononuclear cells (PBMC) isolated from the heparinized blood. They found that the cytotoxicity of the nanocomposites depended on the concentration of AgNO<sub>3</sub> in the initial solutions, so that the lowest concentration (1 mmol dm<sup>-3</sup> AgNO<sub>3</sub> solution) had only slight cytotoxic effects.

### **2.5.3. SILVER RELEASE INVESTIGATIONS**

Kinetics of silver release from Ag/PVA and Ag/PVA/Gr hydrogel nanocomposites was studied as a function of time of exposure to phosphate buffer (PB) at 37 °C [10]. Silver concentration within Ag/PVA and Ag/PVA/Gr hydrogels initially decreased sharply with time, and after 3 days of silver release (16% and 19% of the initial silver content, respectively) a plateau was observed, indicating a significant lowering of the silver release rate. Even after 28 days, both Ag/PVA and Ag/PVA/Gr discs still retained 76% of the initial silver content as a consequence of the stability of

AgNPs within the highly crosslinked PVA hydrogel network. This is very important, because the remaining silver can preserve sterility of the samples over time [10]. Silver release kinetics was also studied from Ag/PVP hydrogel nanocomposites during time of exposure to PB at 37 °C [23]. The remaining silver (about 20% after 28 days) can preserve the sterility of the samples over time [23]. Kinetics of silver release from silver/poly(N-vinyl-2-pyrrolidone) PVP were examined under static conditions, continuous PB perfusion (in perfusion bioreactors), and under dynamic compression coupled with PB perfusion [24]. Diffusion was the dominant mechanism of silver release in static conditions and under PB perfusion, while a slight contribution of dynamic compression was observed in the biomimetic bioreactor. Silver release kinetics modelling provided estimation of the time allowed for peripheral blood mononuclear cells PBMC to be safely exposed to Ag/PVP nanocomposites under static and perfusion conditions (e.g. as wound dressings) of about 3 days. In wound dressing applications, that is a reasonable time for dressing replacement [24]. In another study, freshly prepared Ag/PVA–gum acacia (GA) hydrogel samples were used for the investigation [39], an increase of silver release with increasing in GA concentration was observed. The long time for the release of silver in the low concentrations of GA was explained as the result of a slow swelling nature of the matrix with low GA content [39]. A nano-Ag/PVA hydrogel device was synthesized by *in situ* gamma-irradiation with the aim of designing a hydrogel controlled release system of Ag<sup>+</sup> ions for antibacterial purposes with the advantages of the radiolytic method [13]. *In vitro* Ag<sup>+</sup> ion release study showed sustained and controlled release in a solution with a pH similar to that of the biological fluids. The obtained *in vitro* release profiles of silver were similar to the patterns observed with other drugs. Therefore, elements of the drug-delivery paradigm were applied for the study of Ag<sup>+</sup> ion release kinetics [13].

#### **2.5.4.SORPTION STUDIES**

The increase in swelling ability, as well as the decrease in the hydrogel elasticity, was the consequence of the AgNPs incorporation into the PVP hydrogel [23]. The findings were explained by the fact that AgNPs, when embedded inside the hydrogel network, expand the network, enabling faster SBF diffusion, and due to the retained solution, make the hydrogel slightly stiffer, which lowers the elastic behavior

of the polymer network, but only under dynamic conditions [23]. Sorption studies were performed on PVA and PVA/silica films [130]. It was found that the amount of water adsorbed in the PVA–silica film was slightly higher than that of the PVA film. However, the water uptake of PVA–silica films was not significantly changed by the increase in the sodium silicate concentration [130]. Sorption of different dyes by PVA/clay hydrogel as a function of immersion time at room temperature was investigated using UV spectrophotometric analysis [131]. It was found that the percentage value of dye sorption by the hydrogel differs from one dye to another. Sorption of a reactive dye was found to increase significantly after 3 hours and afterward tends to level off with increasing time of immersion up to next 2 hours. In the case of a basic dye, sorption by the hydrogel was shown to increase substantially by increasing the time of immersion up to 24 hours. Moreover, it was shown that the hydrogel that contained 50% clay had a higher tendency toward the two dyes under investigation than the one that contained 60% clay [131].

## **2.6. HYDROGEL MECHANICAL PROPERTIES**

Polymers resist stresses differently depending on their structure, molecular weight, and intermolecular forces [90]. They can be tested by stretching to determine tensile strength, compression to obtain compressive strength, bending to determine flexural strength, sudden stress to determine impact strength, and by dynamic loading to determine fatigue. With increasing molecular weight and consequently the level of intermolecular forces, polymers display the properties under an applied stress. A flexible polymer can perform better under stretching improved whereas a rigid polymer performs better under compression [90].

Attempts of tissue engineering using hydrogels have produced tissues with significantly poorer mechanical strength than the native tissues [132]. There are several reasons for this result including random alignment of fibres and high water content within the hydrogel. The ability to follow changes in mechanical properties of hydrogels over time is important in the quest to engineer functional tissues. Mechanical properties of hydrogels have been relatively frequently studied but only few methods can be used to measure mechanical properties of cell-seeded hydrogels. Presently, the most commonly used method to determine mechanical properties of hydrogels is tensile

testing or strip extensometry [132]. PVA hydrogels were mechanically characterized for self-healing purposes, depending on PVA concentration, separation time and number of freezing/thawing cycles [1]. It was suggested that these hydrogels have a good balance between amount of free hydroxyl groups of PVA on cut surfaces required for forming interchain H-bonds and sufficient chain mobility ensuring chain diffusion across the interface [1]. Mechanical properties of mixed hydrogels of PVA/PVP prepared by freezing/thawing method followed by gamma-irradiation at different doses (50,100 and 150 kGy) [133]. It was found that the tensile and compressive strengths reached a maximum at the dose of irradiation of 100 kGy and then decreased when dose of irradiation increased [133]. To enhance mechanical properties of hydrogels small amounts of nano-scale particles of metals or carbon nanoparticles CNs were added [7,12,134-180]. Silver/poly(vinyl alcohol)/cellulose/acetate/gelatin nanocomposites (Ag/PVA/CA/GEL) were prepared by gamma irradiation for wound dressing purposes [12] and their mechanical properties were studied. It was found that the tensile strength of the composite membranes was increased with the addition of AgNPs and irradiation doses [12]. Similarly, mechanical properties of Ag/PVA cryogel nanocomposites prepared by freezing/thawing followed by chemical reduction process were studied [7]. It was found that the tensile strength increased with PVA concentration in the hydrogel and with the number of freezing/thawing cycles. It was suggested that the size of crystallite increased with the amount of PVA and the number of freezing/thawing cycles, so that the network structure became more compact and strong due to the increase in intermolecular interactions which resulted in better mechanical properties [7].

Ag/PVP hydrogel (10 wt% PVP) nanocomposites were synthesized by gamma irradiation using Co-60 in the dosage range between 0.5 kGy h<sup>-1</sup> up to 25 kGy h<sup>-1</sup> followed by reduction reaction in the dark [25]. Mechanical properties of both PVP hydrogel and Ag/PVP nanocomposites were studied under bioreactor conditions and it was shown that both samples had highly elastic behavior and the values of Young's moduli for Ag/PVP nanocomposites were higher than that for pure PVP hydrogels [25]. Those results suggested that the presence of AgNPs affected the network structure inducing better mechanical properties more suitable for potential medical applications [25].

### **3. AIMS OF RESEARCH**

This dissertation focuses on the research studies of silver/poly(vinyl alcohol) (Ag/PVA) and silver/poly(vinyl alcohol)/graphene (Ag/PVA/Gr) nanocomposites, produced from pure poly(vinyl alcohol) hydrogels by doping them with silver nanoparticles (AgNPs) using electrochemical synthesis. The aim of this study was to investigate hydrogel morphological and structural properties as well as thermal stability, cytotoxicity, antibacterial activity, silver release and sorption characteristics in order to explore their potential for medical applications as wound dressings, soft tissue implants and drug carriers.

## 4. EXPERIMENTAL PART

### 4.1. MATERIALS

Chemicals used were all p.a. grade, PVA powder ('hot soluble', fully hydrolyzed  $M_w = 70000-100000$  Sigma, St. Louis, USA),  $\text{AgNO}_3$  (M. P. Hemija, Belgrade, Serbia),  $\text{KNO}_3$  (Centrohem, Stara Pazova, Serbia), graphene powder (Graphene Supermarket, USA). In all the experiments ultra-pure water from Milli-Q system (Millipore, Billerica, MA, USA) was used.

### 4.2. PREPARATION OF Ag/PVA AND Ag/PVA/Gr COMPOSITE HYDROGEL DISCS

PVA powder was first dissolved in hot  $\text{dH}_2\text{O}$  ( $90^\circ\text{C}$ ) in order to obtain PVA aqueous solution with the concentration of 10 wt. % PVA. To prepare a PVA/Gr colloid dispersion, graphene (Gr) was added to dissolved PVA under vigorous stirring to yield a final concentration of 10 wt. % PVA and 0.01 wt. % Gr. Subsequently, the dispersion was cooled down to room temperature and sonicated for 30 min to ensure uniformity.

After cooling down, the PVA solution and PVA/Gr colloid dispersion were poured into a Petri dish to the height of 5 mm and subjected to successive freezing and thawing in 5 cycles, where one cycle involved freezing for 16 hours at  $-18^\circ\text{C}$  and thawing for 8 h at  $4^\circ\text{C}$ . The obtained hydrogels were cut into small discs ( $d = 10$  mm). Swelling of PVA and PVA/Gr hydrogels was performed in dark by immersing the pre-weighed hydrogel discs in solutions of different  $\text{AgNO}_3$  concentration (0.25, 0.5, 1 and 3.9 mM  $\text{AgNO}_3$ ) and 0.1 M  $\text{KNO}_3$  at  $25^\circ\text{C}$ , during different periods of swelling time (between 24 h and 72 h) in order to determine the optimal time of swelling at room temperature. The pH of the swelling solution was around 6–7.

Swollen PVA and PVA/Gr hydrogels were used to produce Ag/PVA and Ag/PVA/Gr composites, respectively by electrochemical reduction of  $\text{Ag}^+$  at a constant voltage, by *in situ* synthesis of silver nanoparticles within the PVA and PVA/Gr matrix, respectively [181]. Briefly, specially designed electrochemical cell was employed, with two Pt plates horizontally placed face-to-face, as working and counter electrodes. The

hydrogel discs were placed in between two electrodes in the special glass holder. The polarity of the electrodes was changed after the half of the implementation time, in order to reduce the formation of a thin layer of metallic Ag at the surface of the hydrogel in contact with the working electrode and to ensure the synthesis of AgNPs within the hydrogel matrix. The following parameters were varied: applied voltage (50 V to 200 V) and implementation time (2 min to 4 min), by using MA 8903 Electro-Phoresis Power Supply (Iskra d.d., Ljubljana, Slovenia). The electrodes were cleaned by rinsing in HNO<sub>3</sub> (1:1) during 5 min and dH<sub>2</sub>O water after each experiment.

### **4.3. METHODS OF CHARACTERIZATION**

#### ***4.3.1. UV-VISIBLE SPECTROSCOPY***

UV-Vis spectra of PVA, PVA/Gr, Ag/PVA and Ag/PVA/Gr hydrogels were recorded by CARY 300 Bio (Varian, Palo Alto, CA, USA) spectrophotometer at the wavelength range of scanning between 200-800 nm. Hydrogel discs (1g) were dissolved in 10 ml of boiling DI water and left to cool down prior to UV-Vis measurements. Subsequently, 1 ml of solution was used for UV-Vis measurements. The obtained hydrogels undergo quick dissolution due to disruption of intermolecular hydrogen bonds at high temperatures. All tests were performed seven days after the electrochemical synthesis.

#### ***4.3.2. RAMAN SPECTROSCOPY***

HR-Raman analysis of Ag/PVA and Ag/PVA/Gr hydrogel discs was carried out using an inVia Raman spectrophotometer (Renishaw, Wotton-under-Edge, Gloucestershire, UK) equipped with a 514 nm argon laser. The intensity used was 10 % of total power (50 mW). The spectral range of the analysis was carried out between 3500 - 100 cm<sup>-1</sup>.

#### ***4.3.3. CYCLIC VOLTAMMETRY (CV)***

Cyclic voltammetry (CV) measurements of a Pt electrode in 0.25, 0.5, 1 and 3.9 mM AgNO<sub>3</sub> + 0.1 M KNO<sub>3</sub> solution, as well as of PVA, PVA/Gr, Ag/PVA and Ag/PVA/Gr hydrogels were performed using two platinum electrodes (9 mm × 10 mm)

as working and counter electrodes, and a saturated calomel electrode (SCE) as a reference electrode. CV measurements were acquired using Reference 600 potentiostat/galvanostat/ZRA (Gamry Instruments, Warminster, PA, USA) at a scan rate of  $50 \text{ mV s}^{-1}$ , in the potential region from  $-0.3 \text{ V}$  to  $1 \text{ V}$  vs. SCE, starting from the open circuit potential,  $E_{\text{ocp}}$ . In each experiment, cycling was continued until stabilized voltammograms were obtained (typically 4 cycles).

#### **4.3.4. FIELD EMISSION SCANNING ELECTRON MICROSCOPY (FE-SEM)**

Surface morphology of dried PVA, PVA/Gr, Ag/PVA and Ag/PVA/Gr hydrogels was analyzed by FE-SEM (LEO SUPRA 55, Carl Zeiss, Germany) operated at acceleration voltage of  $10 \text{ kV}$  and TESCAN MIRA 3 XMU.

#### **4.3.5. FOURIER TRANSFORM INFRARED SPECTROSCOPY (FT-IR)**

FT-IR analysis of dried PVA, PVA/Gr, Ag/PVA and Ag/PVA/Gr hydrogel discs was carried out using KBr pellets in a Perkin Elmer (Spectrum One system) spectrophotometer (PerkinElmer, Inc., Waltham, MA, USA). The scan was carried out in the range of  $450 \text{ cm}^{-1}$  to  $4000 \text{ cm}^{-1}$  with a spectral resolution of  $0.5 \text{ cm}^{-1}$ .

#### **4.3.6. X-RAY DIFFRACTION (XRD)**

The crystalline structure was investigated using a X-ray diffractometer (model Bruker AXS-D-8 Discover) with irradiation from  $K\alpha$  line of Cu ( $\lambda = 1.5406 \text{ \AA}$ ). The detector resolution in  $2\theta$  (diffraction angle) was between  $5^\circ$  and  $80^\circ$  at  $25^\circ\text{C}$  while the tube current and voltage maintained at  $300 \text{ mA}$  and  $40 \text{ kV}$ , respectively.

#### **4.3.7. THERMAL ANALYSIS**

Thermal stability of composite hydrogels was investigated using a TA instrument DSC-TGA SDT Q600 (TA Instruments, New Castle, DE, USA) from  $\sim 20^\circ\text{C}$  to  $1000^\circ\text{C}$  under  $\text{N}_2$  ( $50 \text{ ml/min}$ ), heating rate of  $20^\circ\text{C/min}$ .

### **4.3.8. CYTOTOXICITY**

#### **4.3.8.1. Preparation of peripheral blood mononuclear cells**

Peripheral blood mononuclear cells (PBMCs) were washed three times in separating solutions (Histopaque-1077, Sigma Aldrich, St. Louis, MO, USA). Finally, cell slurry was re-suspended in nutrient medium RPMI-1640 (Sigma Aldrich, St. Louis, MO, USA), pH 7.2, supplemented with 10% heat-inactivated for 30 min at 56°C fetal bovine serum (FBS), 3 mM L glutamine, 100 mg dm<sup>-3</sup> streptomycin, 0.1 IU dm<sup>-3</sup> penicillin and 25 mM HEPES). All chemicals acquired from Sigma Aldrich, St. Louis, MO, USA.

#### **4.3.8.2. Treatment of PBMC**

PBMCs were seeded in nutrient medium, in a 24-well plate in which either pure PVA, PVA/Gr hydrogel, Ag/PVA and Ag/PVA/Gr composite hydrogel discs were added. Ag/PVA and Ag/PVA/Gr composites were obtained by electrochemical reduction of PVA and PVA/Gr hydrogels preswollen in 0.25, 0.5, 1 and 3.9 mM AgNO<sub>3</sub> solution. All hydrogels were sterilized prior to experiments by UV irradiation for 30 minutes by placing them under UV-C lamp integrated in the laminar airflow hood. Pure PVA, PVA/Gr hydrogels, Ag/PVA and Ag/PVA/Gr composites in the form of cylinders (d = 2 mm, δ = 5 mm) were placed in the 24-well plate. In the second experimental series, effects of Ag/PVA and Ag/PVA/Gr composite hydrogels on PBMC stimulated for proliferation were studied. Experimental set-up was the same except for addition in this case of mitogen phytohemagglutinin (PHA) that stimulates the proliferation of PBMCs.

#### **4.3.8.3. Determination of target cell survival**

Survival of target cells was determined using MTT test, in order to assess the activity of living cells by their mitochondrial dehydrogenase activity [182]. Standard MTT assay was employed based on reduction of the yellow salt - tetrazolium dye MTT (4,5 dimethyl thiazol - 2-yl) - 2,5 - diphenyl tetrazolium bromide) to its soluble

formazan (purple colored crystals) by mitochondrial dehydrogenase activity of living cells. The absorbance was measured using 570 nm using Multiskan EX Thermo Labsystems (Thermoscientific, Waltham, MA, USA). Since the number of live cells is directly proportional to the absorbance of viable, metabolically active MTT treated cells, for calculation of the cell survival (S), absorbance of newly formed formazan was used:

$$S(\%) = \frac{A_u}{A_c} \times 100 \quad (4.1)$$

$A_u$  is the absorbance of cells grown in the presence of the samples and  $A_c$  is the absorbance of control cells. Cytotoxicity was rated based on the cell survival relative to controls as following: non-cytotoxic (> 90% cell survival), slightly cytotoxic (60–90% cell survival), moderately cytotoxic (30–59% cell survival), and severely cytotoxic ( $\leq$  30% cell survival) [183].

#### **4.3.9. ANTIBACTERIAL ACTIVITY**

Antibacterial activity was determined for Ag/PVA and Ag/PVA/Gr hydrogel discs pre-swollen in the AgNO<sub>3</sub> solution of the lowest concentration of 0.25 mM. Prepared hydrogels samples (cut into  $\sim 1 \text{ mm}^3$  cubes) were sterilized by exposing to UV-C lamp integrated in the laminar air flow hood at a distance of 60 cm between hydrogels and the lamp for a total time of 30 minutes. Antibacterial activity was tested against bacteria strain *Staphylococcus aureus* TL (culture collection–FTM, University of Belgrade, Serbia) and *Escherichia coli* (ATCC 25922) in suspensions using the spread-plate method. The study was performed in modified phosphate-buffered saline (PBS), termed phosphate buffer (PB); salt composition of 0.39 mM KH<sub>2</sub>PO<sub>4</sub> and 0.61 mM K<sub>2</sub>HPO<sub>4</sub>, and was free of Cl<sup>-</sup> ions (in order to avoid eventual precipitation of AgCl). Minimal supply of nutrients is advised in protocols when antibacterial properties of biomaterials are assessed. The number of bacteria in the samples was monitored at the beginning of the experiment and after incubation for 1, 3, and 24 h. After incubation for 24 h at 37 °C, the number of colonies was counted using a colony counter and

expressed as CFU/mL to obtain the number of viable *Staphylococcus aureus* and *Escherichia coli*.

#### **4.3.10. SILVER RELEASE INVESTIGATION**

Silver release from Ag/PVA and Ag/PVA/Gr composite hydrogel discs preswollen in the AgNO<sub>3</sub> solution of the lowest concentration of 0.25 mM was investigated in phosphate buffer (PB) at 37 °C ± 1 °C. PB (pH 7.42) consisted of 0.39 mM KH<sub>2</sub>PO<sub>4</sub> and 0.61 mM K<sub>2</sub>HPO<sub>4</sub>, and was free of Cl<sup>-</sup> ions (in order to avoid eventual precipitation of AgCl). During first 7 days, PB was changed daily and then once a week, up to 28 days. Silver contents were determined initially, at different time points and after the completion of the experiments. The amount of silver in solutions was determined using atomic absorption spectrometer (PYU UNICAM SP9, Philips, Netherlands). Total contents of silver within the composite hydrogels were determined upon treatment in HNO<sub>3</sub> (1:1, v/v) inducing oxidation of all AgNPs into Ag<sup>+</sup>.

#### **4.3.11. SORPTION CHARACTERISTICS**

Dry Ag/PVA and Ag/PVA/Gr hydrogel discs, xerogels ( $d = 4.73 \pm 0.27$  mm,  $\delta = 1.95 \pm 0.05$  mm) were obtained by drying the hydrogel discs ( $d = 10$  mm,  $\delta = 5$  mm) to constant weight. The xerogels were then immersed in Kokubo's solution at pH = 7.2, 37 ± 1 °C, until attainment of equilibrium during 28 days. Kokubo's solution was prepared by dissolving reagent-grade salts in deionized water up to Na<sup>+</sup> 142.0 mM, K<sup>+</sup> 5.0 mM, Mg<sup>2+</sup> 1.5 mM, Ca<sup>2+</sup> 2.5 mM, HCO<sub>3</sub><sup>-</sup> 4.2 mM, Cl<sup>-</sup> 147.8 mM, HPO<sub>4</sub><sup>2-</sup> 1.0 mM, and SO<sub>4</sub><sup>2-</sup> 0.5 mM. The final solution was buffered in Tris and pH adjusted to 7.40 with 1 M hydrochloric acid. The sorption characteristics were determined by periodical gravimetric measurements using an analytical balance.

## **5. RESULTS AND DISCUSSION**

### **5.1. ELECTROCHEMICAL SYNTHESIS OF SILVER NANOPARTICLES INSIDE PVA AND PVA/Gr HYDROGELS**

An innovative method was developed [181,184,185] for the synthesis of AgNPs inside hydrogel matrices based on the electrochemical reduction of  $\text{Ag}^+$  ions. To obtain AgNPs within PVA and PVA/Gr hydrogel discs swollen in 3.9 mM  $\text{AgNO}_3$  solution. Fig.5.1a represents the two-electrode cell consisting of a working electrode and counter electrode made of Pt, with hydrogel discs between, previously swollen in  $\text{AgNO}_3$  solution situated in a specially designed glass holder. The optimal time of swelling was 48 h, as evident from the complete saturation of hydrogel discs with  $\text{AgNO}_3$  solution and appearance of dark brown color on Ag/PVA hydrogel discs after electrochemical synthesis (Fig. 5.1b). The synthesis was performed at the constant voltage of 90 V and implementation time of 4 min. The polarity between the electrodes was periodically changed in order to reduce the electrodeposition of metallic Ag at the cathode surface. When the polarity of the electrode is reversed, the deposited bulk Ag layer is again dissolved and returned into the electrolyte in the form of  $\text{Ag}^+$  ions. For the implementation time exceeding 4 min, significant growth of Ag layer electrodeposited on the cathode was observed. The photographs of synthesized Ag/PVA and Ag/PVA/Gr discs are depicted in Fig. 5.1b.

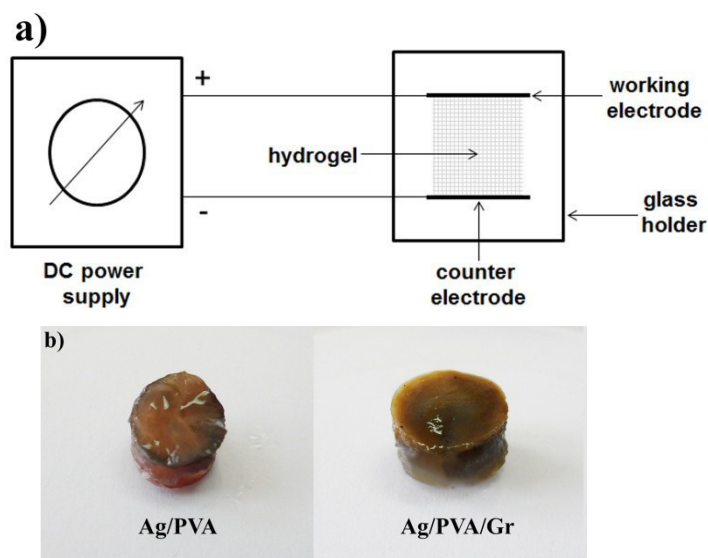


Figure 5. 1. (a) Scheme of the electrochemical cell for AgNP synthesis inside the polymer hydrogel and (b) photographs of synthesized Ag/PVA and Ag/PVA/Gr hydrogels

In general, formation of metal nanoparticles by electrolysis starts with the reduction of their ions at the cathode. Stabilization agents are being introduced to speed up the formation of AgNPs, reduce the metal layer deposition on the cathode surface and limit the agglomeration of nanoparticles in the solution [184]. The reduction of  $\text{Ag}^+$  ions and water occurs at the cathode and is represented by the following equations, respectively:



While the water oxidation occurs at the anode:



The competition between metal nanoparticles formation and the metal layer deposition at the cathode surface can be explained as follows. Silver layer electrodeposition at the cathode surface occurs simultaneously to the hydrogen evolution, contributing to a decrease in the effective surface area for silver nanoparticles

production. Linear polymeric PVA chains promote stabilization of particles by adsorption of polymeric chains on their surface via bonding with the exposed hydroxyl groups in PVA chains. Lone pairs on the oxygen atoms in PVA molecule can occupy two sp orbitals of  $\text{Ag}^+$  to form a metal complex, so the first step is the formation of the  $\text{Ag}_m^{m+}$ -PVA complex by coordinative bonding between  $\text{Ag}^+$  ions and PVA molecules, where  $m$  is the number of  $\text{Ag}^+$  bounded with PVA molecule. The second step is the electrochemical reduction of  $\text{Ag}_m^{m+}$ -PVA complex at the cathode surface, followed by formation of  $\text{Ag}_m^0$ -PVA adatoms stabilized with PVA chains. The presence of PVA ensures that the  $\text{Ag}_m^{m+}$ -PVA complex is being reduced rather than individual  $\text{Ag}^+$  ions since oxygen atoms in PVA chains increase the electron density of sp orbital of the silver ion in respect to the water molecules in hydrated  $\text{Ag}^+$  ions. As a consequence, silver ions in  $\text{Ag}_m^{m+}$ -PVA complex attract the electrons from the cathode easier than individual hydrated silver ions. This means that the reduction of  $\text{Ag}_m^{m+}$ -PVA complex is favored comparing the reduction of individual  $\text{Ag}^+$  ions. Consequently, the deposition of metallic silver layer at the cathode surface is lowered. In the third step the silver nanoparticles nucleation occurs, while the final sstep involves AgNPs growth with particle aggregation being limited by the presence of PVA chains. Similar mechanism was proposed [116] for silver nanoparticles production in the poly(vinyl pyrrolidone) (PVP) solution. Previous research of electrochemical synthesis of silver nanoparticles in the hydrogel matrices of alginate [21, 22], PVP [23, 24] and PVA [184] confirmed the presence of AgNPs inside the hydrogel using UV-visible spectroscopy and field-emission scanning electron microscopy. Moreover, the antibacterial activity of AgNPs was confirmed by both the agar-diffusion test and test in suspension [21, 184], while the kinetics of silver release was monitored in simulated physiological conditions (phosphate buffer, PB) [22, 23, 24, 184].

## 5.2. UV-VIS ANALYSIS

UV-Vis spectroscopy was employed to identify and monitor formation of AgNPs, which exhibit optical properties that are highly sensitive to nanoparticle size, shape, concentration, and agglomeration state. According to Mie theory, metal nanoparticles exhibit characteristic peaks in their absorption spectra due to localized surface plasmon resonance (LSPR) effect [102,186]. It is well known that absorption

spectra of small sphere-like AgNPs exhibit a peak at wavelengths of 405-420 nm [21,118]. The absorption spectra of PVA, PVA/Gr, Ag/PVA, and Ag/PVA/Gr hydrogels are shown in Figure 5.2.

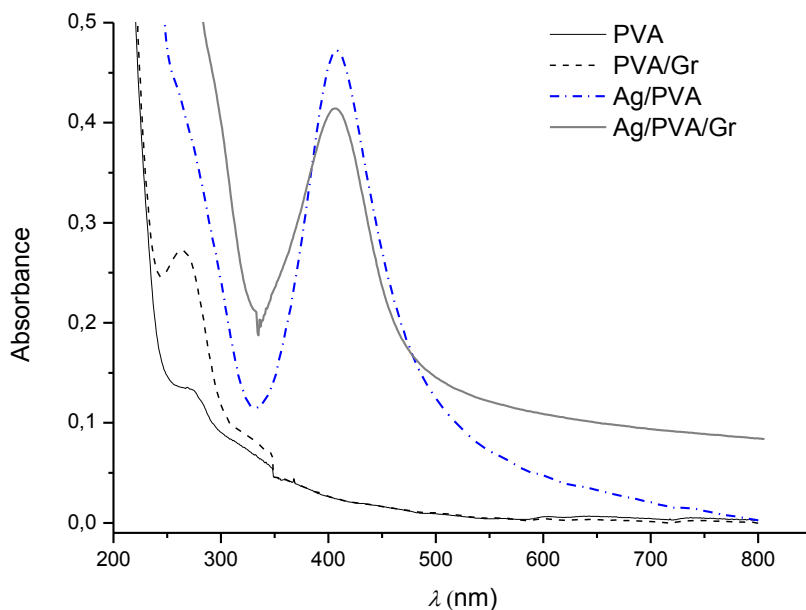


*Figure 5.2. Absorption spectra of PVA, PVA/Gr, Ag/PVA, and Ag/PVA/Gr hydrogels (swelling solution: 3.9 mM AgNO<sub>3</sub> + 0.1 M KNO<sub>3</sub>)*

It can be seen that both Ag/PVA and Ag/PVA/Gr exhibited absorption spectra with bands peaking around 400 nm, which confirmed the formation of AgNPs. Furthermore, the absence of any absorption bands in the longer wavelength region suggests restricted aggregation of AgNPs in the proposed composite systems. Since the concentration of AgNPs is linearly dependent to the absorbance intensity [27], it can be concluded that the amount of AgNPs decreased with the addition of graphene slightly. In addition, the slight shift of the absorbance maximum toward lower wavelength values was observed in the presence of graphene for Ag/PVA/Gr (405 nm) compared to that at 408 nm for Ag/PVA. This indicates somewhat smaller dimensions of AgNPs in the Ag/PVA/Gr hydrogel, suggesting that graphene sheets in these hydrogels hindered aggregation and further growth or agglomeration of AgNPs.

### 5.3. RAMAN SPECTROSCOPY

The Ag/PVA/Gr hydrogels were analyzed using Raman spectroscopy in order to verify exfoliation of graphene sheets into the polymer matrix. The presence of graphene was verified by appearance of two broad, distinct bands at  $1372\text{ cm}^{-1}$  and  $1581\text{ cm}^{-1}$  (Fig. 5.3). The Raman D band at  $1372\text{ cm}^{-1}$  is ascribed to amorphous or disordered structures and defects in graphene layers, while the G band at  $1581\text{ cm}^{-1}$  originates from the in-plane vibration of  $\text{sp}^2$  carbon atoms. Moreover, the G band intensity is directly proportional to the number of graphene layers [187]. The level of disorder and defects can be calculated from the intensity ratio of the D band and G band ( $I_D/I_G$ ), and the average size of  $\text{sp}^2$  domains is also inversely proportional to this ratio [187]. The value of this ratio was calculated to be 0.85, which is close to the value found in literature and indicates significant amount of defects [62].

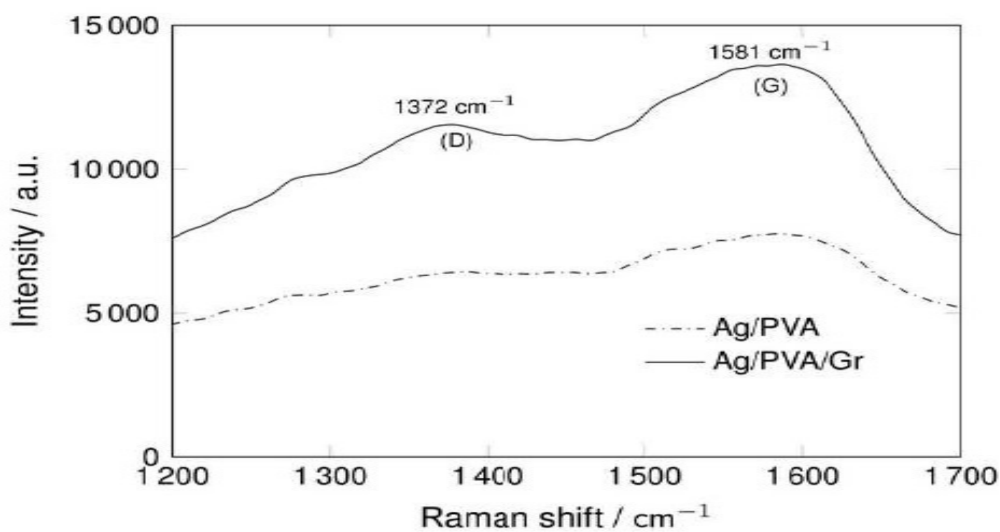


Figure 5.3. Raman spectra of Ag/PVA and Ag/PVA/Gr hydrogels (swelling solution:  $3.9\text{ mM AgNO}_3 + 0.1\text{ M KNO}_3$ )

## 5.4. CYCLIC VOLTAMMETRY

Incorporation of AgNPs into PVA and PVA/Gr polymer matrices was further examined by CV measurements. The voltammetry tests were performed on a polycrystalline Pt working electrode in the potential domain from -0.3 V to 1 V vs. SCE in order to gain better insight into the oxidation/reduction processes occurring at the Pt surface.

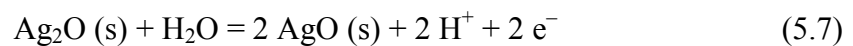
The base curves obtained for pure PVA and PVA/Gr hydrogels in the absence of AgNPs (Fig. 5.4a) exhibit hindered hydrogen adsorption/desorption peaks, indicating that PVA and PVA/Gr are probably adsorbed on the electrode surface. In the case of the pure PVA hydrogel, an intense oxidation process in the 750-1000 mV vs. SCE potential region and its cathodic counterpart at about 450 mV vs. SCE, exhibited as a sharp increase in current density in this potential region, most probably represents the processes related to the oxidation/reduction of the PVA macromolecules at the hydrogel/electrode interface. In contrast, the PVA/Gr hydrogel exhibited a broad anodic peak at about 100 mV vs. SCE, followed by a gradual increase in current density starting at around 300 mV, manifesting a wide anodic shoulder. The only cathodic feature is present at about 100 mV vs. SCE. All these peaks could be ascribed to the redox processes involving the PVA, but also to possible oxidation and reduction of graphene.

To gain insight into the redox processes of silver ions at the Pt electrode, the CV curves were also recorded for a Pt electrode in 3.9 mM AgNO<sub>3</sub> + 0.1 M KNO<sub>3</sub> solution, as shown in Figure 5.4b. The pH of this solution was measured to be around 6.5–7. In the cathodic region, the most prominent peak is around 225–235 mV, corresponding to the reduction of Ag<sup>+</sup> ions and deposition of a bulk silver layer at the surface of the Pt electrode. The anodic peaks between 350 and 650 mV involve the oxidation of the Ag layer deposited on Pt in the cathodic half cycle to Ag<sup>+</sup>, as well as further oxidation of the bulk Ag to Ag<sub>2</sub>O. In the initial cycles (Fig. 5.4b, cycles 1 and 2), there was only one peak at 465 mV, which it was assumed corresponded only to the oxidation of Ag to Ag<sup>+</sup> ions and the dissolution of the bulk silver layer on the Pt surface. In the stationary voltammograms (Fig. 5.4b, cycles 3-5), there was evident doubling of this peak into two peaks at 454 mV and 544 mV. It was assumed that the oxidation of Ag to Ag<sup>+</sup> ions is

represented by the first peak at more negative potentials, whereas the second peak indicates the oxidation of the Ag deposit to the Ag<sub>2</sub>O layer. The third peak at around 850 mV could involve further oxidation of bulk Ag or Ag<sub>2</sub>O to AgO, i.e. the oxidation of Ag(0) and Ag(I) states to Ag(II). In order to check the possibility of these reactions, the theoretical potentials for their occurrence were calculated using the Nernst equation (eq. (5.4)):

$$E = E_r^\ominus - \frac{RT}{zF} \ln \frac{C_{Red}}{C_{Ox}} \quad (5.4)$$

Where  $E$  is the electrode potential,  $E_r^\ominus$  is the standard reversible potential for the given reaction,  $T$  is the temperature,  $R$  and  $F$  are universal gas and Faraday constants, respectively,  $z$  is the number of exchanged electrons and  $C_{Red}$  and  $C_{Ox}$  are concentrations of reductive and oxidative species, respectively. The three anodic processes represented by three peaks in Fig. 5.4b were illustrated by the following reactions. The first anodic peak, at the most negative potential, was ascribed to reaction (5.5), i.e. the oxidation of a bulk silver layer at the Pt electrode surface, which was deposited during the cathodic sweep, bearing in mind that the cycling was started from the cathodic potential region. The electrode potential for this reaction, calculated using eq. (5.4), for a 3.9 mM AgNO<sub>3</sub> solution, is 420 mV vs. SCE. The second anodic process could involve the oxidation of the same bulk Ag layer on the Pt surface to Ag(I) species, i.e. the second peak corresponds to the formation of Ag<sub>2</sub>O oxide, depicted by the reaction (5.6). The potential for this reaction, in a solution of pH ~ 6.5 was calculated to be 545 mV vs. SCE. Finally, the third anodic peak could correspond to further oxidation of Ag(I) to Ag(II) species, i.e. to the formation of AgO oxide, following the reaction (5.7). The electrode potential for reaction (4), calculated using Nernst equation for solution of pH ~ 6.5 was around 780 mV vs. SCE.



The calculated values of the potentials for given reactions are in good agreement with experimentally obtained potentials, with some variations that could be ascribed to

the probable changes in local pH values in the electrolyte layer in contact with the electrode, as well as the influence of mass transfer on the mentioned reactions.

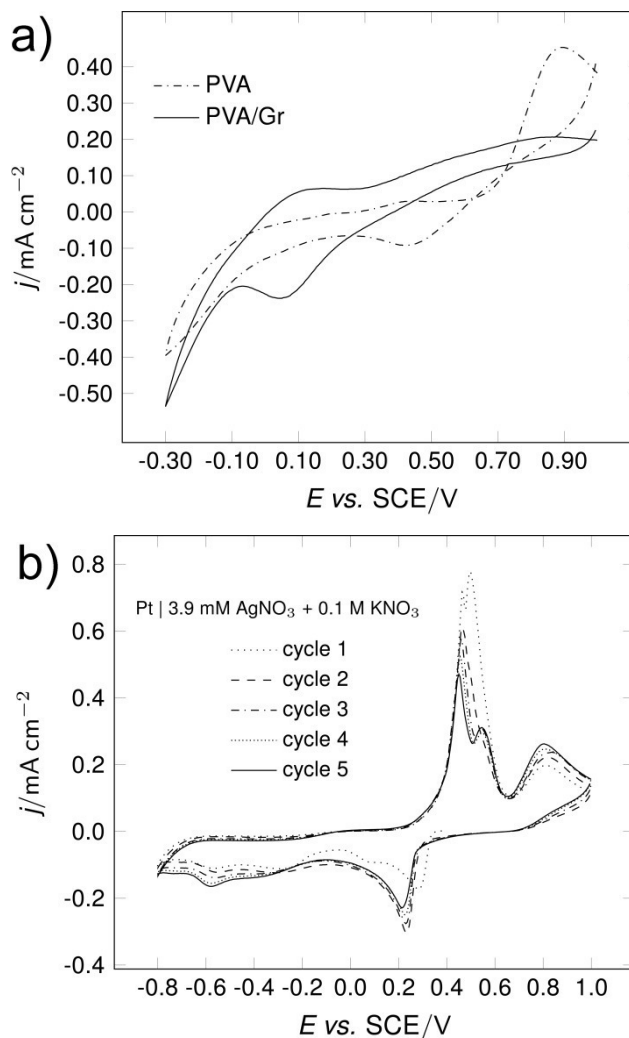


Figure 5.4. Cyclic voltammograms of (a) PVA and PVA/Gr hydrogels and (b) Pt electrode in 3.9 mM AgNO<sub>3</sub> + 0.1 M KNO<sub>3</sub> solution; scan rate 50 mV·s<sup>-1</sup>

Figure 5.5 depicts the cyclic voltammograms of Ag/PVA and Ag/PVA/Gr hydrogels at the Pt electrode, synthesized using 1.0 mM AgNO<sub>3</sub> + 0.1 M KNO<sub>3</sub> swelling solution. After 24 h (Fig. 5.5a), cyclic voltammograms of both Ag/PVA and Ag/PVA/Gr samples exhibited a cathodic peak at 189 mV vs. SCE for Ag/PVA and at 235 mV vs. SCE for Ag/PVA/Gr, which could be ascribed to the reduction of Ag<sup>+</sup> ions leftover in the swollen hydrogel after the synthesis and to the formation of Ag layer at the surface of Pt electrode. In the anodic region, a sharp anodic peak located at 374 mV

vs. SCE (for Ag/PVA) and at 439 mV vs. SCE (for Ag/PVA/Gr) could be ascribed to the oxidation of this newly formed layer, i.e. to the dissolution of Ag layer on the surface of Pt and formation of  $\text{Ag}^+$  ions. The difference of the potential for these peaks could be due to the uncompensated ohmic resistance of the experimental setup, causing discrepancies in the potential values. Other peaks, such as anodic peak at potentials higher than 700 mV and cathodic peak at  $\sim 400$  mV probably correspond to the redox processes of the PVA and PVA/Gr hydrogels.

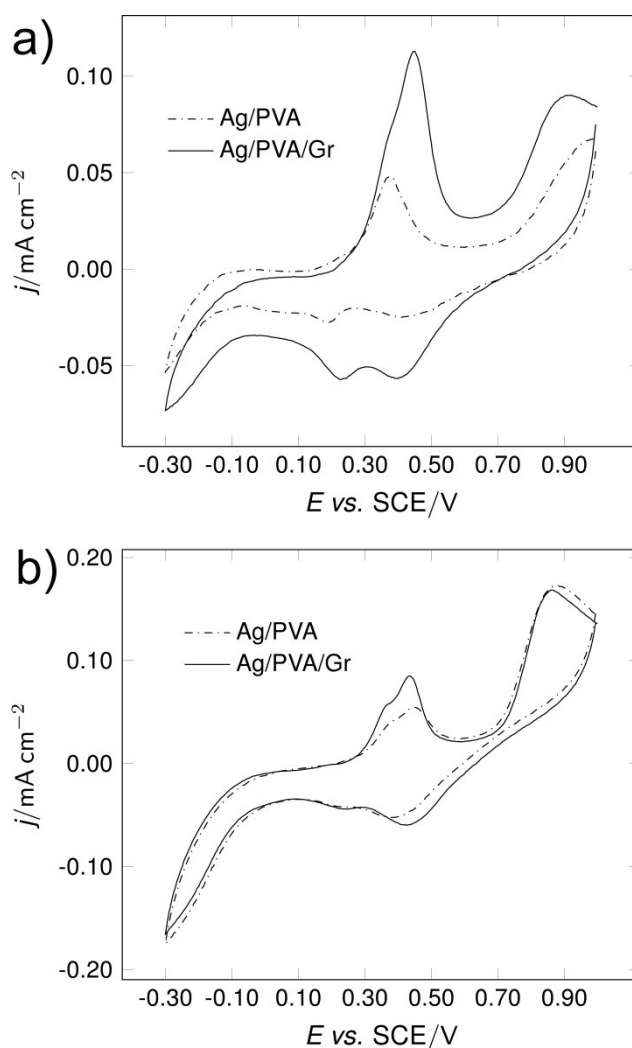
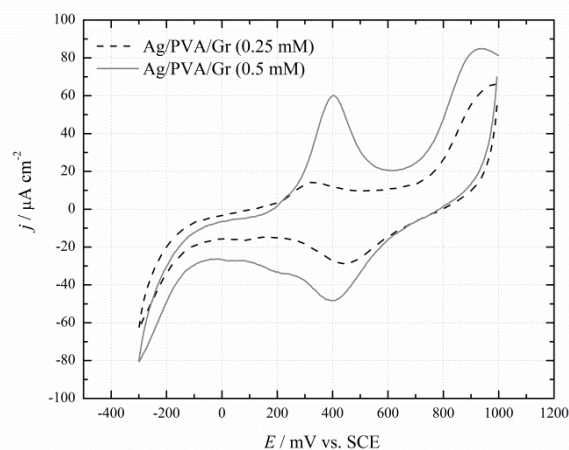


Figure 5.5. Stationary cyclic voltammograms of Ag/PVA and Ag/PVA/Gr hydrogels at (a) 24 h and (b) 5 days after the electrochemical synthesis (swelling solution: 1.0 mM  $\text{AgNO}_3$  + 0.1 M  $\text{KNO}_3$ ); scan rate  $50 \text{ mV}\cdot\text{s}^{-1}$

After five days (Fig. 5.5b), there is a cathodic peak of  $\text{Ag}^+$  reduction at  $\sim 200$  mV for both Ag/PVA and Ag/PVA/Gr hydrogels, and the corresponding anodic peak appears at 444 mV vs. SCE for Ag/PVA hydrogel, and at 425 mV in the case of Ag/PVA/Gr. In the case of the Ag/PVA/Gr sample, two close anodic peaks appeared, probably due to the split into different silver oxidation processes. As discussed above, these processes could involve the oxidation of the bulk Ag layer on the surface of Pt electrode (formed by the reduction of  $\text{Ag}^+$  ions during the cathodic sweep) to the  $\text{Ag}^+$  and  $\text{Ag}_2\text{O}$  species, as illustrated by equations (5.5) and (5.6), respectively. The difference in anodic current densities of these peaks for Ag/PVA and Ag/PVA/Gr hydrogels was less pronounced after five days than it was after 24 h.

Figure 5.6 represents stationary voltammograms (cycle 3) of Ag/PVA/Gr hydrogels obtained from  $\text{AgNO}_3$  swelling solutions with two concentrations of  $\text{Ag}^+$  (0.25 mM and 0.5 mM). The cathodic sweep contains a broad peak at 430 mV for Ag/PVA/Gr from 0.25 mM  $\text{AgNO}_3$ , and at 395 mV for Ag/PVA/Gr from 0.5 mM  $\text{AgNO}_3$ . Anodic process occurs at potentials more positive than 800 mV, seen as a shoulder with high current densities on the CVs. As mentioned previously, these peaks probably correspond to processes related to the reduction and oxidation of both PVA and PVA/Gr hydrogels. A cathodic shoulder at  $\sim 100$ -200 mV corresponds to the reduction of  $\text{Ag}^+$  and deposition of bulk Ag layer at the cathode surface. In the anodic sweep, both CVs contain one prominent peak, at 345 mV for Ag/PVA/Gr swollen in 0.25 mM  $\text{AgNO}_3$ , and at 404 mV for Ag/PVA/Gr swollen in 0.5 mM, probably involving the oxidation of Ag layer on the Pt surface, deposited during the cathodic sweep.



*Figure 5.6. Stationary cyclic voltammograms (cycle 3) of Ag/PVA/Gr hydrogels synthesized from 0.25 mM and 0.5 mM AgNO<sub>3</sub> swelling solutions; scan rate 50 mV·s<sup>-1</sup>*

Figure 5.7 depicts voltammetric sweeps of Ag/PVA/Gr hydrogels obtained from 0.25 and 0.5 mM AgNO<sub>3</sub> swelling solutions. Voltammograms of both hydrogels quickly reach steady state after several cycles. In the cathodic region for both hydrogels, cycle 1 contains peaks at  $\sim 100$  mV, which probably involve reduction of residual Ag<sup>+</sup> ions, remaining unreduced in the hydrogel after the synthesis and to the deposition of Ag layer on the surface of Pt. These peaks almost disappear from cycles 2-5, hinting that almost all Ag<sup>+</sup> ions are reduced in the first cycle of the CV sweep. The cathodic peak at  $\sim 400$  mV, as mentioned above, probably involves some reduction reaction of PVA macromolecules. During cycles 1–5, a continuous decrease of the anodic current density can be observed for the peak of Ag layer oxidation at 320–340 mV for Ag/PVA/Gr obtained in 0.25 mM AgNO<sub>3</sub>, and at 370–390 mV for Ag/PVA/Gr obtained in 0.25 mM AgNO<sub>3</sub>, indicating that there is lesser amount of the species being oxidized at the surface of Pt electrode.

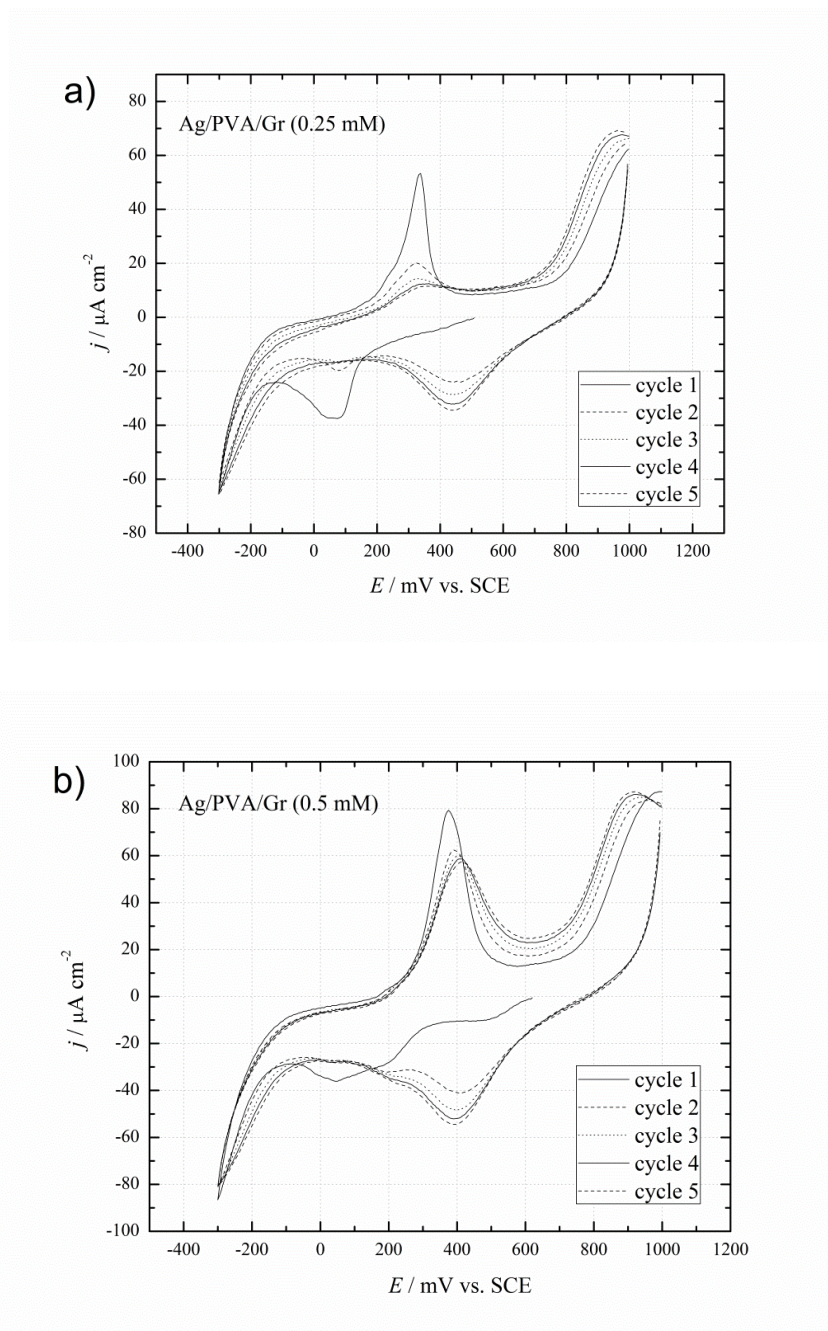
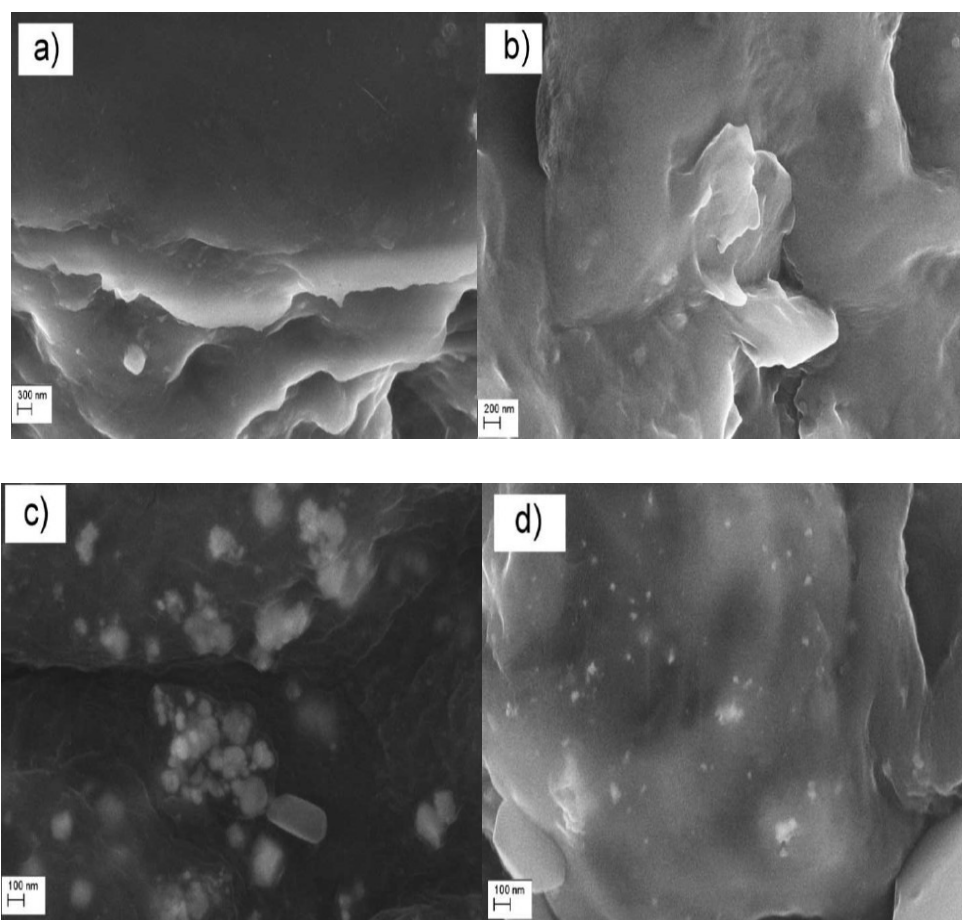


Figure 5.7. Five cycles of cyclic voltammograms of Ag/PVA/Gr hydrogels synthesized from (a) 0.25 mM and (b) 0.5 mM AgNO<sub>3</sub> swelling solutions; scan rate 50 mV·s<sup>-1</sup>

## 5.5. FIELD EMISSION SCANNING ELECTRON MICROSCOPY (FE-SEM)

The FE-SEM micrographs of PVA, PVA/Gr, Ag/PVA, and Ag/PVA/Gr composite hydrogels are shown in Figure 5.8. The separate graphene sheets are not visible in the micrographs of the hydrogels due to the encapsulation of nanosheets by the PVA polymer matrix.



*Figure 5.8. FE-SEM microphotographs of (a) PVA(scale bar=300  $\mu\text{m}$ ), (b) PVA/Gr(scale bar=200  $\mu\text{m}$ ), (c) Ag/PVA, and (d) Ag/PVA/Gr hydrogels (swelling solution: 3.9 mM  $\text{AgNO}_3$  + 0.1 M  $\text{KNO}_3$ )(scale bar=100  $\mu\text{m}$ )*

AgNPs adopt spherical morphologies in appearance at nanoscale levels. The average size of the primary AgNPs was found to be around 37 nm in the Ag/PVA hydrogel (Figure 5.8c) and around 16 nm in the Ag/PVA/Gr hydrogel (Figure 5.8d).

Thus, from FE-SEM micrographs it can be concluded that the size of AgNPs in the Ag/PVA/Gr nanocomposite was reduced compared to that in the Ag/PVA nanocomposite. Hydrogen bonds established between hydrophilic PVA chains and graphene nanosheets regulate the size of the surrounding AgNPs and prevent their further growth and aggregation. This is in agreement with the UV-Vis spectroscopy results, in which the absorption peak positions indicated slightly smaller dimensions for the AgNPs in the Ag/PVA/Gr hydrogels. It was further attempted to examine the types and natures of bonds and interactions in hydrogels and also to identify the functional groups involved in the synthesis of AgNPs using FT-IR spectroscopy.

## 5.6. FOURIER TRANSFORM INFRARED SPECTROSCOPY (FT-IR)

FT-IR spectra and wave numbers data of the PVA hydrogel as shown in Figure 5.9 and Table 5.1, exhibited several characteristic absorption bands, including those at  $3275\text{ cm}^{-1}$  (O–H stretching vibration),  $2949\text{ cm}^{-1}$  (aliphatic C–H stretching and asymmetric stretching of  $-\text{CH}_2$ ) carbonyl (C=O) stretching at  $1642\text{ cm}^{-1}$ , and C–H in-plane bending at  $1428\text{ cm}^{-1}$  [48, 188-190]. Of these, especially interesting is the band at  $\sim 3200\text{-}3300\text{ cm}^{-1}$ , corresponding to the valence vibrations of hydroxyl groups; these valence vibrations are sensitive to interactions with other functional groups, particularly to hydrogen bonding [191]. With the addition of AgNPs into the system, i.e., in the FT-IR spectrum of the Ag/PVA hydrogels, this particular band exhibited a slight red shift and moved from  $3275\text{ cm}^{-1}$  (PVA) to  $3313\text{ cm}^{-1}$  (Ag/PVA). This is evidence of coordination bonding and complex formation between PVA macromolecules and AgNPs during and after the electrochemical synthesis. Moreover, in the FT-IR spectrum of the Ag/PVA/Gr hydrogel, this band shifted again to a lower wave number ( $3299\text{ cm}^{-1}$ ), pointing to the interactions of graphene with PVA and its influence on the weakening of  $\text{Ag}_m\text{-PVA}$  complex bonds. This results in easier release and faster leaching of silver from these hydrogels, as observed also from voltammetric (section 5.3) and silver release investigations (section 5.10). The C-O stretching vibration appeared at  $1095$ ,  $1097$ , and  $1097\text{ cm}^{-1}$  for PVA, Ag/PVA, and Ag/PVA/Gr, respectively. The appearance of this band is often linked to the semi-crystalline structure of PVA [8,190].

Coordination interactions between Ag nanoparticles and hydroxyl groups on the chain of PVA molecules could have caused the red shift of this band. However, the band changed neither position nor shape in the Ag/PVA/Gr hydrogels, leading to the conclusion that silver alone had an impact on the crystallinity of PVA, and graphene did not have any effect.

*Table 5.1. Wave numbers of main characteristic FT-IR bands and corresponding assignments for PVA, Ag/PVA and Ag/PVA/Gr hydrogel discs*

Wave numbers (cm <sup>-1</sup> )			Assignments
PVA	Ag/PVA	Ag/PVA/Gr	
3275	3307	3299	-OH stretching vibration
2949	2950	2951	Asymmetric CH <sub>2</sub> stretching and aliphatic C-H stretching vibrations
1642	1639	1640	Asymmetric and symmetric stretching vibration of –COO
1428	1432	1428	Weak –OH band vibration
1334	-	-	-OH in plane coupling with C-H wagging
1144	-	-	C-C stretching vibration
1095	1097	1097	C-O stretching vibration of secondary alcohols
662	678	665	C-H rocking vibration

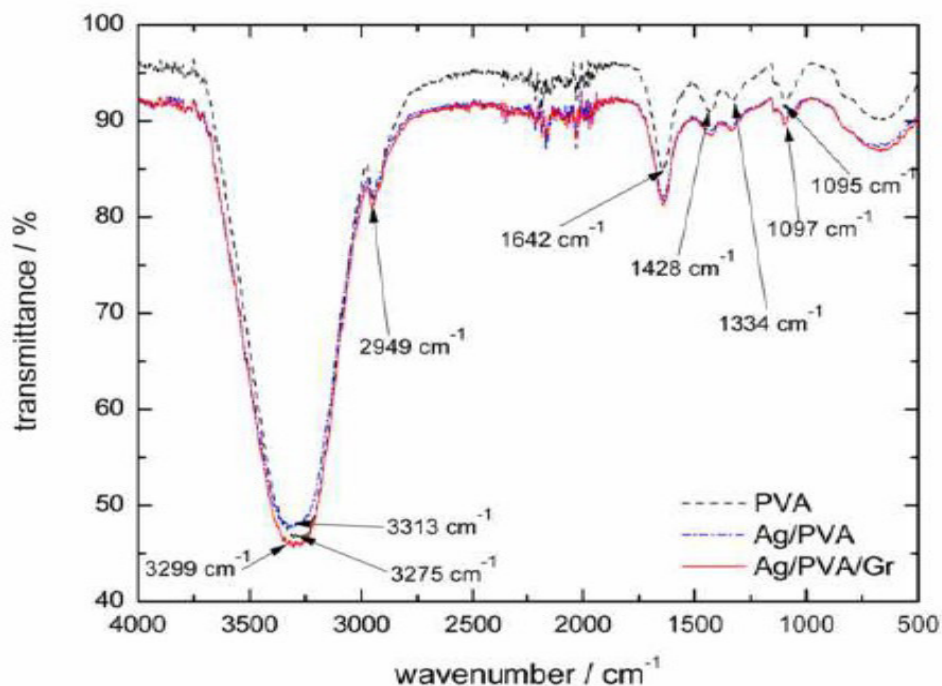


Figure 5.9. FT-IR spectra of PVA, Ag/PVA, and Ag/PVA/Gr hydrogels (swelling solution: 3.9 mM AgNO<sub>3</sub> + 0.1 M KNO<sub>3</sub>)

## 5.7. X-RAY DIFFRACTION (XRD)

Figure 5.10 shows the XRD patterns of Ag/PVA and Ag/PVA/Gr hydrogels. Diffraction maxima at  $2\theta = 19.39^\circ$  (for Ag/PVA) and  $19.74^\circ$  (for Ag/PVA/Gr), are related to the characteristic peak of (002) lattice plane of PVA, demonstrating the semi-crystalline structure of PVA [9,191]. Diffraction peaks for Ag/PVA observed at  $2\theta$  of  $38.36^\circ$  and  $44.11^\circ$  and those of the Ag/PVA/Gr composite hydrogels at  $2\theta$  of  $38.50^\circ$ ,  $44.59^\circ$ ,  $64.59^\circ$ , and  $77.50^\circ$  correspond to Bragg's reflections from the crystal planes (111), (200), (220), and (311), respectively, which are characteristics of the face centered cubic crystal structure of AgNPs, in good agreement with previously reported data [192]. A weak broad peak near  $22.84^\circ$  represents graphene in the Ag/PVA/Gr composite. The interspacing (d-spacing) value of the (002) lattice plane of PVA and

Ag/PVA hydrogels was calculated to be 0.457 nm, while the obtained value changed slightly with the introduction of graphene sheets (0.449 nm for Ag/PVA/Gr nanocomposite), indicating the additional interactions established between the PVA molecules and graphene sheets and the AgNPs incorporated in the Ag/PVA/Gr nanocomposite. It can be considered that the cross-section of graphene produced a weak interface with the (002) plane of PVA due to the lattice mismatch; as a consequence, the distance between graphene sheets increased from 0.340 nm in pure multi-layered graphene to 0.449 nm in the Ag/PVA/Gr nanocomposite, indicating strong hydrogen bonding between the hydroxyl groups present in PVA and the oxygen-containing groups in graphene. This supports the hypothesis that graphene sheets, incorporated between the polymer chains, prevent aggregation and growth of AgNPs in hydrogels, as observed by FE-SEM and FT-IR .

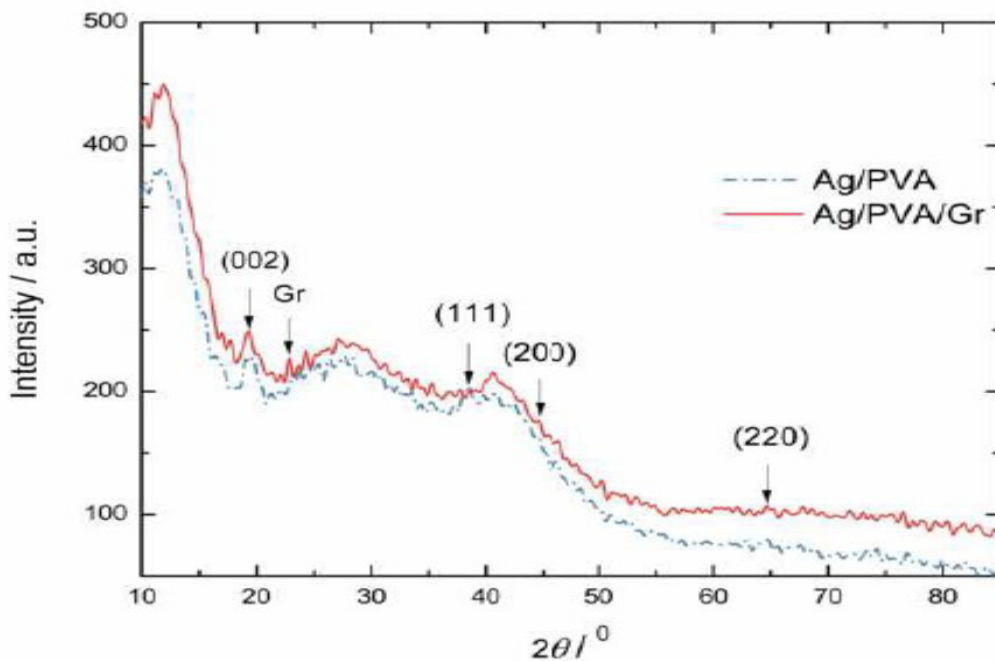


Figure 5.10. XRD patterns of Ag/PVA and Ag/PVA/Gr hydrogels (swelling solution: 3.9 mM AgNO<sub>3</sub> + 0.1 M KNO<sub>3</sub>)

## 5.8. THERMAL ANALYSIS

Thermogravimetric analysis (TGA) was employed to investigate the influence of graphene on thermal properties of the hydrogel structure, and corresponding differential thermogravimetric (DTG) curves were calculated. In Figure 5.11a, PVA underwent a three-step weight loss, starting with a sudden drop in wt. % at about 100-110 °C, which was immediately followed by another weight loss at higher temperatures (~170 °C) reaching the maximum weight loss rate, as seen from the DTG curve of PVA. In this range, around 80 wt. % of the initial mass was lost due to the dehydration processes and evaporation of water from the hydrogels. The second step was a slight steady weight loss peaking at about 278 °C, suggesting PVA backbone degradation. This peak on the DTG curve of Ag/PVA (Figure 5.11a) is sharper and shifted slightly toward a higher temperature (284 °C), indicating the influence of the coordination bonding of silver on PVA thermal stability. However, the Ag/PVA hydrogel exhibited a higher weight percent loss, with only 1.5 wt. % residue at 600 °C. From Figure 5.11b, showing both the TGA and DTG curves of PVA/Gr and Ag/PVA/Gr hydrogels, it is obvious that the presence of graphene leads to an increase in the thermal stability of both PVA/Gr and Ag/PVA/Gr. At the temperature of 450 °C (Figure 5.11b), Ag/PVA/Gr had a smaller weight loss (94.6 wt. %) compared to that of PVA/Gr (96 wt. %) or Ag/PVA (97.6 wt. %), demonstrating increased stability and stronger interactions between the molecules of the Ag/PVA/Gr hydrogel composite. Graphene also increased temperature required for the thermal decomposition of the polymer backbone since PVA and Ag/PVA exhibited lower thermal stability (about 278 °C and 283 °C, respectively) compared to those of PVA/Gr (288 °C) and Ag/PVA/Gr (311 °C). Even after being heated to 600 °C, approximately 5 wt. % of graphene-containing residue was still present. These findings indicate that the addition of graphene at such an exceptionally low concentration can improve the thermal stability of PVA-based composite hydrogels.

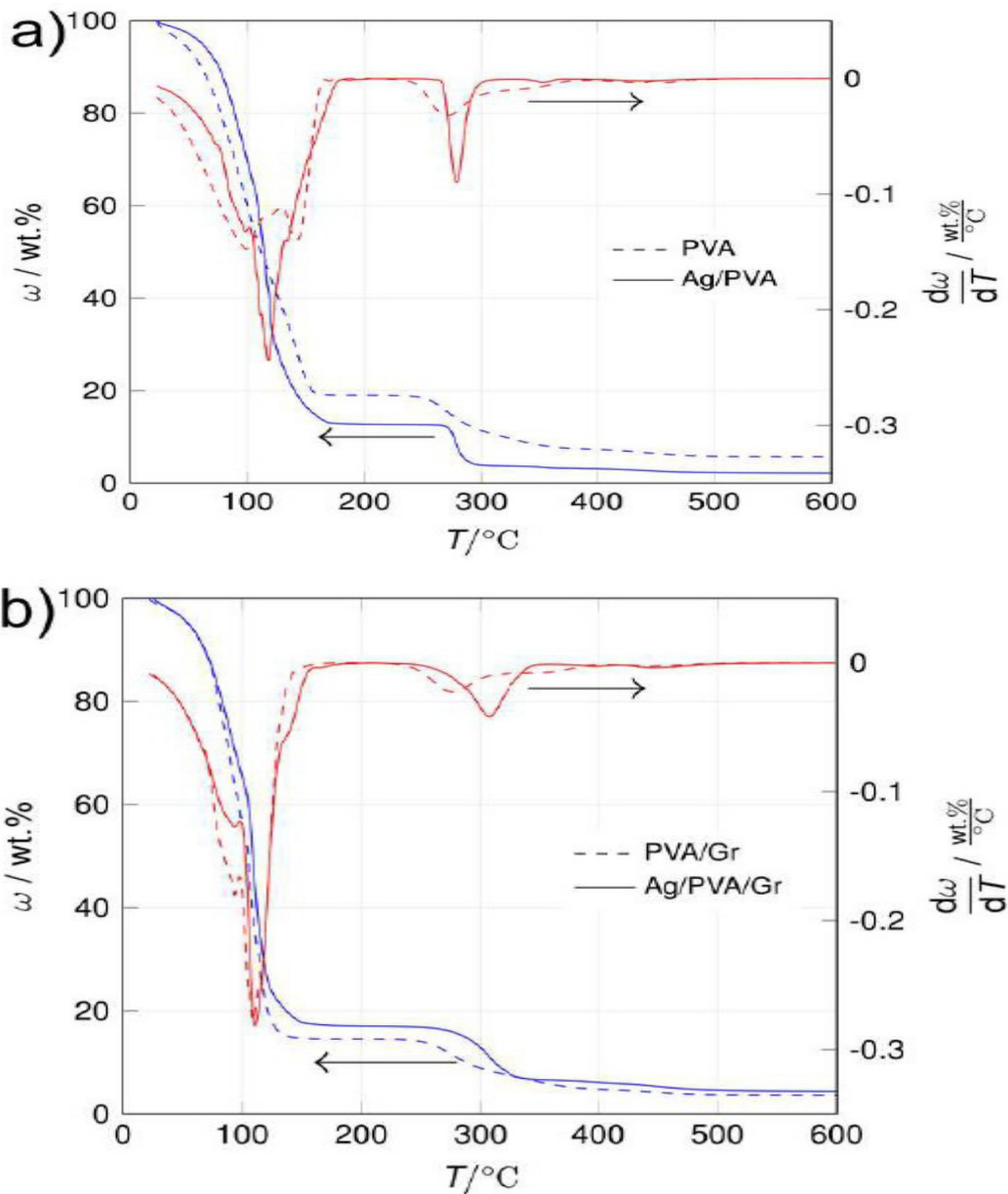


Figure 5.11. TGA (left axis) and DTG (right axis) curves of (a) PVA and Ag/PVA and (b) PVA/Gr and Ag/PVA/Gr hydrogels (swelling solution: 3.9 mM AgNO<sub>3</sub> + 0.1 M KNO<sub>3</sub>)

The DSC thermograms of both PVA/Gr (as a reference) and Ag/PVA/Gr hydrogels exhibit endothermic changes in the range of 20-1000 °C (Figure 5.12). The first endothermic peak, at 119.13 °C for PVA/Gr and at 119.60 °C for Ag/PVA/Gr, is related to the evaporation and loss of water from the hydrogel network upon heating the samples. The high temperature of this event (~ 120 °C) indicates that water molecules are strongly hydrogen bonded to hydroxyl groups on the PVA chain, as well as to

oxidized groups in the graphene structure. This is bound water with highly oriented and ordered dipoles that usually evaporates at higher temperatures [193]. The area of this peak does not change significantly upon addition of AgNPs to the PVA/Gr hydrogel, which implies that AgNPs have a small influence on the binding and orientation of H<sub>2</sub>O molecules in the polymer matrix. The loss of free water at temperatures lower than 100 °C did not result in any significant peaks on both DSC curves, so it was concluded that the main state of water in hydrogels is bound H<sub>2</sub>O, due to the presence of a large number of oxygen-containing groups in PVA macromolecules.

The second endothermic peak on DSC curves of PVA/Gr and Ag/PVA/Gr is located at 287.45 °C and 311.19 °C, respectively, and is related to melting of the polymer. The melting point,  $T_m$ , of pure PVA is reported to be in the range of 200-220 °C [194-196]  $T_m$  of PVA/Gr hydrogel is shifted to significantly higher temperatures (287.45 °C) with respect to PVA, indicating increased thermal stability due to incorporated graphene. Graphene and graphene-oxide nanofillers are known to improve thermal properties of polymer materials, often owed to the incorporation inside the hydrogel structure, as well as to interactions with polymer chains that lead to lowered mobility and higher stability of the polymer matrix. It is well known that graphene always possesses a certain amount of oxygen-containing groups, present as impurities or residues from the manufacturing process, which allow it to be dispersed in aqueous media and form bonds with various materials. The interactions with PVA are achieved *via* hydrogen bonding between these oxygenated groups of graphene, and –OH groups of PVA. Several studies have shown the influence of graphene fillers on thermal stability and thermal degradation of polymeric networks, such as poly(methyl methacrylate) (PMMA), [197,198] PVA films [199] and PVA/starch blends [200,201].

Further more, melting of Ag/PVA/Gr hydrogel occurs at even higher  $T_m = 311.19$  °C, exhibiting much better thermal stability due to the presence of AgNPs together with graphene. This corroborates the assumption that AgNPs form complexes mainly with -OH groups of PVA macromolecule, which has a strong influence on both thermal stability and crystallinity of PVA polymer.

Finally, at temperatures higher than 400 °C, the DSC curves exhibit stable endothermic regions with small change over the analyzed temperature range. This region of the curve probably covers mostly slow thermal oxidation of graphene sheets

incorporated in the hydrogels, as also seen by small-area endothermic peak on the DSC curve of PVA/Gr at around 825 °C.

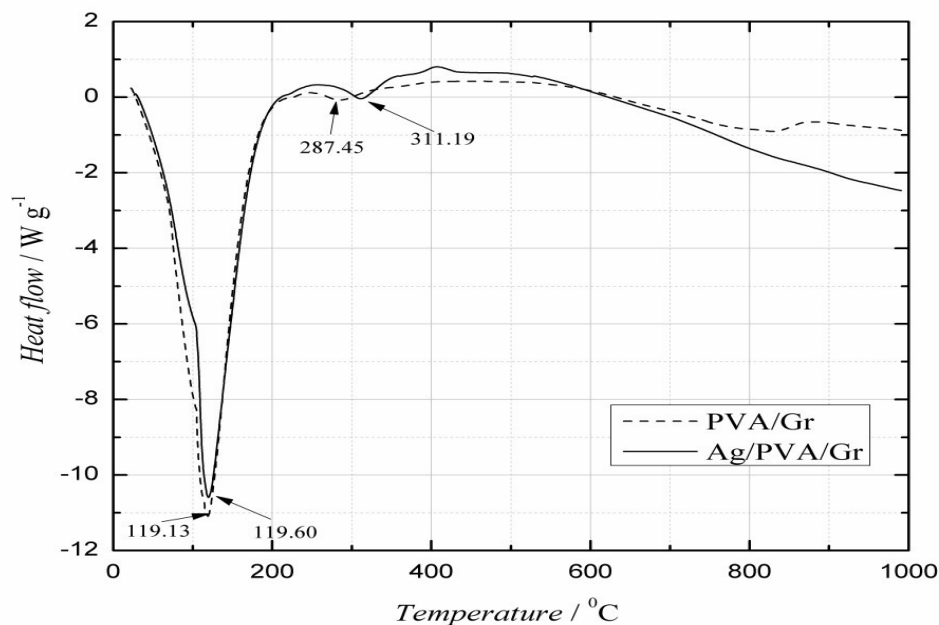


Figure 5.12.. DSC curves of PVA/Gr and Ag/PVA/Gr hydrogels (swelling solution: 3.9 mM AgNO<sub>3</sub>)

## 5.9. CYTOTOXICITY

Determining dose-dependent cytotoxicity of AgNPs and Ag<sup>+</sup> ions incorporated into hydrogels was the primary concern in the quest for the best-suited composite. PBMCs mainly consist of lymphocytes and monocytes, thus representing one of the main populations of the human immune system cells. In the blood, leukocytes represent a cellular host defense system that is able to release various inflammatory mediators after cell activation. Therefore for the initial testing of this composite system, it was opted for PBMCs as a first line of defense against any type of implant in the human body, before proceeding to tissue specific cells. The experiments (as shown in Tables 5.2, 5.3 and figure 5.13) determined survival, S, of non-stimulated and PHA-stimulated PBMCs exposed to PVA, Ag/PVA, PVA/Gr and Ag/PVA/Gr hydrogels swollen in solutions of different AgNO<sub>3</sub> concentrations (0.25, 0.5, 1 and 3.9 mM). Increased silver

concentration in AgNO<sub>3</sub> solutions induced a decrease in target cell survival. Presence of pure PVA hydrogel leads only to a slight decrease in the survival of non-stimulated and PHA-stimulated PBMCs, i.e.  $90.77 \pm 0.88\%$  and  $84.01 \pm 7.86\%$ , respectively. Survival of PBMCs remarkably decreased in the presence of a high dosage of AgNPs in the Ag/PVA composite hydrogel. It can be concluded that the release of silver from Ag/PVA composites obtained from PVA hydrogels swollen in 0.25 mM AgNO<sub>3</sub> solutions demonstrated the lowest cytotoxicity (cytotoxicity scale in Section 4.3.8.3) in non-stimulated PBMC culture, while Ag/PVA composites obtained from PVA swollen in more concentrated AgNO<sub>3</sub> solutions exerted pronounced cytotoxicity. Also, when stimulated to proliferation (induced PHA into the culture medium) cells retained high survival rate as cytotoxic effects of hydrogels were not significantly different in non-stimulated and stimulated for proliferation PBMC cells. The presence of PVA/Gr hydrogel leads only to a slight decrease in the survival of non-stimulated and PHA-stimulated PBMCs, i.e.  $84.15 \pm 6.69\%$  and  $72.73 \pm 6.24\%$ , respectively. Survival of PBMCs remarkably decreased in the presence of Ag/PVA/Gr when the loading of Ag increased. The release of silver from Ag/PVA/Gr (swollen in 0.25 mM AgNO<sub>3</sub>) exhibited the lowest cytotoxicity towards non-stimulated PBMC, while Ag/PVA/Gr obtained from PVA/Gr hydrogels swollen in more concentrated AgNO<sub>3</sub> solutions exerted pronounced cytotoxicity. PHA had negligible effects on the overall cell survival since cytotoxic effects were not significantly different in non-stimulated and proliferated PBMC cells. These results are in good agreement with the data which have been published previously [10].

*Table 5.2. Survival, S, of non-stimulated and PHA-stimulated PBMC cultured in the presence of PVA hydrogels swollen in different concentrations of AgNO<sub>3</sub> solutions, C (AgNO<sub>3</sub>)*

	<b>PVA hydrogels</b>				
C/AgNO <sub>3</sub> [mM]	PVA	0.25	0.5	1	3.9
PBMC	90.77	82.52	63.86	35.88	08.87
PBMC+PHA	84.01	75.58	61.03	38.34	05.26

*Table 5.3. Survival, S, of non-stimulated and PHA-stimulated PBMC cultured in the presence of PVA hydrogels swollen in different concentrations of AgNO<sub>3</sub> solutions, C (AgNO<sub>3</sub>)*

	<b>PVA/Gr hydrogels</b>				
C/AgNO <sub>3</sub> [mM]	PVA/Gr	0.25	0.5	1	3.9
PBMC	84.15	69.39	53.07	34.33	8.51
PBMC+PHA	72.73	67.95	59.69	34.23	7.05

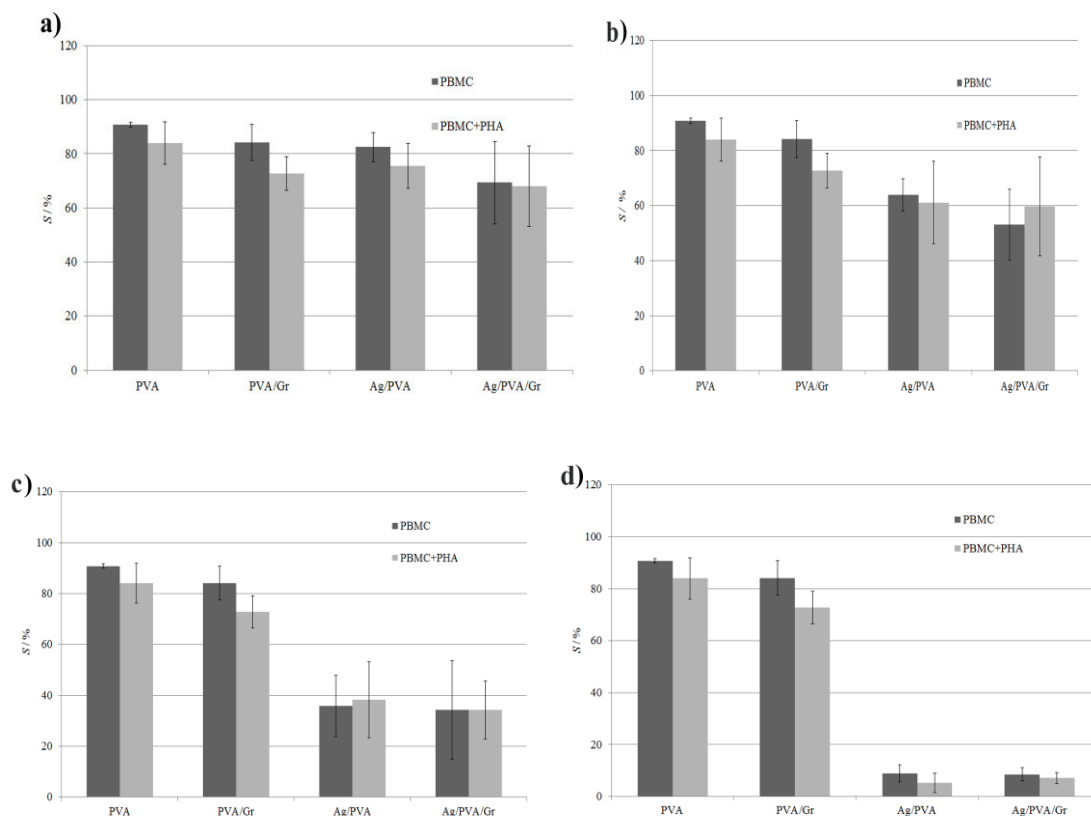
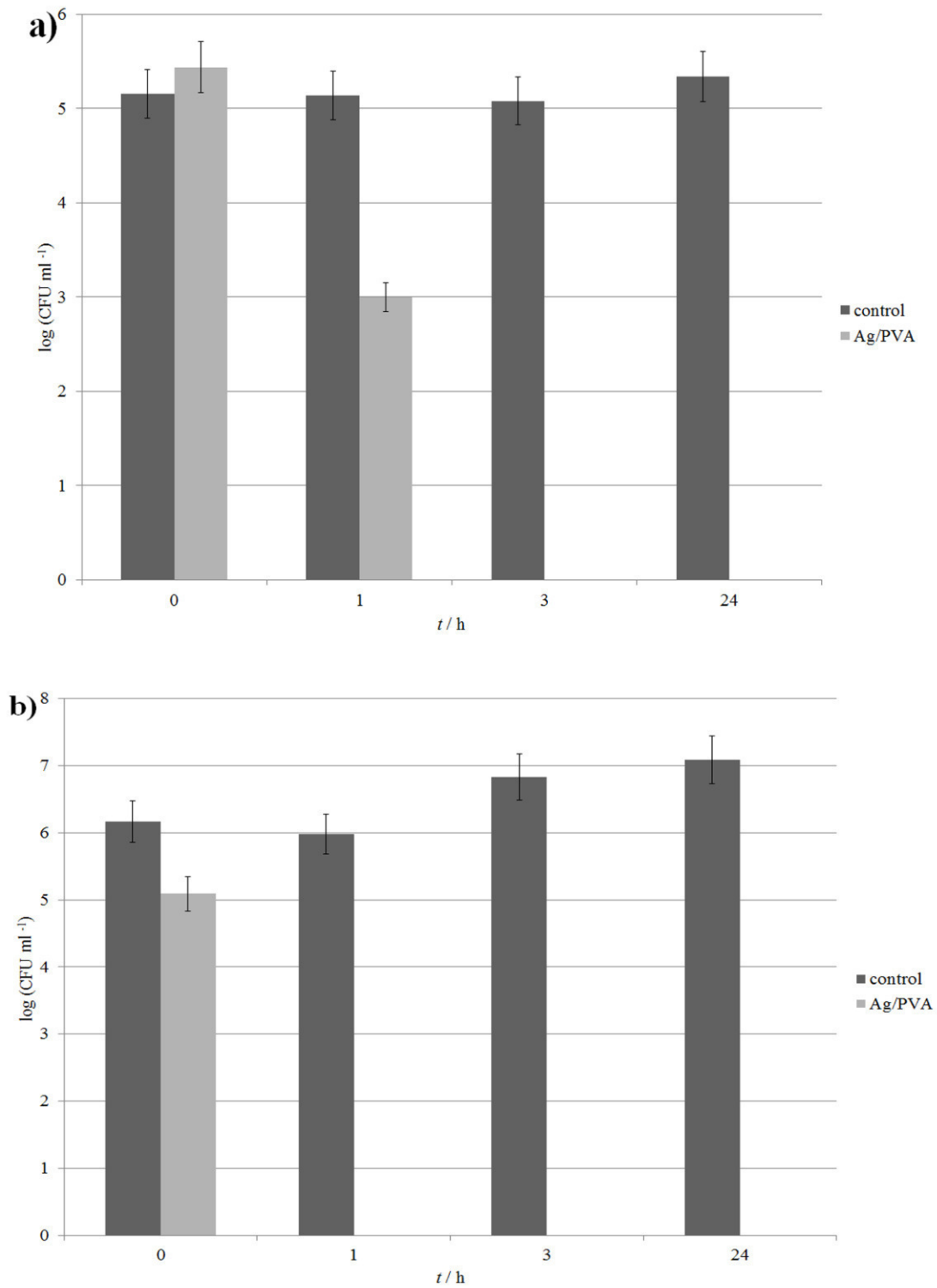


Figure 5.13. Survival,  $S$ , in the presence of PVA, PVA/Gr, Ag/PVA and Ag/PVA/Gr hydrogel for non-stimulated and PHA-stimulated PBMC cultured cells as a function of the concentration of AgNO<sub>3</sub> in hydrogels: a) 0.25 mM, b) 0.5 mM, c) 1 mM and d) 3.9 mM.

Therefore, for the observed exposure time of 72 h, PBMCs affected by AgNPs incorporated into hydrogels, confirmed the fact that silver cytotoxicity to human cells is dependent not only on the ion concentration and exposure period, but also on the cell type, too. Based on *in vitro* experiments here presented, AgNPs and Ag<sup>+</sup> ions exhibited dose-dependent cytotoxicity in PBMC cultures. In addition, there were no remarkable differences in cytotoxicity of the investigated agents in non-stimulated and PHA-stimulated PBMC. The results suggest that the similar, slight cytotoxic effect was observed for both Ag/PVA and Ag/PVA/Gr hydrogel discs preswollen in 0.25 mM AgNO<sub>3</sub> solution.

## 5.10. ANTIBACTERIAL ACTIVITY

Antibacterial activity of Ag/PVA and Ag/PVA/Gr hydrogel discs was tested against, *Staphylococcus aureus* (Gram-positive bacterium) and *Escherichia coli* (Gram-negative bacterium) that are responsible for most of the inter-hospital infections. Figure 5.14 depicts the antibacterial activity of Ag/PVA hydrogel discs against the investigated strains in PB. Antibacterial activity of the Ag/PVA composite hydrogel could be noticed immediately after inoculation of samples and subsequently more than one logarithmic unit reduction in cell viability is achieved after only 1 h of incubation. Calculations based on the initial number of cells in samples and 1 h post-incubation revealed that Ag/PVA hydrogel discs exhibited reduction of both bacteria, *Staphylococcus aureus* TL (44.8 % of cell reduction) and *Escherichia coli* (100 % of cell reduction). Thus, Ag/PVA composite hydrogel exhibited strong antibacterial activity within 1 h of exposure.



*Fig. 5.14. Reduction of viable cell number of: a) Staphylococcus aureus and b) Escherichia coli after contact with the Ag/PVA hydrogel for 0, 1, 3 and 24 h in PB as compared to the control w/o samples.*

Figure 5.15 depicts the antibacterial activity of Ag/PVA/Gr hydrogel discs against the investigated strains in PB. Here also, antibacterial activity of the Ag/PVA/Gr could be noticed immediately after inoculation of samples and imminent reduction of cell viability is achieved after only 1 h of incubation for more than 3 logarithmic units. Calculations based on the initial number of cells in samples and 1 h post-incubation revealed that Ag/PVA/Gr exhibited reduction of both bacteria, *Staphylococcus aureus* TL (97 % of cell reduction) and *Escherichia coli* (complete reduction of cell numbers). Thus, Ag/PVA/Gr hydrogel discs exhibited strong antibacterial activity after 1 h of exposure. Total reduction of bacterial cell numbers within 3 h of exposure (Figs. 5.14 and 5.15) indicated that both hydrogels, Ag/PVA and Ag/PVA/Gr with 0.25 mM of silver loading, are successful candidates for future excellent antibacterial medical devices.

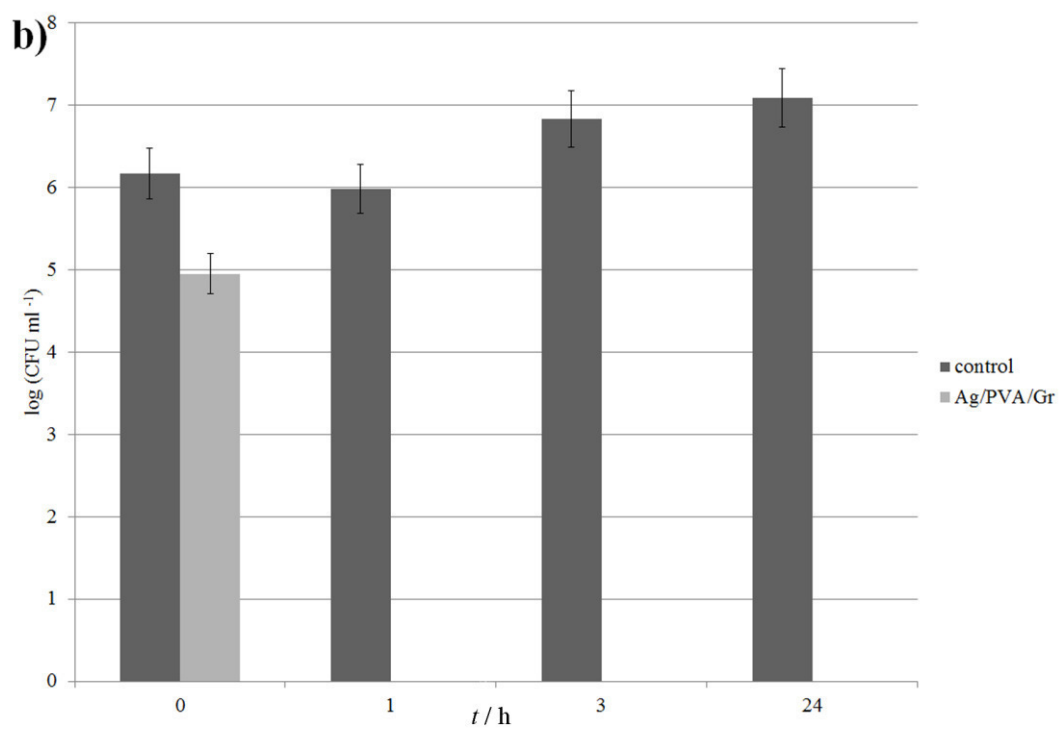
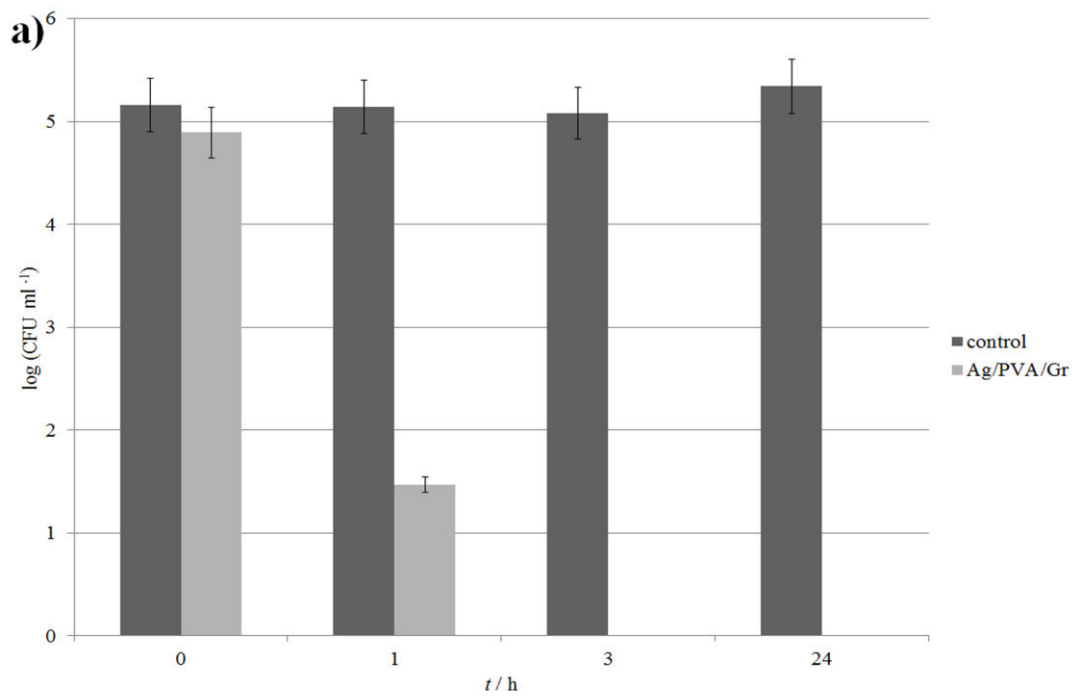


Fig. 5.15. Reduction of viable cell number of: a) *Staphylococcus aureus* and b) *Escherichia coli* after contact with the Ag/PVA/Gr hydrogel discs for 0, 1, 3 and 24 h in PB as compared to the control w/o samples.

Current trends in development of new medical devices are aiming for new products that would be suited for releasing drugs depending on the clinical need (antibiotics, antimicrobial agents etc.) in a predictable manner, according to kinetic laws. However, the action mechanism of silver, a well-known inorganic antimicrobial agent, is still not completely revealed, but bactericidal effects of metal nanoparticles has been associated with their small size and high surface to volume ratio, which allows them close contact with microbial membranes [202]. Silver is assumed to disrupt the bacterial cell integrity by binding to enzymes and proteins within the bacteria, thus accelerating their death. Based on the antibacterial results for the Ag/PVA, it can be concluded that an immediate silver ion release (section 3.6) induce the imminent drop in CFU numbers even after 1 h of exposure, which is sufficient bactericidal effect necessary to prevent any biofilm formation. In order to fully understand the antibacterial mechanism of Ag/PVA/Gr hydrogel, it is necessary to consider a synergistic action of both silver and graphene. Physical damage on bacterial membranes occurs upon direct contact by graphene-based materials e.g. low thickness graphene sharp edges cut through membranes resulting in release of intracellular contents [182, 203]. Graphene may also chemically increase the cellular oxidative stress through formation of reactive oxygen species (ROS). These effects are more pronounced in the case of pure graphene due to stronger interaction between sharp sheet edges and the bacteria's cell membrane and/or better charge transfer between the bacteria and the graphene-based material itself [203]. For the present, antibacterial activity of Gr remains controversial [204] and it should be a subjected to further investigations.

## **5.11. SILVER RELEASE INVESTIGATIONS**

### ***5.11.1. SILVER RELEASE FROM HYDROGELS WITH $0.25 \times 10^{-3}$ M $\text{AgNO}_3$***

The key feature for any type of antibacterial medical device represents its antibacterial efficiency, evaluated by the release of the incorporated antimicrobial into the physiological environment [205]. The silver release kinetics from Ag/PVA and Ag/PVA/Gr hydrogel nanocomposites with  $0.25 \times 10^{-3}$  M  $\text{AgNO}_3$  during time of exposure to PB at  $37^\circ \text{C}$  is shown in (Appendix) and Figure 5.16, as the amount of silver

remaining inside a sample as a function of time. It can be observed that the silver concentration inside Ag/PVA and Ag/PVA/Gr hydrogels initially decreased slightly sharply with time, and after 2 days of silver release (26 % and 25 % of the initial silver content, respectively) a plateau was observed, indicating a significant lowering of the silver release rate. However, it can also be seen that even after 28 days, both Ag/PVA and Ag/PVA/Gr had still retained 67-68 % of the initial silver content, as a consequence of stability of AgNPs inside the highly crosslinked PVA hydrogel network. High initial concentration of antibacterial agent in the direct-contact surrounding tissue is particularly important in the immediate period of post-application since it prevents initial adhesion of bacteria. However, continuous silver ion release after this critical period is also desirable to prevent bacteria biofilm formation and the remaining silver can preserve the sterility of the samples over time. As a result, these Ag/PVA and Ag/PVA/Gr composites could be suited for an extensive continuous application, preserving the sterility of a soft tissue implant, especially considering their antibacterial effect against *Staphylococcus aureus* and *Escherichia coli*. The time dependence of the cumulative silver ratio ( $C_{Ag}/C_{tot}$ ) for Ag/PVA and Ag/PVA/Gr hydrogels during release was calculated as shown in Figure 5.17.

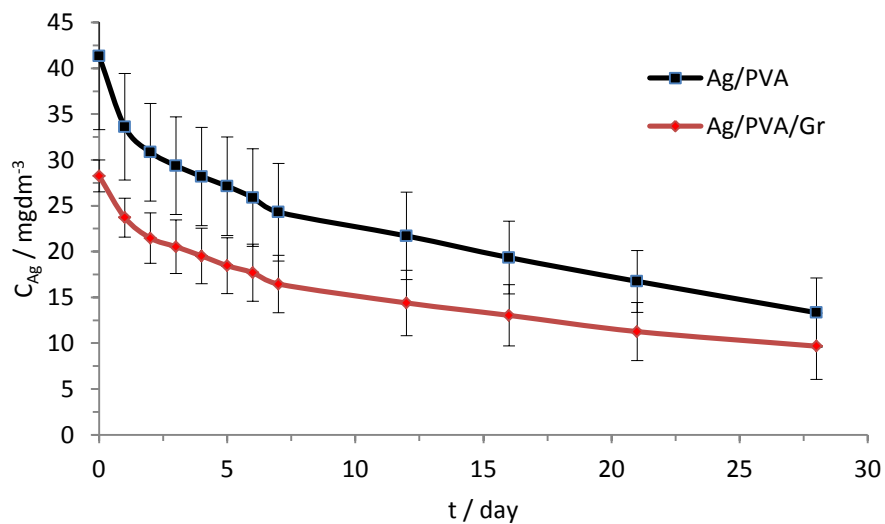


Figure 5.16. Time dependence of the silver concentration inside Ag/PVA and Ag/PVA/Gr hydrogels during exposure to PB at 37 °C (data represent average of three measurements,  $0.25 \times 10^{-3}$  M  $\text{AgNO}_3$  swelling solution)

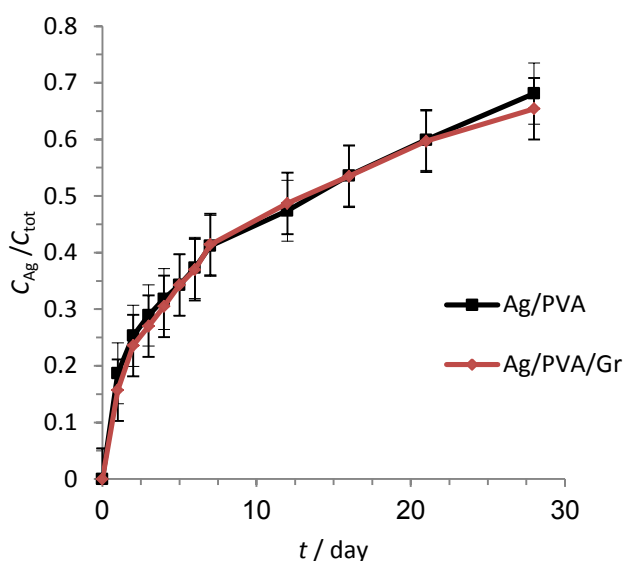


Figure 5.17. Time dependence of the cumulative silver release ratio ( $C_{Ag}/C_{tot}$ ) release from Ag/PVA and Ag/PVA/Gr hydrogels during exposure to PB at 37 °C (data represent average of three measurements,  $0.25 \times 10^{-3}$  M AgNO<sub>3</sub> swelling solution)

### 5.11.2. SILVER RELEASE FROM HYDROGELS WITH $0.5 \times 10^{-3}$ M AgNO<sub>3</sub>

Silver release kinetics from Ag/PVA and Ag/PVA/Gr hydrogel nanocomposites with  $0.5 \times 10^{-3}$  M AgNO<sub>3</sub> during exposure to PB at 37 °C is depicted in Figure 5.18, as the amount of silver remaining inside the sample as a function of time. It can be observed that the silver concentration inside Ag/PVA and Ag/PVA/Gr hydrogels initially decreased slightly with time, and after 7 days of silver release (34 % and 44 % of the initial silver content, respectively) a plateau was observed, indicating a significant lowering of the silver release rate. However, it can also be seen that even after 28 days, the both Ag/PVA and Ag/PVA/Gr had still retained 48-57 % of the initial silver content, as a consequence of stability of AgNPs inside the highly crosslinked PVA hydrogel network. This is very important since the remaining silver can preserve the sterility of the samples over time. As a result, these hydrogels could be used for a prolonged period of time, preserving the sterility of a soft tissue implant for example. Furthermore, the

potential application of Ag/PVA and Ag/PVA/Gr hydrogel nanocomposites as antibacterial agents were demonstrated by their effect against *Staphylococcus aureus* and *Escherichia coli*. The time dependence of the cumulative release silver ratio ( $C_{Ag}/C_{tot}$ ) for Ag/PVA and Ag/PVA/Gr hydrogels is shown in Figure 5.19.

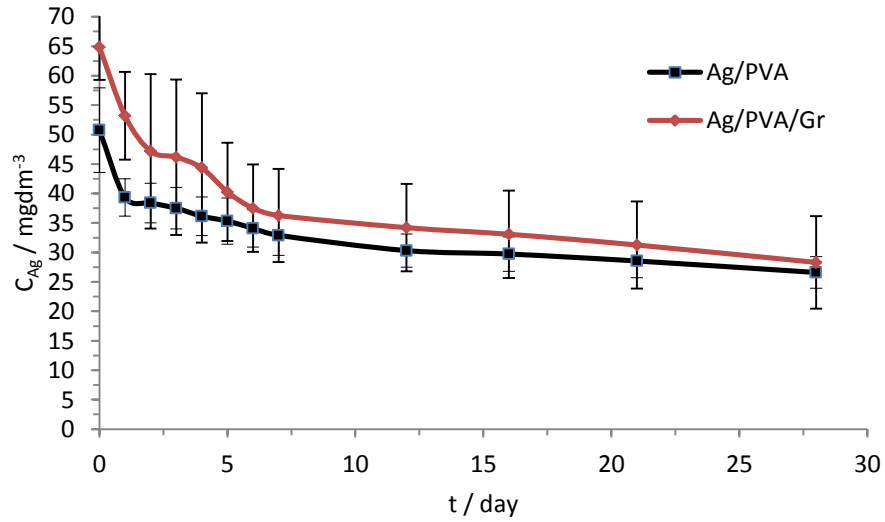


Figure 5.18. Time dependence of the silver concentration within Ag/PVA and Ag/PVA/Gr hydrogels during exposure to PB at  $37^{\circ}\text{C}$  (data represent average of three measurements,  $0.5 \times 10^{-3} \text{ M AgNO}_3$  swelling solution)

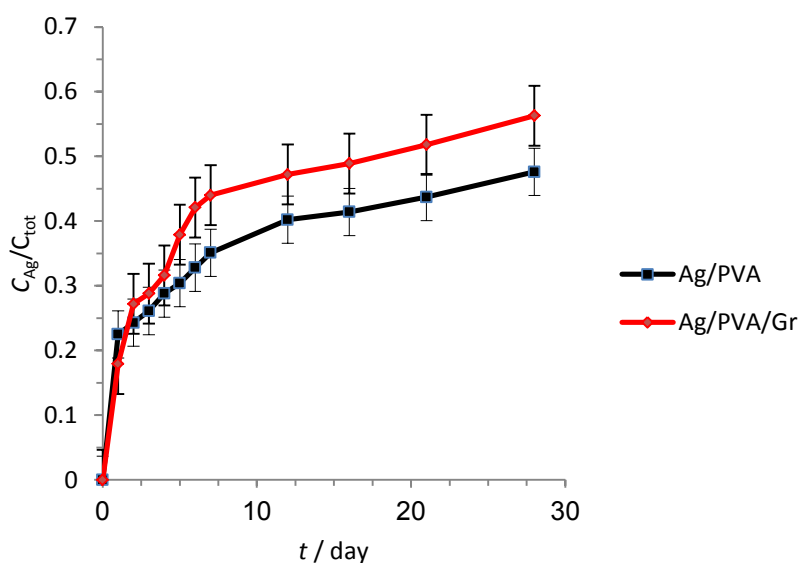


Figure 5.19. Time dependence of the cumulative silver ratio ( $C_{Ag}/C_{tot}$ ) for Ag/PVA and Ag/PVA/Gr hydrogels during exposure to PB at 37 °C (data represent average of three measurements,  $0.5 \times 10^{-3}$  M AgNO<sub>3</sub> swelling solution)

### 5.11.3. SILVER RELEASE FROM HYDROGELS WITH $1 \times 10^{-3}$ M AgNO<sub>3</sub>

Silver release profiles from Ag/PVA and Ag/PVA/Gr hydrogels obtained from  $1 \times 10^{-3}$  M AgNO<sub>3</sub> during exposure to PB at 37 °C in depicted swelling solution are given in Figure 5.20 as the amount of silver remaining inside the sample as a function of time. All data are given as the arithmetic mean of three measurements.

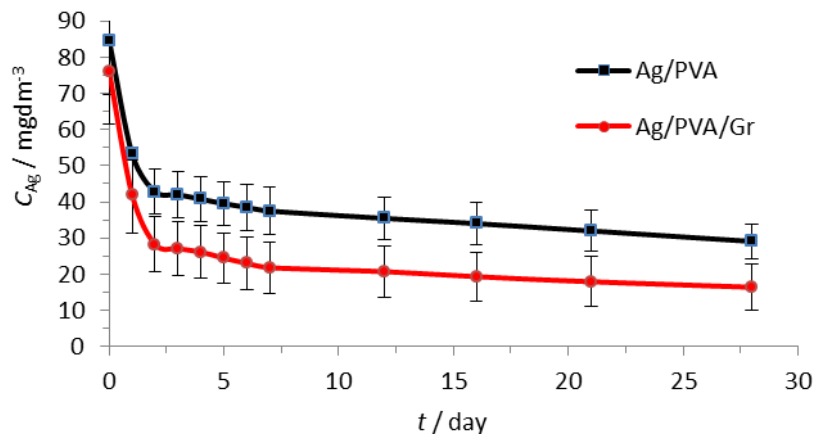


Figure 5.20. Time dependence of the silver concentration within Ag/PVA and Ag/PVA/Gr hydrogels during exposure to PB at 37 °C (data represent average of three measurements,  $1.0 \times 10^{-3} M$  AgNO<sub>3</sub> swelling solution).

Both profiles start with a steep and fast release in the first two days, eventually reaching a plateau toward the end of each experiment. This indicates a “burst release” in the first 48 h, during which roughly 48 wt. % of Ag was released from the Ag/PVA hydrogel, and nearly 63 wt.% was released from the Ag/PVA/Gr hydrogel. After this period, the antibacterial substance was slowly released. After 28 days, the Ag/PVA gels retained on average 35 wt.% and the Ag/PVA/Gr gels around 23 wt.% of the total initial concentration of AgNPs. Such behavior in a release profile is desirable for the application of hydrogels as anti-inflammatory wound dressings. The fast initial release ensures the sterilization of the wound and prevents the adhesion of bacteria, whereas the slow and steady late-time release profile is suitable for the prolonged protection of the wound from infection.

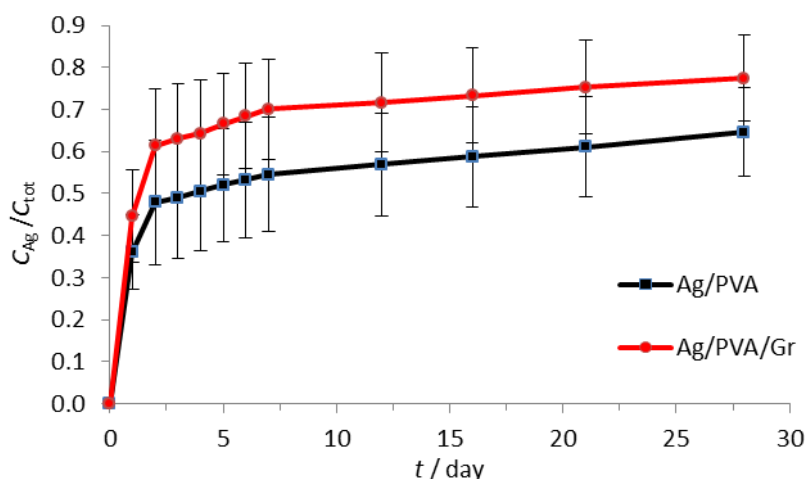


Figure 5.21. Time dependence of the cumulative silver ratio ( $C_{Ag}/C_{tot}$ ) for Ag/PVA and Ag/PVA/Gr hydrogels during exposure to PB at 37 °C (data represent average of three measurements,  $1.0 \times 10^{-3}$  M AgNO<sub>3</sub> swelling solution)

The cumulative profile of silver release from the Ag/PVA hydrogels with  $1.0 \times 10^{-3}$  M AgNO<sub>3</sub> (Figure 5.21) follows a slower trend compared to the release from Ag/PVA/Gr samples. The Ag/PVA samples retained a higher percentage of the total initial concentration of AgNPs after the 28-day release period. Additionally, the synthesis itself was more successful in Ag/PVA hydrogels; it was determined that the total concentrations of Ag in these samples were roughly 11 wt. % higher than those in the Ag/PVA/Gr hydrogels.

All of these findings support the conclusion that the presence of graphene sheets in the hydrogel matrix causes the destabilization of AgNPs due to the repulsive electrostatic interactions with silver and also by shielding active binding sites on the PVA chains, which weakens the bonds between PVA and AgNPs, ultimately enabling the easier release of the AgNPs. This is corroborated by the results of the voltammetric measurements, which showed more intense oxidation of AgNPs from Ag/PVA/Gr hydrogels.

#### 5.11.4. SILVER RELEASE FROM HYDROGELS WITH $3.9 \times 10^{-3}$ M AgNO<sub>3</sub>

Silver release kinetics from Ag/PVA and Ag/PVA/Gr hydrogel nanocomposites with  $3.9 \times 10^{-3}$  M AgNO<sub>3</sub> during exposure to PB at 37 °C is depicted in Figure 5.22, as

the amount of silver remaining inside a sample as a function of time. It can be observed that the silver concentration inside Ag/PVA and Ag/PVA/Gr hydrogels initially decreased sharply with time, and after 2 days of silver release (68 % and 71 % of the initial silver content, respectively) a plateau was observed, indicating a significant lowering of the silver release rate. However, it can also be seen that even after 28 days, both Ag/PVA and Ag/PVA/Gr had still retained 22-27 % of the initial silver content, as in previous experiments. In this case, also hydrogels can preserve sterility which inducing strong bactericidal effects as shown in studies of antibacterial activity. The relation between time dependence of the cumulative silver ratio ( $C_{Ag}/C_{tot}$ ) for Ag/PVA and Ag/PVA/Gr hydrogels during release is shown in Figure 5.23.

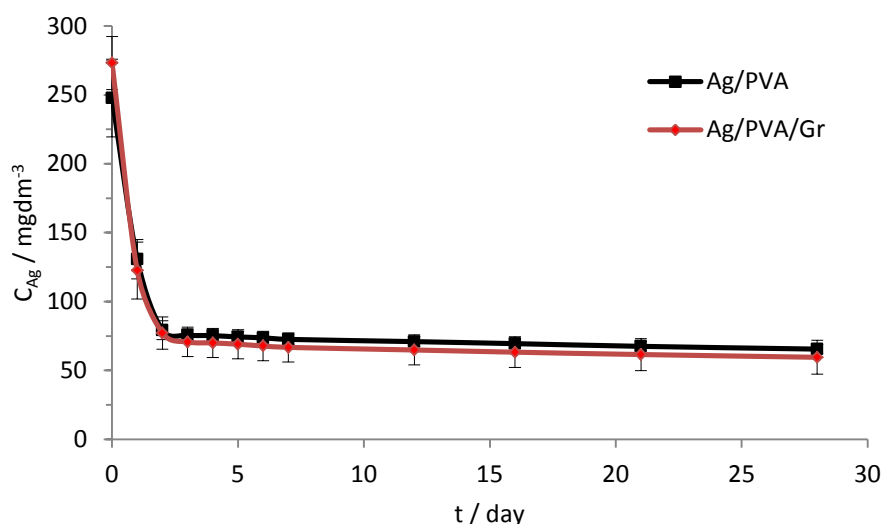


*Figure 5.22. Time dependence of silver concentration inside Ag/PVA and Ag/PVA/Gr hydrogels during exposure to PB at 37 °C (data represent average of three measurements  $3.9 \times 10^{-3} M AgNO_3$ ).*

High initial concentration of antibacterial agent in the direct-contact surrounding tissue is particularly important in the immediate period of post-application since it prevents initial adhesion of bacteria. However, from the presented data no definite conclusion about the initial silver content could be drawn. Silver content embedded in the polymeric network vastly depends on the biomaterial itself, different conditions of electrochemical syntheses, inconsistency in cross-linking, discrepancies in terms of

density and viscosity. Overall, all those deviations are minor, within the margin of error [184].

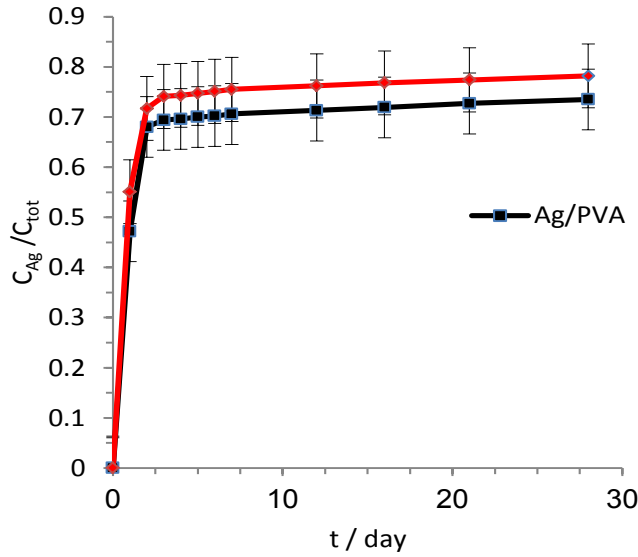


Figure 5.23. Time dependence of cumulative silver ratio ( $C_{Ag}/C_{tot}$ ) for Ag/PVA and Ag/PVA/Gr hydrogels during exposure to PB at 37 °C (data represent average of three measurements,  $3.9 \times 10^{-3} M AgNO_3$  swelling solution)

## 5.12. SORPTION CHARACTERISTICS

In order to determine sorption characteristics of the pure PVA, PVA/Gr, Ag/PVA and Ag/PVA/Gr xerogels (dry gels), the intake of simulated body fluid was monitored gravimetrically for 72 h at  $37 \pm 1^\circ C$  (sorption curves, Fig. 5.24a). The reduced sorption curves (Fig. 5.24b) are plotted as a dependence  $m_t / m_\infty$  vs.  $t^{1/2} / \delta$ , following the second Fickian diffusion law given by following equation, for a flat plane and short times ( $\frac{m_t}{m_\infty} < 0.6$ ) [23]:

$$\frac{m_t}{m_\infty} = \frac{4}{\delta} \frac{D^{1/2}}{\pi^{1/2}} t^{1/2} \quad (5.8)$$

where  $m_t$  is the amount of SBF absorbed at time  $t$ ,  $m_\infty$  is the amount of SBF absorbed at equilibrium,  $D$  is the diffusion coefficient of SBF through hydrogels, and  $\delta$  is the thickness of the hydrogel sample.

As it can be observed in figure 5.24a, the initial sorption of SBF was approximately linear until a steady state was reached. The values of diffusion coefficient,  $D$  ( Table 5.4), of SBF through PVA, PVA/Gr, Ag/PVA and Ag/PVA/Gr hydrogels were calculated from the slopes of the initial linear region of the reduced sorption curves (Fig. 5.24b). The values obtained were  $3.3 \times 10^{-2} \text{ cm}^2 \text{ min}^{-1}$  for PVA and  $2.5 \times 10^{-2} \text{ cm}^2 \text{ min}^{-1}$  for PVA/Gr hydrogel nanocomposites. The diffusion coefficient of SBF in the PVA was higher than in PVA/Gr hydrogel, by about 24%, indicating the facilitated absorption of SBF into the pure PVA hydrogel, compared to PVA/Gr hydrogel.

*Table 5.4. Diffusion coefficient values calculated from the slopes of the initial linear region of the reduced sorption curves*

Samples	PVA	PVA/Gr	Ag/PVA	Ag/PVA/Gr
Diffusion coefficient ( $D$ ) $\text{cm}^2 \cdot \text{min}^{-1}$	$3.3 \times 10^{-2}$	$2.5 \times 10^{-2}$	$2.2 \times 10^{-2}$	$2.8 \times 10^{-2}$

The diffusion coefficient of SBF in the Ag/PVA/Gr ( $2.8 \times 10^{-2} \text{ cm}^2 \text{ min}^{-1}$ ) was higher than that in the Ag/ PVA hydrogel ( $2.2 \times 10^{-2} \text{ cm}^2 \text{ min}^{-1}$ ), by about 21%, indicating the facilitated absorption of SBF into the formed nanocomposite. It could be presumed that the presence of AgNPs with graphene sheets expands the PVA hydrogel network, enabling slightly faster SBF diffusion, and therefore promotes the sorption ability of the Ag/PVA/Gr nanocomposites. This is a consequence of established hydrogen bonding interactions between the  $\text{OH}^-$  groups present in PVA and residual oxygen containing groups in graphene sheets situated between the polymer chains of Ag/PVA/Gr. This type of interaction enables the PVA hydrogel network expansion, causing slightly faster SBF diffusion, and therefore promoting the sorption ability of the Ag/PVA/Gr hydrogel. This property is important in the biomedical application of composite hydrogel as wound dressings because, compared to Ag/PVA hydrogel,

Ag/PVA/Gr can further absorb slight to moderate amounts of wound exudate by swelling and generally speed up the wound healing process.

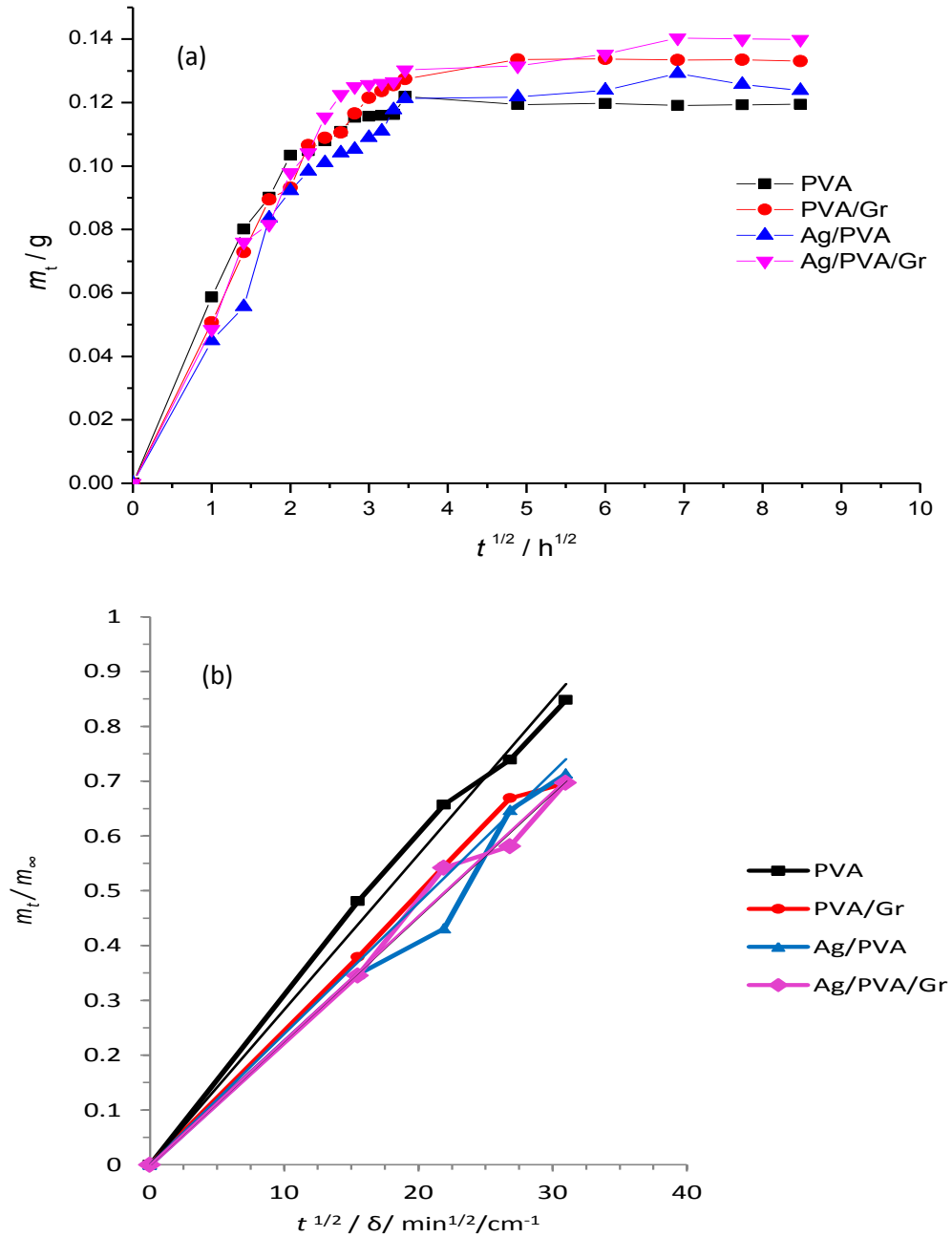


Figure 5.24. Sorption curves (a), and reduced sorption curves (b) of PVA, PVA/Gr, Ag/PVA and Ag/PVA/Gr nanocomposites in SBF at 37 °C.

## 6. CONCLUSION

- PVA/Gr hydrogel was successfully obtained from a PVA/Gr colloid solution by cross linking using the freezing-thawing method. Then silver nanoparticles (AgNPs) have been successfully incorporated into the matrices of PVA and PVA/Gr hydrogels using the electrochemical method of silver ions reduction to obtain nanocomposite hydrogels, at the applied voltage of 90 V and for the implementation time of 4 min.
- Both Ag/PVA and Ag/PVA/Gr hydrogels exhibited UV-Vis absorption spectra with bands peaking at around 400 nm, which confirmed the formation of AgNPs. Further more, the absence of any absorption bands in the longer wavelength region suggests the restrictive aggregation of AgNPs in the synthesized composite hydrogels. UV-Vis results indicated somewhat smaller dimensions of AgNPs in Ag/PVA/Gr hydrogels than in Ag/PVA, suggesting that graphene sheets situated between the polymer chains prevented further growth and aggregation or agglomeration of AgNPs.
- CV and FE-SEM studies proved smaller dimensions of AgNPs in Ag/PVA/Gr nanocomposites due to graphene sheets situated between PVA chains.
- XRD and FT-IR analyses have shown interactions between AgNPs and hydroxyl groups in PVA, as well as between PVA molecules and graphene sheets. These findings support the hypothesis that graphene sheets situated between the polymer chains prevent further growth and aggregation or agglomeration of AgNPs, as indicated by UV-Vis and FE-SEM results.
- Based on TGA, DTG and DSC studies the Ag/PVA/Gr nanocomposite exhibited the highest thermal stability. According to DTG results, PVA and Ag/PVA exhibited the lowest thermal stability as compared to PVA/Gr and Ag/PVA/Gr which decomposed gradually. The increased temperature required for thermal degradation of the hydrogels containing silver and especially graphene indicate that graphene enhanced the thermal stability of both PVA and Ag/PVA hydrogels.

- Silver release kinetics investigations revealed slower leaching of silver from the Ag/PVA hydrogel (1.0 mM AgNO<sub>3</sub> swelling solution) compared to the release profile of the Ag/PVA/Gr hydrogel due to the repulsive electrostatic interactions of AgNPs and graphene and the influence of graphene on the destabilization of Ag<sub>m</sub>-PVA complexes.
- Ag/PVA/Gr and Ag/PVA hydrogels obtained from 0.25 mM AgNO<sub>3</sub> swelling solution exerted the lowest cytotoxicity towards non-stimulated PBMC culture.
- Ag/PVA and Ag/PVA/Gr obtained from 0.25 mM AgNO<sub>3</sub> swelling solution exhibited strong antibacterial activity against *Staphylococcus aureus* and *Escherichia coli* after first hour of exposure.
- The slow silver release, as well as high remaining silver content of ~ 68 % after 28 days in simulated body fluid confirmed that both Ag/PVA/Gr and Ag/PVA hydrogels can preserve sterility over time, and along with observed low cytotoxicity and strong antibacterial activity, can be excellent candidates for soft tissue implants and wound dressings.

## 7. REFERENCES

- [1] H. Zhang, H. Xia, Y. Zhao, „Poly(vinyl alcohol) hydrogel can autonomously Self-Heal", *American Chemical Society*, **1** (2012) 1233–1236, doi: 10.1021/mz300451r.
- [2] J. L. Holloway, A. M. Lowmanb, G. R. Palmese, „The role of crystallization and phase separation in the formation of physically cross-linked PVA hydrogels". *Soft Matter*, **9** (2013) 826-833, doi: 10.1039/c2sm26763b.
- [3] S. Gupta, S. Goswami, A. Sinha, „A combined effect of freeze–thaw cycles and polymer concentration on the structure and mechanical properties of transparent PVA gels" , *Biomed. Mater.* **7** (2012) 1-8, doi:10.1088/1748-6041/7/1/015006.
- [4] J. Soledad Gonzalez, V. Alejandra Alvarez, „The effect of the annealing on the poly(vinyl alcohol) obtained by freezing–thawing", *Thermochimica Acta* **521** (2011) 184–190 , doi:10.1016/j.tca.2011.04.022.
- [5] M. Sirousazara, M. Yaric, „Dehydration kinetics of poly(vinyl alcohol) hydrogel wound dressing during wound healing process", *Chinese Journal of Polymer Science*, **28** (4) (2010) 573–580, doi: 10.1007/s10118-010-9099-5.
- [6] C. M. Hassan, N. A. Peppas, „Structure and morphology of freeze/thawed PVA hydrogels", *Macromolecules*, **33** (7) (2000) 2472-2479, doi:10.1021/ma9907587.
- [7] A. Chaturvedi, A.K. Bajpai, J. Bajpai, „Preparation and characterization of poly(vinyl alcohol) cryogel-silver nanocomposites and evaluation of blood compatibility, cytotoxicity, and antimicrobial behaviors", *Polymer Composites*, (2014) 1-15, doi: 10.1002/pc.23108.
- [8] R. Surudžić, Ž. Jovanović, N. Bibić, B. Nikolić, V. Mišković-Stanković, „Electrochemical synthesis of silver nanoparticles in poly(vinyl alcohol) solution", *J. Serb. Chem. Soc.* **78** (2013) 2087–2098, doi: 10.2298/JSC131017124S.
- [9] R. Surudžić, A. Janković, M. Mitrić, I. Matić, Z. D. Juranić, L. Živković, V. Mišković-Stanković, K. Yop Rhee, S. Jin Park , D. Hui, „The effect of graphene loading on mechanical, thermal and biological properties of poly(vinyl

- alcohol)/graphene nanocomposites", *Journal of Industrial and Engineering Chemistry* **34** (2016) 250-257, doi: 10.1016/j.jiec.2015.11.016.
- [10] R. Surudžić, A. Janković, N. Bibić, M. Vukašinović-Sekulić, A. Perić-Grujić, V. Mišković-Stanković, S. Jin Park, K. Yop Rhee, „Physicochemical and mechanical properties and antibacterial activity of silver/poly(vinyl alcohol)/graphene nanocomposites obtained by electrochemical method", *Composites Part B* **85** (2016) 102-112, doi: 10.1016/j.compositesb.2015.09.029.
- [11] J. Kui Li, N. Wang, X. Shen Wu, „Poly(vinyl alcohol) nanoparticles prepared by freezing–thawing process for protein / peptide drug deliver", *Journal of Controlled Release*, **56** (1998) 117-126.
- [12] H. L. Abd El-Mohdy, Radiation synthesis of nanosilver/poly(vinyl alcohol)/cellulose acetate/gelatin hydrogels for wound dressing", *J Polym Res*, volume, **20 (177)** (2013)1-12, doi: 10.1007/s10965-013-0177-6.
- [13] J. Krstić, J. Spasojević, A. Radosavljević, A. Perić-Grujić, Momčilo - Đurić, Z. Kacarević-Popović, Srd-an Popović, „In Vitro Silver ion release kinetics from nanosilver/poly(vinyl alcohol) hydrogels synthesized by Gamma Irradiation", *J APPL POLYM*, **40321** (2014) 1-14, doi: 10.1002/APP.40321.
- [14] Thi-H. Nguyen, Young-H. Kim, Ho-Y. Song, Byong-T. Lee, „Nano Ag loaded PVA nano-fibrous mats for skin applications", *Journal of Biomedical Materials research B: Applied Biomaterials*, **96 (B)** (2011) 225-233, doi: 10.1002/jbm.b.31756.
- [15] B. Lili, Y. Wu, X. Qunji, G. Jinzhang, „Antibacterial properties of silver /poly(vinyl alcohol) colloids", *CJI*, **9 (12)** (2007) 52-62, [://www.chemistrymag.org/cji/2007/09c052pe.htm](http://www.chemistrymag.org/cji/2007/09c052pe.htm).
- [16] D. Van Phu, L. Anh Quoc, N. Ngoc Duy, N. Thi Kim Lan, B. Duy Du, L. Q. Luan, N. Quoc Hien, „Study on antibacterial activity of silver nanoparticles synthesized by gamma irradiation method using different stabilizers", *Van Phu et al Nanoscale Research Letters*, **9 (162)** (2014) (1-5) ,[www.nanoscalereslett.com/content/9/1/162](http://www.nanoscalereslett.com/content/9/1/162).
- [17] S. Kr. Saha, P. Chowdhury, P. Saini, S. P. Sinha Babu, „Ultrasound assisted green synthesis of poly(vinyl alcohol) capped silver nanoparticles for the study

- of its antifilarial efficacy", *Applied Surface Science*, **288** (2014) 625-632, doi: 10.1016/j.apsusc.2013.10.085.
- [18] R. N. Oliveira<sup>1</sup>, R. Rouze', B. Quilty, G. G. Alves, G. D. A. Soares, R. M. S. M. Thire', G. B. McGuinness, „Mechanical properties and *in vitro* characterization of poly(vinyl alcohol) nano-silver hydrogel wound dressings", *Interface Focus* **4 (0049)** (2013)1-11, doi: 10.1098/rsfs.2013.0049.
- [19] C. Xiao, F. Gao, Y. Gao, „Controlled preparation of physically crosslinked chitosan-g-poly(vinyl alcohol) hydrogel", *Journal of Applied Polymer Science*,**117** (2010) 2946-2950, doi: 10.1002/app.32202.
- [20] A. Janković, S. Eraković , M. Vukašinović-Sekulić , V. Mišković-Stanković, S. Jin Park , K. Yop Rhee, „Graphene-based antibacterial composite coatings electrodeposited on titanium for biomedical applications", *Progress in organic Coatings*, **83** (2015) 1-10, doi: 10.1016/j.porgcoat.2015.01.019.
- [21] Ž. Jovanović, J. Stojkovska, B. Obradović, V. Mišković-Stanković, „Alginate hydrogel microbeads incorporated with Ag nanoparticles obtained by electrochemical method", *Materials Chemistry and Physics*,**133** (2012) 182-189, doi:10.1016/j.matchemphys.2012.01.005.
- [22] J. Stojkovska, J.Zvicer, Ž. Jovanović, V. Mišković-Stanković, B. Obradović, „Controlled production of alginate nanocomposites with incorporated silver nanoparticles aimed for biomedical applications", *Journal of the Serbian Chemical Society*, **77 (12)** (2012). 1709-1722, doi: 10.2298/JSC121108148S.
- [23] Ž. Jovanović , A. Radosavljević , J. Stojkovska, B. Nikolić , B. Obradovic, Z. Kačarević -Popović , V. Mišković –Stanković, „Silver/Poly(N-vinyl-2-pyrrolidone) hydrogel nanocomposites obtained by electrochemical synthesis of silver nanoparticles inside the polymer hydrogel aimed for biomedical applications", *Polymer Composites*, **35** (2014) 217-226, doi: 10.1002/pc.2265.
- [24] Ž. Jovanović, A. Radosavljević, Z. Kačarević-Popović, J. Stojkovska, A. Perić-Grujić, M. Ristić, I. Z. Matić, Z.D. Juranić, B. Obradovic,V. Mišković-Stanković, „Bioreactor validation and biocompatibility of Ag/poly(N-vinyl-2-pyrrolidone)hydrogel nanocomposites", *Colloids and Surfaces B: Biointerfaces*, **105** (2013) 230-235, doi: 10.1016/j.colsurfb.2012.12.055.

- [25] Ž. Jovanović, A. Krklješ, J. Stojkowska, S. Tomić, B. Obradović, V. Mišković-Stanković, Z. Kačarević-Popović, „Synthesis and characterization of silver/poly(N-vinyl-2-pyrrolidone) hydrogel nanocomposite obtained by *in situ* radiolytic method", *Radiation Physics and Chemistry*, **80** (2011) 1208-1215, doi:10.1016/j.radphyschem.2011.06.005.
- [26] Ž. Jovanović, A. Radosavljević, M. Šiljegović, N. Bibić, V. Mišković-Stanković, Z. Kačarević-Popović, „Structural and optical characteristics of silver/poly(N-vinyl-2-pyrrolidone) nano systems synthesized by  $\gamma$ -irradiation", *Radiation Physics and Chemistry*, **81** (2012) 1720-1728, doi: 10.1016/j.radphyschem.2012.05.019.
- [27] L. Lu, A. Kobayashi, K. Tawa, Y. Ozaki, „Silver nanoplates with special shapes: controlled synthesis and their surface plasmon resonance and surface-enhanced raman scattering properties", *Chem. Mater*, **18** (2006) 4894-4901, doi: 10.1021/cm0615875.
- [28] M. Eid, M. B. El-Arnaouty, M. Salah, El-S. Soliman, El-S. A. Hegazy, „Radiation synthesis and characterization of poly(vinyl alcohol)/poly(N-vinyl-2-pyrrolidone) based hydrogels containing silver nanoparticles", *J Polym Res*, **19** (9835) (2012) 1-10, doi: 10.1007/s10965-012-9835-3.
- [29] X. Zan, M. Kozlov, T. J. McCarthy, Z. Su, „Covalently attached, silver-doped poly(vinyl alcohol) hydrogel films on poly(L-lactic acid)", *Biomacromolecules*, **11** (2010) 1082-1088, doi: 10.1021/bm100048q.
- [30] W. Li, J. Wang, H. Chi, G. Wei, J. Zhang, L. Dai, „Preparation and antibacterial activity of poly(vinyl alcohol)/regenerated silk fibroin composite fibers containing Ag nanoparticles", *Journal of applied Polymer science*, **123** (2012) 20-25, doi: 10.1002/app.34434.
- [31] S. K. Mishra, J.M.F. Ferreira, S. Kannan, „Mechanically stable antimicrobial chitosan–PVA–silver nanocomposite coatings deposited on titanium implants", *Carbohydrate Polymers*, **121** (2015) 37-43, doi: 10.1016/j.carbpol.2014.12.027.
- [32] Ngoc-T. Nguyen, Jui-H. Liu, „A green method for *in situ* synthesis of poly(vinyl alcohol)/chitosan hydrogel thin films with entrapped silver nanoparticles",

- Journal of the Taiwan Institute of Chemical Engineers*, **45** (2014) 2827-2833, doi: 10.1016/j.jtice.2014.06.017.
- [33] X. Xu, Yi-Q. Yang, Ying-Y. Xing, Jiu-F. Yang, Shi-F. Wang, „Properties of novel poly(vinyl alcohol)/cellulose nanocrystals/ silver nanoparticles blend membranes", *Carbohydrate Polymers*, **98**, (2013) 1573-1577, doi: 10.1016/j.carbpol.2013.07.065.
- [34] D. Erdonmez, S. Mosayyebi, K. Erkan, K. Salimi, N. Nagizade, N. Saglam, Z.M.O. Rzeyev, „Nanofabrication and characterization of PVA-organofiller/Ag nanocoatings on pMAD plasmids", *Appl Surf Sci*, **318** (2014) 127-31, .doi: 10.1016/j.apsusc.2014.02.007.
- [35] Z. Liu, J. Yan, Y-E. Miao, Y. Huang, T. Liu,,Catalytic and antibacterial activities of green-synthesized silver nanoparticles on electrospun polystyrene nanofiber membranes using tea polyphenols", *Compos Part B Eng*, **79** (2015) 217–23,doi: 10.1016/j.compositesb.2015.04.037.
- [36] L. Bo, W. Yang, Q. Xue, J. Gao, „Antibacterial properties of silver/poly(vinyl alcohol) colloids", *Chem Org*, **9** (2007) 52.
- [37] H. Ghasemzadeh , F. Ghanaat, „Antimicrobial alginate/PVA silver nanocomposite hydrogel, synthesis and characterization", *J Polym Res*, **21 (355)** (2014), 1-14, doi: 10.1007/s10965-014-0355-1.
- [38] H. Guen Kim, J. Ho Kim, „Preparation and properties of antibacterial poly(vinyl alcohol) nanofibers by nanoparticles", *Fibers and Polymers* ,**12** (2011) 602-609, doi: 10.1007/s12221-011-0602-6.
- [39] K.A. Jubya, C. Dwivedia, M. Kumara , S. Kotab, H.S. Misrab, P.N. Bajaja, „Silver nanoparticle-loaded PVA/gum acacia hydrogel: Synthesis, characterization and antibacterial study", *Carbohydrate polymers*, **89** (2012) 906-913,doi: 10.1016/j.carbpol.2012.04.033.
- [40] D. Erdonmez , S. Mosayyebi K. Erkan, K. Salimi, N. Nagizade, N. Saglam, Z.M.O. Rzeyev, „Nanofabrication and characterization of PVA–organofiller/ Ag nanocoatings on pMAD plasmids", *Applied Surface Science* , (2014) 1-5, doi: 10.1016/j.apsusc.2014.02.007.
- [41] M. Jae Kim, T. Hwan Oh, S. Soo Han, S. Woo Joo, H. Yong Jeon, D. Wook Chang, „Preparation of poly(vinyl alcohol)/silver-zeolite composite hydrogels

- by UV-irradiation", *Fibers and Polymers*, **15** (2014) 101-107, doi: 10.1007/s12221-014-0101-7.
- [42] V. Chaudhary , A. K. Bhowmick, „Synthesis, optical, and electrical properties of RNA-mediated Ag/PVA nanobiocomposites", *J Nanopart Res*, **15 (1508)** (2013) 1-8, doi: 10.1007/s11051-013-1508-6.
- [43] K. Hong, J. Lyoul Park, I. Hwan Sul, J. Ho Youk, T. Jin Kang, „Preparation of antimicrobial poly(vinyl alcohol) nanofibers containing silver nanoparticles", *Journal of Polymer science*, **44** (2006) 2468-2474, doi: 10.1002/polb.20913.
- [44] S. Mallakpour , M. Dinari, M. Talebi, „A facile, efficient, and green fabrication of nanocomposites based on L-leucine containing poly(amide-imide) and PVA-modified Ag nanoparticles by ultrasonic irradiation", *Colloid Polym Sci*, **293** (2015) 1827-1833, doi: 10.1007/s00396-015-3581-0.
- [45] J. Cveticanin, A. Krkljes , Z. Kacarevic-Popovic , M. Mitric , Z. Rakocevic, D. Trpkov, O. Neskovic, „Functionalization of carbon nanotubes with silver clusters", *Applied Surface Science* ,**256** (2010) 7048-7055, doi: 10.1016/j.apsusc.2010.05.023.
- [46] J. Krstić, J. Spasojević, A. Radosavljević, M. Šiljegović, Z. Kačarević-Popović, „Optical and structural properties of radiolytically *in situ* synthesized silver nanoparticles stabilized by chitosan /poly(vinylalcohol)blends",*Radiation Physics and Chemistry*, **96** (2014) 158-166, doi: 10.1016/j.radphyschem.2013.09.013.
- [47] R. Abargues, P. J. Rodriguez-Canto, S. Albert, I. Suarez and J. P. Martinez-Pastor, „Plasmonic optical sensors printed from Ag–PVA nanoinks",*J Mater.Chem.C*, **2** (2014) 908-915, doi: 10.1039/c3tc31596g.
- [48] I. Saini , Jyoti Rozra , N. Chandak , S. Aggarwal , P. K. Sharma , A. Sharma, „Tailoring of electrical, optical and structural properties of PVA by addition of Ag nanoparticles", *Materials Chemistry and Physics* , **139** (2013) 802-810, doi: 10.1016/j.matchemphys.2013.02.035.
- [49] M. Ghanipour, D. Dorranean, „Effect of Ag-Nanoparticles Doped in poly(vinyl alcohol) on the structural and optical properties of PVA films", *Journal of Nanomaterials*, **ID 897043** (2013) 1-10, doi: 10.1155/2013/897043.

- [50] V. Agabekov, N. Ivanova, V. Dlugunovich, I. Vostchula, „Optical properties of poly(vinyl alcohol) films modified with silver nanoparticles", *Journal of Nanomaterials*, **ID 206384** (2012) 1-5, doi:10.1155/2012/206384.
- [51] A.G. El-Shamy, W. Attia, K.M. Abd El-Kader, „The optical and mechanical properties of PVA-Ag nanocomposite films", *Journal of Alloys and Compounds*, **590** (2014) 309-312, doi: 10.1016/j.jallcom.2013.11.203.
- [52] W. Zhang, W. Li, J. Wang, C. Qin, and L. Dai, „Composites of poly(vinyl alcohol) and carbon nanotubes decorated with silver nanoparticles", *Fibers and Polymers*, **11** (2010) 1132-1136, doi: 10.1007/s12221-010-1132-3.
- [53] J. He, T. Kunitake, „Formation of silver nanoparticles and nanocraters on silicon wafers", *Langmuir*, **22** (2006) 7881-7884, doi: 10.1021/la0610349.
- [54] Z. Gong, C. Wang, C. Wang, C. Tang, F. Cheng, H. Du, M. Fan, A. G. Brolo, „A silver nanoparticle embedded hydrogel as a substrate for surface contamination analysis by surface-enhanced Raman scattering", *Analyst*, **139** (2014) 5283-5289, doi: 10.1039/c4an00968a.
- [55] Y. Wang, J. Chen, J. Cao , Y. Liu, Y. Zhou, Jia-H. Ouyang, D. Jia, „Graphene/carbon black hybrid film for flexible and high rate performance supercapacitor", *Journal of Power Sources*, **271** (2014) 269-277, doi: 10.1016/j.jpowsour.2014.08.007.
- [56] N. Wang, P. R. Chang, P. Zheng, X. Ma, „Graphene–poly(vinyl alcohol) composites: Fabrication, adsorption and electrochemical properties", *Applied Surface Science*, **314** (2014) 815-821, doi: 10.1016/j.apsusc.2014.07.075.
- [57] Wei-L. Song, W. Wang, L. Monica Veca, C. Yi Kong, Mao-S. Cao, P. Wang, M. J. Meziani, H. Qian, G. E. LeCroy, L. Cao, Ya-P. Sun, „Polymer/carbon nanocomposites for enhanced thermal transport properties – carbon nanotubes versus graphene sheets as nanoscale fillers", *Journal of Materials Chemistry*, **22** (2012) 17133-17139, doi: 10.1039/c2jm32469e.
- [58] V. Sridhar, Il-K. Oh, „A coagulation technique for purification of graphene sheets with graphene–reinforced PVA hydrogel as byproduct", *Journal of Colloid and Interface Science*, **348** (2010) 384-387, doi:10.1016/j.jcis.2010.04.054.

- [59] Yun-S.Ye , Ming-Y. Cheng , Xiao-L. Xie , J. Rick , Yao-J. Huang , Feng-C. Chang , Bing-J. Hwang, „Alkali doped poly(vinyl alcohol)/graphene electrolyte for direct methanol alkaline fuel cells", *Journal of Power Sources*, **239** (2013) 424-432, doi: 10.1016/j.jpowsour.2013.03.021.
- [60] J. Jose, M. A. Al-Harhi, M. Al-Ali AlMa'adeed, J. Bhadra Dakua, S. K. De, „Effect of graphene loading on thermomechanical properties of poly(vinyl alcohol)/starch blend", *J.Appl. Polym. Sci.*, **132** (2015) 41827(1-8), doi: 10.1002/app.41827
- [61] J. Wang, X. Wang, C. Xu, M. Zhanga, X. Shanga, „Preparation of graphene/poly(vinyl alcohol) nanocomposites with enhanced mechanical properties and water resistance", *Polym Int*, **60** (2011) 816–822, doi: 10.1002/pi.3025.
- [62] S. Lee, Jin-Y. Hong, J. Jang, „The effect of graphene nanofiller on the crystallization behavior and mechanical properties of poly(vinyl alcohol)", *Polym Int* , **62** (2013) 901-908, doi: 10.1002/pi.4370
- [63] I. Tantis, G. C. Psarras, D. Tasis, „Functionalized graphene – poly(vinyl alcohol) nanocomposites: physical and dielectric properties", *eXPRESS Polymer Letters*, **6 (4)** (2012) 283-292, doi: 10.3144/expresspolymlett.2012.31.
- [64] G. Huang, J. Gao, X. Wang , H. Liang, C. Ge, „How can graphene reduce the flammability of polymer nanocomposites?", *Materials Letters*, **66** (2012) 187-189, doi:10.1016/j.matlet.2011.08.063.
- [65] J. Guo, L. Ren, R. Wang, C. Zhang, Y. Yang, T. Liu, „Water dispersible graphene noncovalently functionalized with tryptophan and its poly(vinyl alcohol) nanocomposite", *Composites : Part B*, **42** (2011) 2130-2135, doi:10.1016/j.compositesb.2011.05.008.
- [66] S. Mitra, O. Mondal, D. Ranjan Saha, A. Datta, S. Banerjee, D. Chakravorty, „Magnetodielectric effect in graphene-PVA nanocomposites", *J. Phys. Chem. C*, **115** (2011) 14285-14289, doi: 10.1021/jp203724f.
- [67] A. Janković, S. Eraković, M. Mitrić, I. Z. Matić, Z. D. Juranić, G. C.P. Tsui. Chak-yin Tang , V. Mišković-Stanković, K. Yop Rhee , S. Jin Park, „Bioactive hydroxyapatite/graphene composite coating and its corrosion stability in

- simulated body fluid", *Journal of Alloys and compounds*, **624** (2015) 148-157, doi: 10.1016/j.jallcom.2014.11.078.
- [68] M. Moradi, J. Aghazadeh Mohandesi, D. Fatmehsari Haghshenas, „Mechanical properties of the poly(vinyl alcohol) based nanocomposites at low content of surfactant wrapped graphene sheets", *Polymer*, **60** (2015) 207-214, doi: 10.1016/j.polymer.2015.01.044.
- [69] Y. Toumia, S. Orlanducci, F. Basoli, S. Licoccia, G. Paradossi, „Soft” Confinement of Graphene in Hydrogel Matrixes", *J. Phys. Chem. B*, **119** (2015) 2051-2061, doi: 10.1021/jp510654h.
- [70] F. Barzegar, A. Bello, M. Fabiane, S. Khamlich, D. Momodu, F. Taghizadeh, J. Dangbegnon, N. Manyala, „Preparation and characterization of poly(vinylalcohol)/graphene nanofibers synthesized by electrospinning", *Journal of Physics and Chemistry of Solids*, **77** (2015) 139-145, doi: 10.1016/j.jpcs.2014.09.015.
- [71] Yuan-C. Cao, W. Wei, J. Liu, Q. You, F. Liu, Q. Lan, C. Zhang, C. Liu, J. Zhao, „The preparation of graphene reinforced poly(vinyl alcohol) antibacterial nanocomposite thin film", *International Journal of Polymer Science*, **ID 407043** (2015) 1-7, doi: 10.1155/2015/407043
- [72] A. Joshi, A. Bajaj, R. Singh, P S Alegaonkar, K Balasubramanian, S. Datar, „Graphene nanoribbon–PVA composite as EMI shielding material in the X band", *Nanotechnology*, **24 (455705)** (2013) (1-8), doi:10.1088/0957-4484/25/23/239501.
- [73] X. Yang , L. Li , S. Shang , Xiao-m. Tao, „Synthesis and characterization of layer-aligned poly(vinyl alcohol)/graphene nanocomposites", *Polymer*, **51** (2010) 3431-3435, doi:10.1016/j.polymer.2010.05.034.
- [74] X. Zhao, Q. Zhang, D. Chen, „Enhanced mechanical properties of graphene-based poly(vinyl alcohol) composites", *Macromolecules*, **43** (2010) 2357-2363, doi: 10.1021/ma902862u.
- [75] A. K. Gaharwar, N. A. Peppas, A. Khademhosseini, „Nanocomposite hydrogels for biomedical applications", *Biotechnology and Bioengineering*, **111 (3)** (2014) 441-453, doi: 10.1002/bit.25160.
- [76] L. Kou, C. Gao, „Bioinspired design and macroscopic assembly of poly(vinyl

- alcohol)-coated graphene into kilometers-long fibers", *Nanoscale*, **5** (2013) 4370–4378, doi: 10.1039/c3nr00455d.
- [77] G-Q. Qi, J. Cao, R-Y. Bao, Z-Y. Liu, W. Yang, B-H. Xie, M-B. Yanga, „Tuning the structure of graphene oxide and the properties of poly(vinyl alcohol)/graphene oxide nanocomposites by ultrasonication", *J Mater Chem A*, **1** (2013) 3163-3170, doi: 10.1039/c3ta01360j.
- [78] C. Bao, Y. Guo, L. Song, Y. Hu, „Poly(vinyl alcohol) nanocomposites based on graphene and graphite oxide: a comparative investigation of property and mechanism", *J Mater Chem*, **21** (2011) 13942–13950, doi: 10.1039/C1JM11662B.
- [79] W. Yao, C. Geng, D. Han, F. Chen and Q. Fu, „Strong and conductive double-network graphene/ PVA gel", *RSC Advances*, **4** (2014) 39588-39595, doi: 10.1039/c4ra02674h.
- [80] L. Blandón, M. V. Vázquez, D. M. Benjumea, G. Ciro, „Electrochemical synthesis of silver nanoparticles and their potential use as antimicrobial agent: a Case Study on *Escherichia Coli* ", *Portugaliae Electrochimica Acta*, **30 (2)** (2012) 135-144, doi: 10.4152/pea.201202135.
- [81] ML. Rodríguez-Sánchez, MJ. Rodríguez, MC. Blanco, J. Rivas, MA. López-Quintela, „Kinetics and mechanism of the formation of Ag nanoparticles by electrochemical techniques: A plasmon and cluster time-resolved spectroscopic study", *J Phys Chem B*, **109** (2005) 1183–119, doi: 10.1021/jp046056n.
- [82] F. Liu, Y. Yuan, L. Li, S. Shang, X. Yu, Q. Zhang, S. Jiangb, Y. Wua, „Synthesis of polypyrrole nanocomposites decorated with silver nanoparticles with electrocatalysis and antibacterial property", *Compos Part B Eng*, **69** (2015)232–236, 10.1016/j.compositesb.2014.09.030.
- [83] MA. del Valle, M. Gacitúa, FR. Díaz, F. Armijo, R. del Río, „Electrosynthesis of polythiophene nanowires via mesoporous silica thin film templates", *Electrochem Commun*, **11** (2009) 2117–2120, doi: 10.1016/J.elecom.2009.09.009.
- [84] SC. Tang, XK. Meng, S. Vongehr, „An additive-free electrochemical route to rapid synthesis of large-area copper nano-octahedra on gold film substrates", *Electrochem Commun*, **11** (2009) 867–870, doi:

- 10.1016/J.elecom.2009.02.016.
- [85] RM. Stiger, S. Gorer, B. Craft, RM. Penner, „Investigations of electrochemical silver nanocrystal growth on hydrogen-terminated silicon(100)", *Langmuir*, **15** (1999) 790–79, doi: 10.1021/La980800b.
- [86] M. Starowicz, B. Stypuła, J. Banaś, „Electrochemical synthesis of silver nanoparticles", *Electrochem Commun*, **8** (2006) 227–230, doi: 10.1016/J.elecom.2005.11.018.
- [87] L-P. Jiang, A-N. Wang, Y. Zhao, J-R. Zhang, J-J. Zhu, „A novel route for the preparation of monodisperse silver nanoparticles via a pulsed sonoelectrochemical technique", *Inorg Chem Commun*, **7** (2004) 506–509, doi: 10.1016/j.inoche.2004.02.003.
- [88] I. Haas, S. Shanmugam, A. Gedanken, „Pulsed sonoelectrochemical synthesis of size-controlled copper nanoparticles stabilized by poly(N-vinylpyrrolidone)", *J Phys Chem B*, **110** (2006) 16947–16952, doi: 10.1021/jp064216k.
- [89] G. Sandmann, H. Dietz, W. Plieth, „Preparation of silver nanoparticles on ITO surfaces by a double-pulse method", *J Electroanal Chem*, **491** (2000) 78–86, doi: 10.1016/S0022-0728(00)00301-6.
- [90] Kinam Park, Patrick Sinko, „Pharmaceutical polymers", 6<sup>th</sup> Edn. 492-515, [http://downloads.lww.com/wolterskluwer\\_vitalstream\\_com/sample-content/9780781797665sinko/samples/chapter20.pdf](http://downloads.lww.com/wolterskluwer_vitalstream_com/sample-content/9780781797665sinko/samples/chapter20.pdf).
- [91] V. Gowda Kadajji, G. V. Betageri, „Water soluble polymers for pharmaceutical applications", *Polymers* **3** (2011) 1972-2009, doi:10.3390/polym3041972.
- [92] R. Pal Chahal, S. Mahendia, A.K. Tomar, S. Kumar, „ $\gamma$ -Irradiated PVA/Ag nanocomposite films: materials for optical applications", *Journal of Alloys and Compounds*, **538** (2012) 212-219, doi: 10.1016/j.jallcom.2012.05.085
- [93] A. Krklješ, J.M. Nedeljković, Z.M. Kačarević-Popović, „Fabrication of Ag-PVA hydrogel nanocomposite by  $\gamma$ -irradiation", *Polymer Bulletin*, **58** (2007) 271-279, doi: 10.1007/s00289-006-0593-4.
- [94] M. Kumar, L. Varshney, S. Francis, „Radiolytic formation of Ag clusters in aqueous poly(vinyl alcohol) solution and hydrogel matrix", *Radiation Physics and Chemistry*, **73** (2005) 21-27, doi:10.1016/j.radphyschem.2004.06.006.

- [95] K. Hareesh, R.P. Joshi, S.S. Dahiwale, V.N. Bhoraskar, S.D. Dhole, „Synthesis of Ag-reduced graphene oxide nanocomposite by gamma radiation assisted method and its photocatalytic activity", *Vacuum*, **124** (2016) 40-45, doi: 10.1016/j.vacuum.2015.11.011.
- [96] W. H. Eisa, Y. K. Abdel-Moneam, Y. Shaaban, A. A. Abdel-Fattah, A. M. Abou Zeid, „Gamma-irradiation assisted seeded growth of Ag nanoparticles within PVA matrix", *Materials Chemistry and Physics*, **128** (2011) 109-113, doi:10.1016/j.matchemphys.2011.02.076.
- [97] W. H. Eisa , A.A. Shabaka, „Ag seeds mediated growth of Au nanoparticles within PVA matrix: An eco-friendly catalyst for degradation of 4-nitrophenol", *Reactive & Functional Polymers*, **73** (2013) 1510-1516, doi: 10.1016/j.reactfunctpolym.2013.07.018.
- [98] G. Mustatea, I. Calinescu, A. Diacon, L. Balan, „Photoinduced synthesis of silver/polymer nanocomposites", *Materiale Plastice*, **51 (1)** (2014) 17-21, ISSN: 00255289, <http://www.revmaterialeplastice.ro>.
- [99] A. Gautam, S. Ram, „Preparation and thermomechanical properties of Ag-PVA nanocomposite", films *Materials Chemistry and Physics* , **119** (2010) 266-271, doi:10.1016/j.matchemphys.2009.08.050.
- [100] A. Zielinska, E. Skwarek, A. Zaleska, M. Gazda, J. Hupka, „Preparation of silver nanoparticles with controlled particle size", *Procedia Chemistry*, **1** (2009) 1560-1566, doi:10.1016/j.proche.2009.11.004.
- [101] F. Delbecq , F. Kono , T. Kawai, „Preparation of PVP–PVA–exfoliated graphite cross-linked composite hydrogels for the incorporation of small tin nanoparticles", *European Polymer Journal*, **49** (2013) 2654-2659, doi: 10.1016/j.eurpolymj.2013.06.014.
- [102] M. Rachele Guascito, D. Chirizzi, R. Anna Picca, E. Mazzotta, C. Malitesta, „Ag nanoparticles capped by a nontoxic polymer: electrochemical and spectroscopic characterization of a novel nanomaterial for glucose detection", *Materials Science and Engineering C*, **31** (2011) 606-611, doi:10.1016/j.msec.2010.11.022.

- [103] R. Pal Chahal, S. Mahendia, A.K. Tomar, S. Kumar, „UV irradiated PVA–Ag nanocomposites for optical applications", *Applied Surface Science*, **343** (2015) 160-165, doi: 10.1016/j.apsusc.2015.03.074.
- [104] M. Jamal Uddin, T. R Middy, B. K Chaudhuri, „Preparation of silver-hydroxyapatite/PVA nanocomposites: Giant dielectric material for industrial and clinical applications", *IOP Conf. Series: Materials Science and Engineering*, **73** (2015) (1-5), doi:10.1088/1757-899X/73/1/012070.
- [105] O. Bashir, S. Hussain, Z. Khan, S. Ahmed AL-Thabaiti, „Encapsulation of silver nanocomposites and effects of stabilizers", *Carbohydrate Polymers*, **107** (2014) 167-173.
- [106] Xin-G. Li, Jia-L. Zhang, Mei-R. Huang, „Chemical response of nanocomposite membranes of electroactive polydiaminonaphthalene nanoparticles to heavy metal ions", *J Phys. Chem. C*, **118** (2014) 11990-11999, doi: 10.1021/jp5016005.
- [107] B. Sadeghi, M.A.S. Sadjadi, R.A.R. Vahdati, „Nanoplates controlled synthesis and catalytic activities of silver nanocrystals", *Superlattices and Microstructures*, **46** (2009) 858-863, doi:10.1016/j.spmi.2009.10.006.
- [108] R. Pal Chahal, S. Mahendia, A.K. Tomar, S. Kumar, „SHI irradiated PVA/Ag nanocomposites and possibility of UV blocking", *Optical materials*, **52** (2016) 237-241, doi: 10.1016/j.optmat.2015.12.049.
- [109] P. Li, X. Xu, L. Wu, B. Li, Y. Zhao, „Synthesis of silver nanoparticle-loaded sulfadiazine/poly(vinyl alcohol) nanorods and their antibacterial activities", *Med. Chem. Commun.*, **6** (2015) 2204-2208, doi: 10.1039/c5md00331h.
- [110] E. Fortunati, F. Luzi, D. Puglia, A. Terenzia M. Vercellino, L. Visai, C. Santulli, L. Torre, J.M. Kenny, „Ternary PVA nanocomposites containing cellulose nanocrystals from different sources and silver particles: Part II", *Carbohydrate Polymers*, **97** (2013) 837-848, doi: 10.1016/j.carbpol.2013.05.015.
- [111] S. M. Alshehri, A. Aldabahi, A. Baker Al-hajji, A. Ahmad Chaudhary, M. in het Panhuis, N. Alhokbany, T. Ahamad, „Development of carboxymethyl cellulose-based hydrogel and nanosilver composite as antimicrobial agents for UTI pathogens", *Carbohydrate Polymers*, **138** (2016) 229-236, doi: 10.1016/j.carbpol.2015.11.004.

- [112] G. Reza Mahdavinia, H. Etemadi, „*In situ* synthesis of magnetic CarapVA IPN nanocomposite hydrogels and controlled drug release", *Materials Science and Engineering C*, **45** (2014) 250-260, doi: 10.1016/j.msec.2014.09.023.
- [113] S. Sarma, B. Moses Mothudi, M. Simon Dhlamini, „Observed coexistence of memristive, memcapacitive and meminductive characteristics in poly(vinyl alcohol)/cadmium sulphide nanocomposites", *J Mater Sci: Mater Electron*, (2016) 1-8, doi 10. 1007/s10854-016-4330-y.
- [114] J. Kakati, P. Datta, „Schottky junction UV photodetector based on CdS and visible photodetector based on CdS:Cu quantum dots", *Optic*, **126** (2015) 1656-1661, doi: 10.1016/j.ijleo.2015.05.054.
- [115] E. Hariprasad, T. P. Radhakrishnan, „*In situ* fabricated polymer–silver nanocomposite thin film as an inexpensive and efficient substrate for surface-enhanced Raman scattering", *Langmuir*, **29** (2013) 13050-13057, doi: 10.1021/la402594j.
- [116] B. Yin, H. Ma, S. Wang, S. Chen, „Electrochemical Synthesis of Silver Nanoparticles under Protection of Poly( N -vinylpyrrolidone)", *J Phys Chem B*, **107** (2003) 8898–8904, doi: 10.1021/jp0349031
- [117] N. Dobre, A. Petică, M. Buda, L. Anicăi, T. Vişan, „Electrochemical synthesis of silver nanoparticles in aqueous electrolytes", **76 (4)** (2014) 127-136, ISSN 1454 – 2331.
- [118] B. Obradović, J. Stojkowska, Ž. Jovanović, V. Mišković-Stanković, „Novel alginate based nanocomposite hydrogels with incorporated silver nanoparticles", *J Mater Sci: Mater Med*, **23** (2012) 99-107, doi: 10.1007/s10856-011-4522-1.
- [119] H. Jiang, Y. Zuo, L. Zhang, J. Li, A. Zhang, Y. Li, X. Yang, „Property-based design: optimization and characterization of poly(vinyl alcohol) (PVA) hydrogel and PVA-matrix composite for artificial cornea", *J Mater Sci: Mater Med*, **25** (2014) 941-952, doi: 10.1007/s10856-013-5121-0.
- [120] C. Li, M. She, X. She, J. Dai, L. Kong, „Functionalization of poly(vinyl alcohol)hydrogels with graphene oxide for potential dye removal", *Journal of Applied Polymer Sci*, **131** (2014) 1-8, doi: 10.1002/app.39872.
- [121] A.I. Ayesh, S. Qadri, V.J. Baboo, M.Y. Haik, Y. Haik, „Nano-floating gate organic memory devices utilizing Ag–Cunanoparticles embedded in PVA-PAA-

- glycerol polymer", *Synthetic Materials*, **183** (2013) 24-28, doi: 10.1016/j.synthmet.2013.09.018.
- [122] <https://www.fda.gov/aboutfda/centersoffices/oc/officeofscientificandmedicalprograms/nctr/whatwedo/researchdivisions/ucm079048.htm>
- [123] <https://www.fda.gov/scienceresearch/specialtopics/regulatoryscience/ucm452938.htm>
- [124] <http://investorintel.com/wp-content/uploads/2016/02/The-structure-of-graphene.png>
- [125] M. J. D. Nugent, A. Hanley, P. T. Tomkins, C. L. Higginbotham, „Investigation of a novel freeze-thaw process for the production of drug delivery hydrogels", *Journal of Materials Science: Materials in Medicine*, **16** (2005) 1149-1158.
- [126] H. Hong , H. Liao, S. Chen, H. Zhang, „Facile method to prepare self-healable PVA hydrogels with high water stability", *Materials Letters*, **122** (2014) 227-229, doi: 10.1016/j.matlet.2014.02.036.
- [127] K.H. Mahmoud, „Synthesis, characterization, optical and antimicrobial studies of poly(vinyl alcohol)/silver nanocomposites", *Spectrochimica Acta Part A: Molecular and Biomolecular Spectroscopy*, **138** (2015) 434-440, doi: 10.1016/j.saa.2014.11.074.
- [128] Yuan-Q. Li, T. Yu, Tian-Y. Yang, Lian-X. Zheng, K. Liao, „Bio-inspired nacre-like composite films based on graphene with superior mechanical, electrical, and biocompatible properties", *Advanced Materials*, **24** (2012) 3426-3431, doi: 10.1002/adma.201200452.
- [129] Yuan-H. Yu, Chih-C. Chan, Yu-C. Lai, Yan-Y. Lin, Ying-C. Huang, Wen-F. Chi, Che-W. Kuo, Hsui-M. Lin, Pao-C. Chen, „Biocompatible electrospinning poly(vinyl alcohol) nanofibres embedded with graphene-based derivatives with enhanced conductivity, mechanical strength and thermal stability", *RSC Adv.*, **4** (2014) 56373-56384, doi: 10.1039/c4ra10620b.
- [130] F. Pan, H. Jia , Q. Cheng, Z. Jiang, „Bio-inspired fabrication of composite membranes with ultrathin polymer–silica nanohybrid skin layer", *Journal of Membrane Science*, **362** (2010) 119-126, doi:10.1016/j.memsci.2010.06.027.
- [131] S. M Ibrahim, A. A El-Naggar, „Preparation of poly(vinyl alcohol)/ clay hydrogel through freezing and thawing followed by electron beam irradiation for

- the treatment of wastewater", *Journal of Thermoplastic Composite Materials*, **26** (10) (2012) 1332-1348, doi: 10.1177/0892705712439567.
- [132] M. Ahearne, Y. Yang, K-K. Lui. „Mechanical characterization of hydrogels for tissue engineering applications", *Topics in Tissue Engineering*, **4** (2008) 1-16, [http://www.oulu.fi/spareparts/ebook\\_topics\\_in\\_t\\_e\\_vol4/abstracts/ahearne.pdf](http://www.oulu.fi/spareparts/ebook_topics_in_t_e_vol4/abstracts/ahearne.pdf).
- [133] Y. Shi, D. Xiong , J. Zhang, „Effect of irradiation dose on mechanical and biotribological properties of PVA/PVP hydrogels as articular cartilage", *Tribology International*, **78** (2014) 60-67 , doi: 10.1016/j.triboint.2014.05.001.
- [134] Z. H. Mbhele, M. G. Salemane, C. G. C. E. van Sittert, J. M. Nedeljkovic', V. Djokovic', and A. S. Luyt, „Fabrication and characterization of silver-poly(vinyl alcohol)nanocomposites", *Chem.Mater*, volume **15** (2003) 5019-5024, doi: 10.1021/cm034505a.
- [135] P. A. McCarron, D. J. Murphy, C. Little, J. McDonald, O. J. Kelly, M. G. Jenkins, „Preliminary clinical assessment of poly(vinyl alcohol)–tetrahydroxyborate hydrogels as potential topical formulations for local anesthesia of lacerations", *Academic Emergency Medicine* , **18** (2011) 333-339, doi: 10.1111/j.1553-2712.2011.01032.x.
- [136] Y. Zu, Y. Zhang, X. Zhao, C. Shan, S. Zu, K. Wang, Y. Li, Y. Ge, „Preparation and characterization of chitosan–poly(vinyl alcohol) blend hydrogels for the controlled release of nano-insulin", *International Journal of Biological Macromolecules*, **50** (2012) 82-87, doi:10.1016/j.ijbiomac.2011.10.006.
- [137] J. L. Holloway , K. L. Spiller , A. M. Lowman , G. R. Palmese, „Analysis of the *in vitro* swelling behavior of poly(vinyl alcohol) hydrogels in osmotic pressure solution for soft tissue replacement", *Acta Biomaterialia*, **7** (2011) 2477-2482, doi:10.1016/j.actbio.2011.02.016.
- [138] E. Ant Bursali, S. Coskun, Murat Kizil , M. Yurdakoc, „Synthesis, characterization and *in vitro* antimicrobial activities of boron/starch/ poly(vinyl alcohol) hydrogels", *Carbohydrate Polymers*, **83** (2011) 1377-1383, doi:10.1016/j.carbpol.2010.09.056.
- [139] A. M. AL-Sabagh, Z. Abdeen, „Preparation and characterization of hydrogel based on poly(vinyl alcohol) cross-linked by different cross-linkers used to dry

- organic solvents", *J Polym Environ* , **18** (2010) 576-583, doi: 10.1007/s10924-010-0200-5.
- [140] E. S. Costa-Júnior , E.F. Barbosa-Stancioli , A. A.P. Mansur , W. L. Vasconcelos , H. S. Mansur, „Preparation and characterization of chitosan/poly(vinyl alcohol) chemically crosslinked blends for biomedical applications", *Carbohydrate Polymers*, **76** (2009) 472-481, doi:10.1016/j.carbpol.2008.11.015.
- [141] Y. Zheng, Y. Wang, X. Chen, L. Qing, H. Yang, „Preparation and characterization of poly(vinyl alcohol)/hydroxylapatite hybrid hydrogels", *Journal of Composite Materials*, **41** (17) (2007) 2071-2082, doi: 10.1177/0021998307074126.
- [142] H. Xu, Y. Wang, Y. Zheng, X. Chen, L. Ren, G. Wu, X. Huang, „Preparation and characterization of bioglass/poly(vinyl alcohol) composite hydrogel", *Biomedical Materials* , **2** (2007) 62-66, doi:10.1088/1748-6041/2/2/002.
- [143] V. A. Bershtein, V. M. Gun'ko, L. M. Egorova, Z. Wang, M. Illsley, E. F. Voronin, G. P. Prikhod'ko, P. N. Yakushev, R. Leboda, J. Skubiszewska-Zięba, S. V. Mikhalovsky, „Dynamics, thermal behaviour and elastic properties of thin films of poly(vinyl alcohol) nanocomposites", *RSC Advances*, **2** (2012) 1424-1431, doi: 10.1039/c1ra00535a.
- [144] C. YU, B. LI, „Morphology and properties of conducting poly(vinyl alcohol)hydrosulfate/graphite nanosheet composites", *Journal of Composite Materials*, **42** (15) ( 2008) 1491-1504, doi: 10.1177/0021998308092200.
- [145] L. Zhang, Z. Wang, C. Xu, Y. Li, J. Gao, W. Wang, Y. Liu, „High strength graphene oxide/poly(vinyl alcohol) composite hydrogels", *Journal of Materials Chemistry*, **21** (2011) 10399-10406, doi: 10.1039/c0jm04043f.
- [146] K. Liu , Y. Li , F. Xu , Y. Zuo , L. Zhang , H. Wang , J. Liao, „Graphite/poly (vinyl alcohol) hydrogel composite as porous ringy skirt for artificial cornea", *Materials Science and Engineering C*, **29** (2009) 261-266, doi:10.1016/j.msec.2008.06.023.
- [147] Chieh-F. Lo , Jung-F. Wu , Hsieh-Y. Li , Wei-S. Hung , Chao-M. Shih , Chien-C. Hu , Ying-L. Liu , S. Jessie Lue, „Novel poly(vinyl alcohol) nanocomposites containing carbon nano-tubes with Fe<sub>3</sub>O<sub>4</sub> pendants for alkaline fuel cell

- applications", *Journal of Membrane Science*, **444** (2013) 41-49, doi: 10.1016/j.memsci.2013.05.001.
- [148] Y. Pan, D. Xiong, „Stress-relaxation models of nano-HA/PVA gel biocomposites", *Mech Time-Depend Mater*, **17** (2013) 195-204, doi: 10.1007/s11043-012-9186-9.
- [149] E. Fortunati, D. Puglia, F. Luzi, C. Santulli, J.M. Kenny, L. Torre, „Binary PVA bio-nanocomposites containing cellulose nanocrystals extracted from different natural sources: Part I", *Carbohydrate Polymers*, **97** (2013) 825-836, <http://dx.doi.org/10.1016/j.carbpol.2013.03.075>.
- [150] Q. Wen Yeang, S. Hussein Sharif Zein, A. Sulong, S. Huat Tan, „Comparison of the pervaporation performance of various types of carbon nanotube-based nanocomposites in the dehydration of acetone", *Separation and Purification Technology*, **107** (2013) 252-263, doi:10.1016/j.seppur.2013.01.031.
- [151] Xian-L. Hu, Gao-M. Hou, Ming-Q. Zhang, Min-Z. Rong, Wen-H. Ruan, E. P. Giannelis, „A new nanocomposite polymer electrolyte based on poly(vinyl alcohol) incorporating hypergrafted nano-silica", *J. Mater. Chem.*, **22** (2012) 18961-18967, doi: 10.1039/c2jm33156j.
- [152] K. Qiu, A. N. Netravali, „Fabrication and characterization of biodegradable composites based on microfibrillated cellulose and poly(vinyl alcohol)", *Composites Science and Technology*, **72** (2012) 1588-1594, doi:10.1016/j.compscitech.2012.06.010.
- [153] S. Morimune, M. Kotera, T. Nishino, K. Goto, K. Hata, „Poly(vinyl alcohol) nanocomposites with nanodiamond", *Macromolecules*, **44** (2011) 4415-4421, doi: 10.1021/ma200176r.
- [154] Y. Pan, D. Xiong, „Friction properties of nano-hydroxyapatite reinforced poly(vinyl alcohol) gel composites as an articular cartilage", *Wear*, **266** (2009) 699-703, doi:10.1016/j.wear.2008.08.012.
- [155] P. Yusong, X. Dangsheng, C. Xiaolin, „Mechanical properties of nanohydroxyapatite reinforced poly(vinyl alcohol) gel composites as biomaterial", *J Mater Sci*, **42** (2007) 5129-5134, doi:10.1007/s10853-006-1264-4.

- [156] H. Kuo Feng Cheng, N. Gopal Sahoo, Y. Pei Tan, Y. Pan, H. Bao, Lin Li, S. Hwa Chan, J. Zhao, „Poly(vinyl alcohol) nanocomposites filled with poly(vinyl alcohol)-grafted graphene oxide", *Appl. Mater. Interfaces*, **4** (2012) 2387-2394, doi: 10.1021/am300550n.
- [157] X. Qi, X. Yao, S. Deng, T. Zhou, Q. Fu, „Water-induced shape memory effect of graphene oxide reinforced poly(vinyl alcohol) nanocomposites", *J. Mater. Chem.A*, **2** (2014) 2240-2249, doi: 10.1039/c3ta14340f.
- [158] A. Javadi, Q. Zheng, F. Payen, A. Javadi, Y. Altin, Z. Cai, R. Sabo, S. Gong, „Poly(vinyl alcohol)-cellulose nanofibrils-graphene oxide hybrid organic aerogels", *Appl. Mater. Interfaces*, **5** (2013) 5969-5975, doi: 10.1021/am400171y.
- [159] S. Morimune, M. Kotera, T. Nishino, T. Goto, „Uniaxial drawing of poly(vinyl alcohol)/graphene oxide nanocomposites", *Carbon*, **70** (2014) 38-45, doi: 10.1016/j.carbon.2013.12.055.
- [160] Jen-M. Yang, Shen-A. Wang, „Preparation of graphene-based poly(vinyl alcohol)/chitosan nanocomposites membrane for alkaline solid electrolytes membrane", *Journal of Membrane Science*, **477** (2015) 49-57, doi: 10.1016/j.memsci.2014.12.028.
- [161] S. Mo, L. Peng, C. Yuan, C. Zhao, W. Tang, C. Ma, J. Shen, W. Yang, Y. Yu, Y. Min, A. J. Epstein, „Enhanced properties of poly(vinyl alcohol) composite films with functionalized graphene", *RSC Adv.*, **5** (2015) 97738-97745, doi: 10.1039/c5ra15984a.
- [162] S. Ghobadi, S. Sadighikia, M. Papila, F. Çakmak Cebeci, S. Alkan Gürsel, „Graphene-reinforced poly(vinyl alcohol) electrospun fibers as building blocks for high performance nanocomposites", *RSC Adv.*, **5** (2015) 85009-85018, doi: 10.1039/c5ra15689k.
- [163] N. Eghbalifam, M. Frounchi, S. Dadbin, „Antibacterial silver nanoparticles in polyvinyl alcohol/sodium alginate blend produced by gamma irradiation", *International Journal of Biological Macromolecules*, **80** (2015) 170-176, doi: 10.1016/j.ijbiomac.2015.06.042.
- [164] Yan-L. Luo, Qing-B. Wei, F. Xu, Ya-S. Chen, Li-H. Fan, Chang-H. Zhang, „Assembly, characterization and swelling kinetics of Ag nanoparticles in

- PDMAA-g-PVA hydrogel networks", *Materials chemistry and Physics*, **118** (2009) 329-336, doi:10.1016/j.matchemphys.2009.07.063.
- [165] Y. Ma, T. Bai, F. Wang, „The physical and chemical properties of the poly(vinyl alcohol)/ Poly(vinyl pyrrolidone)/hydroxyapatite composite hydrogel", *Materials Science and Engineering C*, **59** (2016) 948-957, doi: 10.1016/j.msec.2015.10.081.
- [166] G. Li, H. Zhang, D. Fortin, H. Xia, Y. Zhao, „Poly(vinyl alcohol)–poly(ethylene glycol) double-network hydrogel: a general approach to shape memory and Self-Healing functionalities", *Langmuir*, **31** (2015) 11709-11716, doi: 10.1021/acs.langmuir.5b03474.
- [167] C. Wang, Y. Zheng, K. Qiao, Y. Xie, X. Zhou, „An environmentally friendly preparation and characterization of waterborne polyurethane hydrogels by poly(vinyl alcohol) physical crosslinking to improve water absorption", *RSC Adv.*, **5** (2015) 73882-73891, doi: 10.1039/c5ra11109a.
- [168] T. Iwatsubo, R. Kishi, T. Miura, T. Ohzono, T. Yamaguchi, „Formation of hydroxyapatite skeletal materials from hydrogel matrices via artificial biomineralization", *J. Phys. Chem. B*, **119** (2015) 8793-8799, doi: 10.1021/acs.jpcc.5b03181.
- [169] G. Li, Q. Yan, H. Xia, Y. Zhao, „Therapeutic-ultrasound-triggered shape memory of a melamine-enhanced poly(vinyl alcohol) physical hydrogel", *ACS Appl. Mater. Interfaces*, **7** (2015) 12067-12073, doi: 10.1021/acsami.5b02234.
- [170] X. Qi, X. Hu, W. Wei, H. Yu, J. Li, J. Zhang, W. Dong, „Investigation of Salecan/poly(vinyl alcohol) hydrogels prepared by freeze/thaw method", *Carbohydrate Polymers*, **118** (2015) 60-69, doi: 10.1016/j.carpol.2014.11.021.
- [171] Z. Li, Y. Su, B. Xie, X. Liu, X. Gao, D. Wang, „A novel biocompatible double network hydrogel consisting of konjac glucomannan with high mechanical strength and ability to be freely shaped", *J. Mater. Chem. B*, **3** (2015) 1769-1778, doi: 10.1039/c4tb01653j.
- [172] T. Ho Kim, D. Bi An, S. Heang Oh, M. Kwan Kang, H. Hoon Song, J. Ho Lee, „Creating stiffness gradient poly(vinyl alcohol) hydrogel using a simple gradual freezing/thawing method to investigate stem cell differentiation behaviors", *Biomaterials*, **40** (2015) 51-60, doi: 10.1016/j.biomaterials.2014.11.017.

- [173] J. S. Gonzalez, L. N. Ludueña, A. Ponce, V. A. Alvarez, „Poly(vinyl alcohol)/cellulose nanowhiskers nanocomposite hydrogels for potential wound dressings", *Materials Science and Engineering C*, **34** (2014) 54-61, doi: 10.1016/j.msec.2013.10.006.
- [174] Z. Lian, L. Ye, „Structure and properties of PVA/ PEO hydrogel prepared by freezing/ thawing method", *Journal of Thermoplastic Composite Materials*, **26(7)**(2011) 912-922, doi: 10.1177/0892705711430857.
- [175] L. Zhang, J. Zhao, J. Zhu, C. He, H. Wang, „Anisotropic tough poly(vinyl alcohol) hydrogels", *Soft Matter*, **8** (2012) 10439-10447, doi: 10.1039/c2sm26102b.
- [176] A. Sebastián Maiolo, M. Nicolás Amado, J. Soledad Gonzalez, V. Alejandra Alvarez, „Development and characterization of Poly (vinyl alcohol) based hydrogels for potential use as an articular cartilage replacement", *Materials Science and Engineering C*, **32** (2012) 1490-1495, doi:10.1016/j.msec.2012.04.030.
- [177] S. Huang, Z. Yang, H. Zhu, L. Ren, W. Weei Tjiu, T. Liu, „Poly(vinly alcohol) nano-sized layered double hydroxides nanocomposite hydrogels prepared by cyclic freezing and thawing", *Macromolecular Research*, **20 (6)** (2012) 568-577, doi: 10.1007/s13233-012-0069-3.
- [178] S. Jiang, S. Liu, W. Feng, „PVA hydrogel properties for biomedical application", *Journal of the Mechanical Behavior of Biomedical Materials*, **4** (2011) 1228-1233, doi:10.1016/j.jmbbm.2011.04.005.
- [179] M. Ru-yin, X. Dang-sheng, „Synthesis and properties of physically crosslinked poly(vinyl alcohol) hydrogels", *J China Univ Mining & Technol*, **18** (2008) 0271-0274, [www.elsevier.com/locate/jcumt](http://www.elsevier.com/locate/jcumt).
- [180] N. Cai, C. Li, X. Luo, Y. Xue, L. Shen, F. Yu, „A strategy for improving mechanical properties of composite nanofibers through surface functionalization of fillers with hyperbranched polyglycerol", *J Mater Sci*, **51** (2016) 797-808, doi: 10.1007/s10853-015-9403-4.
- [181] V. Mišković-Stanković, I. Jevremović, A. Janković, patent application no. P-2015/ 0784, The Intellectual Property Office of the Republic of Serbia, dated 25.11.2015.

- [182] CM. Santos, J. Mangadlao, F. Ahmed, A. Leon, RC. Advincula, DF. Rodrigues, „Graphene nanocomposite for biomedical applications: fabrication, antimicrobial and cytotoxic investigations", *Nanotechnology*, **23** (2012) 395101, doi: 10.1088/0957-4484/23/39/395101.
- [183] G. Sjogren, G. Sletten, JE. Dahl, „Cytotoxicity of dental alloys, metals, and ceramics assessed by millipore filter, agar overlay, and MTT tests", *J ProsthetDent*, **84** (2000) 229-236, doi: 10.1067/mpr.2000.107227.
- [184] M.M. Abudabbus, I. Jevremović, A. Janković, A. Perić Grujić, I. Matić, M. Vukašinović-Sekulić, D. Hui, K.Y. Rhee, V. Mišković-Stanković, „Biological activity of electrochemically synthesized silver doped polyvinyl alcohol/graphene composite hydrogel discs for biomedical applications", *Compos. Part B Eng.* **104** (2016) 26-34, doi: 10.1016/j.compositesb.2016.08.024.
- [185] K. Nešović, M. M. Abudabbus, Kyong Yop Rhee, Vesna Mišković-Stanković, „Graphene Based Composite Hydrogel for Biomedical Applications", *Croat. Chem. Acta*, **90** (2) (2017) 1-7, doi: 10.5562/cca3133.
- [186] J.H. Hodak, A. Henglein, G. V Hartland, „Electron-phonon coupling dynamics in very small (between 2 and 8 nm diameter) Au nanoparticles", *J. Chem. Phys.*, **112** (2000) 5942–5947, doi: 10.1063/1.481167.
- [187] Z. Ni, Y. Wang, T. Yu, Z. Shen, „Raman spectroscopy and imaging of graphene", *Nano Res*, **1** (2008) 273-291, doi: 10.1007/s12274-008-8036-1.
- [188] J. H. Jang, J. K. Kim, D. S. Huh, „Incorporation of graphene oxide to pH responsive hydrogel for rapid adsorption-desorption of nanoparticles on patterned hydrogel surface", *Macromol. Res.*, **22** (2014) 1132-1135, doi: 10.1007/s13233-014-2144-4.
- [189] D. Mayo, F. Miller, R. Hannah, „Course notes on interpretation of infrared and Raman spectra", *John Wiley and Sons Ltd*, 2003, p. 567
- [190] M. Miya, R. Iwamoto, S. Mima, „FT-IR Study of intermolecular interactions in polymer blends", *J. Polym. Sci Pol. Phys.*, **22** (1984) 1149-1151, doi: 10.1002/pol.1984.180220615.

- [191] R. Bryaskova, D. Pencheva, G. M. Kale, U. Lad, T. Kantardjiev, „Synthesis, characterisation and antibacterial activity of PVA/TEOS/Ag-Np hybrid thin films", *J. Colloid Interf. Sci*, **349** (2010) 77-85, doi: 10.1016/j.jcis.2010.04.091.
- [192] J. Krstić, J. Spasojević, A. Radosavljević, M. Šiljegović, Z. Kačarević-Popović, „Optical and structural properties of radiolytically *in situ* synthesized silver nanoparticles stabilized by chitosan/poly(vinyl alcohol) blends", *Radiat. Phys. Chem*, **96** (2014) 158-166, doi: 10.1016/j.radphyschem.2013.09.013.
- [193] T. Wang, S. Gunasekaran, „State of water in chitosan–PVA hydrogel", *J. Appl. Polym. Sci*, **101** (2006) 3227-3232, doi: 10.1002/app.23526.
- [194] S. R. Sudhamani, M. S. Prasad, K. UdayaSankar, „DSC and FTIR studies on gellan and poly(vinyl alcohol) (PVA) blend films", *Food Hydrocoll*, **17** (2003), 245-250, doi: 10.1016/S0268-005X(02)00057-7.
- [195] N. A. Peppas, E. W. Merrill, „Differential scanning calorimetry of crystallized PVA hydrogels", *J. Appl. Polym. Sci*, **20** (1976), 1457-1465, doi: 10.1002/app.1976.070200604.
- [196] H. Feng, Z. Feng, L. Shen, „A high resolution solid-state NMR and DSC study of miscibility and crystallization behaviour of poly(vinyl alcohol), poly(N-vinyl-2-pyrrolidone) blends", *Polymer*, **34** (1993), 2516-2519, doi: 10.1016/0032-3861(93)90581-T.
- [197] S. Villar-Rodil, J. I. Paredes, A. Martínez-Alonso, J. M. D. Tascón, „Preparation of graphene dispersions and graphene-polymer composites in organic media", *J. Mater. Chem.*, **19** (2009), 3591-3593, doi: 10.1039/B904935E.
- [198] T. Ramanathan, A. A. Abdala, S. Stankovich, D. A. Dikin, M. Herrera-Alonso, R. D. Piner, D. H. Adamson, H. C. Schniepp, X. Chen, R. S. Ruoff, et al., „Functionalized graphene sheets for polymer nanocomposites", *Nat. Nanotechnol.*, **3** (2008), 327-331, doi: 10.1038/nnano.2008.96
- [199] J. Liang, Y. Huang, L. Zhang, Y. Wang, Y. Ma, T. Cuo, Y. Chen, „Molecular-level dispersion of graphene into poly(vinyl alcohol) and effective reinforcement of their nanocomposites", *Adv. Funct. Mater.* **19** (2009), 2297-2302, doi: 10.1002/adfm.200801776.

- [200] J. Jose, M. A. Al-Harhi, M. A. A. AlMa'adeed, J. B. Dakua, S. K. De, „Effect of graphene loading on thermomechanical properties of poly(vinyl alcohol)/starch blend", *J. Appl. Polym. Sci.*, **132** (2015), 1, doi: 10.1002/app.41827.
- [201] R. Li, C. Liu, J. Ma, „Studies on the properties of graphene oxide-reinforced starch biocomposites", *Carbohydr. Polym.*, **84** (2011), 631-637, doi: 10.1016/j.carbpol.2010.12.041.
- [202] JP. Ruparelia, AK. Chatterjee, SP. Duttagupta, S. Mukherji, „Strain specificity in antimicrobial activity of silver and copper nanoparticles", *Acta Biomater.*, **4** (2008) 707-716, doi: 10.1016/j.actbio.2007.11.006.
- [203] S. Liu, TH. Zeng, M. Hofmann, E. Burcombe, J. Wei, R. Jiang, „Antibacterial activity of graphite, graphite oxide, graphene oxide, and reduced graphene Oxide : membrane and oxidative stress", *ACS Nano*, **5** (2011) 6971-6980, doi: 10.1021/nn202451x.
- [204] W. Hu, C. Peng, W. Luo, M. Lv, X. Li, D. Li, et al., „Graphene-based antibacterial paper", *ACS Nano*, **4** (2010) 4317-4323, doi: 10.1021/nn101097v.
- [205] Y. Chen, X. Zheng, Y. Xie, H. Ji, C. Ding, H. Li, et al., „Silver release from silvercontaining hydroxyapatite coatings", *Surf Coat Technol.*, **205** (2010) 1892-1896, doi: 10.1016/j.surfcoat.2010.08.073.

## 8. APPENDIX

Table A.1. Silver release data ( $0.25 \times 10^{-3} \text{ M AgNO}_3$ ) for Ag/PVA hydrogel

Ag/PVA											
	Measured silver concentration in the buffer (AAS) ( $\text{mg}/\text{dm}^3$ )			Silver content in 10 ml buffer solution (mg)			Silver concentration released from the hydrogel ( $\text{mg}/\text{dm}^3$ )				
Day	Sample 1	Sample 2	Sample 3	Sample 1	Sample 2	Sample 3	Sample 1	Sample 2	Sample 3	Average	Standard deviation
1	0.4	0.32	0.59	0.004	0.0032	0.0059	7.077140835	5.661713	10.43878	7.72	2.45
2	0.14	0.14	0.19	0.0014	0.0014	0.0019	2.476999292	2.476999	3.361642	2.77	0.51
3	0.1	0.06	0.09	0.001	0.0006	0.0009	1.769285209	1.061571	1.592357	1.47	0.36
4	0.06	0.08	0.06	0.0006	0.0008	0.0006	1.061571125	1.415428	1.061571	1.17	0.20
5	0.06	0.06	0.06	0.0006	0.0006	0.0006	1.061571125	1.061571	1.061571	1.06	0
6	0.06	0.08	0.07	0.0006	0.0008	0.0007	1.061571125	1.415428	1.2385	1.23	0.17
7	0.09	0.09	0.09	0.0009	0.0009	0.0009	1.592356688	1.592357	1.592357	1.59	2.71
12	0.14	0.11	0.19	0.0014	0.0011	0.0019	2.476999292	1.946214	3.361642	2.59	0.71
16	0.12	0.08	0.2	0.0012	0.0008	0.002	2.123142251	1.415428	3.53857	2.35	1.08
21	0.14	0.07	0.23	0.0014	0.0007	0.0023	2.476999292	1.2385	4.069356	2.59	1.41
28	0.22	0.11	0.25	0.0022	0.0011	0.0025	3.892427459	1.946214	4.423213	3.42	1.30
HNO <sub>3</sub>	0.51	0.91	0.84	0.0051	0.0091	0.0084	9.023354565	16.1005	14.862	13.32	3.77
sum	2.04	2.11	2.86	0.0204	0.0211	0.0286	36.09341826	37.33192	50.60156	41.34	8.04

Table A.2. Time dependences of the silver concentration inside hydrogels (data represent average of three measurements) and the cumulative silver release from Ag/PVA hydrogel ( $0.25 \times 10^{-3} \text{ M AgNO}_3$ )

Day	Conc. Ag remaining inside hydrogels ( $\text{mg}/\text{dm}^3$ )			Conc. Ag inside hydrogels ( $\text{mg}/\text{dm}^3$ )	Standard deviation	Cumulative $c_{\text{Ag}}$ released ( $\text{mg}/\text{dm}^3$ )	$c_{\text{Ag}}/c_{\text{tot}}$
	Sample 1	Sample 2	Sample 3				
0	36.0934183	37.3319179	50.601557	41.3	8.04	0	0
1	29.0162774	31.6702052	40.1627742	33.6	5.82	7.7	0.1868
2	26.5392781	29.1932059	36.8011323	30.8	5.32	10.4	0.253
3	24.7699929	28.1316348	35.2087757	29.3	5.32	11.9	0.289
4	23.7084218	26.7162067	34.1472045	28.1	5.37	13.1	0.318
5	22.6468507	25.6546355	33.0856334	27.1	5.37	14.2	0.343
6	21.5852795	24.2392074	31.8471338	25.8	5.32	15.4	0.373
7	19.9929229	22.6468507	30.2547771	24.3	5.32	17.0	0.412
12	17.5159236	20.7006369	26.8931352	21.7	4.76	19.6	0.474
16	15.3927813	19.2852088	23.3545648	19.3	3.98	21.9	0.536
21	12.915782	18.0467091	19.2852088	16.7	3.37	24.5	0.599
28	9.02335456	16.1004954	14.8619958	13.3	3.77	28.0	0.681

Table B.1. Silver release data ( $0.25 \times 10^{-3} \text{ M AgNO}_3$ ) for

*Ag/PVA/Gr hydrogel*

Ag/PVA/Gr											
	Measured silver concentration (AAS) ( $\text{mg}/\text{dm}^3$ )			Silver content in 10 ml buffer solution (mg)			Silver concentration released from the hydrogel ( $\text{mg}/\text{dm}^3$ )				
Day	Sample 1	Sample 2	Sample 3	Sample 1	Sample 2	Sample 3	Sample 1	Sample 2	Sample 3	Average	Standard deviation
1	0.19	0.33	0.25	0.0019	0.0033	0.0025	3.361642	5.838641	4.423213	4.54	1.24
2	0.11	0.17	0.1	0.0011	0.0017	0.001	1.946214	3.007785	1.769285	2.24	0.66
3	0.06	0.06	0.04	0.0006	0.0006	0.0004	1.061571	1.061571	0.707714	0.94	0.20
4	0.04	0.07	0.06	0.0004	0.0007	0.0006	0.707714	1.2385	1.061571	1.00	0.27
5	0.06	0.06	0.06	0.0006	0.0006	0.0006	1.061571	1.061571	1.061571	1.06	0
6	0.04	0.05	0.04	0.0004	0.0005	0.0004	0.707714	0.884643	0.707714	0.76	0.10
7	0.07	0.07	0.07	0.0007	0.0007	0.0007	1.2385	1.2385	1.2385	1.23	0
12	0.09	0.15	0.11	0.0009	0.0015	0.0011	1.592357	2.653928	1.946214	2.06	0.54
16	0.09	0.06	0.08	0.0009	0.0006	0.0008	1.592357	1.061571	1.415428	1.35	0.27
21	0.1	0.09	0.11	0.001	0.0009	0.0011	1.769285	1.592357	1.946214	1.76	0.17
28	0.08	0.12	0.07	0.0008	0.0012	0.0007	1.415428	2.123142	1.2385	1.59	0.46
HNO <sub>3</sub>	0.6	0.32	0.72	0.006	0.0032	0.0072	10.61571	5.661713	12.73885	9.67	3.63
sum	1.53	1.55	1.71	0.0153	0.0155	0.0171	27.07006	27.42392	30.25478	28.24	1.74

Table B.2. Time dependences of the silver concentration inside hydrogels (data represent average of three measurements) and the cumulative silver release from Ag/PVA/Gr hydrogel ( $0.25 \times 10^{-3} \text{ M AgNO}_3$ )

Day	Conc. Ag remaining inside hydrogels ( $\text{mg}/\text{dm}^3$ )			conc. Ag inside hydrogels ( $\text{mg}/\text{dm}^3$ )	Standard deviation	Cumulative $c_{\text{Ag}}$ released ( $\text{mg}/\text{dm}^3$ )	$c_{\text{Ag}}/c_{\text{tot}}$
	Sample 1	Sample 2	Sample 3				
0	27.0700637	27.4239207	30.2547771	28.2	1.74	0	0
1	23.7084218	21.5852795	25.831564	23.7	2.12	4.5	0.157
2	21.7622081	18.5774947	24.0622788	21.4	2.75	6.7	0.236
3	20.7006369	17.5159236	23.3545648	20.5	2.92	7.7	0.27
4	19.9929229	16.2774239	22.2929936	19.5	3.03	8.7	0.305
5	18.9313517	15.2158528	21.2314225	18.4	3.03	9.7	0.343
6	18.2236377	14.3312102	20.5237084	17.6	3.13	10.5	0.37
7	16.985138	13.0927105	19.2852088	16.4	3.13	11.7	0.414
12	15.3927813	10.4387827	17.338995	14.3	3.55	13.8	0.487
16	13.8004246	9.37721161	15.9235669	13.0	3.33	15.2	0.535
21	12.0311394	7.78485492	13.9773531	11.2	3.16	16.8	0.597
28	10.6157113	5.66171267	12.7388535	9.6	3.63	18.5	0.654

## 9. BIOGRAPHY

**Mohamed Mohamed Abudabbus** was born 01/01/1966 in Misurata, Libya. He graduated (BSc) in 1988 and completed his MSc degree in 1996 at the Faculty of Science in Chemistry, University of Misurata, Misurata, Libya. He was an Associate at College of Teachers, University of Misurata, Libya, from 2003 to 2006; Faculty of Sciences, University of Elmergab at Msillata, Libya, from 2005 to 2006; Faculty of Teachers, University of Elmergab at Zliten, Libya, from 2006 to 2007; and at the Faculty of Sciences, University of Misurata, Libya, for several years. He was elected Assistant Lecturer at the Faculty of Education, University of Misurata, in November 2011, and promoted to a Lecturer in July 2013 at the same university.

Mohamed Mohamed Abudabbus enrolled in doctoral studies at the Faculty of Technology and Metallurgy, University of Belgrade, Serbia, in school year 2013/2014. His choice was a Chemistry program, under the mentorship of Prof. dr. Vesna Miskovic-Stankovic. He successfully fulfilled all the program requirements and completed all the courses, including the Final exam. PhD candidate, Mohamed Mohamed Abudabbus, co-authored two papers in the international journal of exceptional value - category M21a, one paper in the international journal, category M23 and participated at two international meetings (conference proceedings published in abstract), category M34. He is fluent in English and actively learning Serbian (Certificate of successfully completed level A2-2 - Serbian language).

### List of Publications:

#### 1. Articles published in international research journals – category M20

##### 1.1. International journal of exceptional value - category M21a

1. **M.M. Abudabbus**, I. Jevremović, A. Janković, A. Perić Grujić, I. Matić, M. Vukašinović-Sekulić, D. Hui, K.Y. Rhee, V. Mišković-Stanković, Biological activity of electrochemically synthesized silver doped polyvinyl alcohol/graphene composite hydrogel discs for biomedical applications, *Compos. Part B Eng.* **104** (2016) 26-34. ISSN 1359-8368, IF 2015 = 3.85 doi: 10.1016/j.compositesb.2016.08.024. <http://www.sciencedirect.com/science/article/pii/S1359836816302943>

2. **M. M. Abudabbus**, I. Jevremović, K. Nešović, A. Perić-Grujić, K. Yop Rhee, V. Mišković-Stanković *In situ* electrochemical synthesis of silver-doped poly(vinyl alcohol)/graphene composite hydrogels and their physico-chemical and thermal properties, *Compos. Part B : Engineering* (2017), (Engineering, Multidisciplinary 3/85, IF(2016) = 4.727) in press, <https://doi.org/10.1016/j.compositesb.2017.12.017>

## 1.2. International journal – category M23

1. Katarina Nešović, **Mohamed M. Abudabbus**, Kyong Yop Rhee, Vesna Mišković-Stanković, Graphene Based Composite Hydrogel for Biomedical Applications, *Croat. Chem. Acta*, **90** (2) (2017) 207-213, doi: 10.5562/cca3133. (Chemistry, Multidisciplinary, 144/166, IF (2016) =0,586) ISSN 0011-1643. [https://hrcak.srce.hr/index.php?show=clanak&id\\_clanak\\_jezik=272785](https://hrcak.srce.hr/index.php?show=clanak&id_clanak_jezik=272785)

## 2. International conferences – category M30

### 2.1. Conference proceedings published in abstract – category M34

1. Abdulali Ben Saleh, **Mohamed Mohamed Abudabbus**, "Removal of Methylene Blue Dye Using Roselle Petals from Aqueous Solutions", WASET 2013, June 20-21, 2013, Istanbul, Turkey, *World Academy of Science, Engineering and Technology*, **78** (2013) 388-391.

2. Katarina Nešović, **Mohamed Mohamed Abudabbus**, Ivana Jevremovic, Ivana Matić, Aleksandra Perić-Grujić, Vesna Mišković-Stanković, „Electrochemical synthesis of silver/polyvinyl alcohol hydrogel nanocomposites“, Fourteenth Young Researchers' Conference - Materials Science and Engineering, Serbian Academy of Sciences and Arts, Belgrade, Serbia, December 9-11, 2015, Programme and the Book of Abstracts, 2-1, p. 7.

**Прилог 1.**

**Изјава о ауторству**

Потписани                      Mohamed Mohamed Abudabbus

број индекса                    ДС - 2013/4049

**Изјављујем**

да је докторска дисертација под насловом

**Elektrohemijska sinteza i karakterizacija nanokompozita polivinil-alkohola I  
nanočestica srebra  
(Electrochemical synthesis and characterization of poly(vinyl alcohol)  
nanocomposites with silver nanoparticles)**

- резултат сопственог истраживачког рада,
- да предложена дисертација у целини ни у деловима није била предложена за добијање било које дипломе према студијским програмима других високошколских установа,
- да су резултати коректно наведени и
- да нисам кршила ауторска права и користила интелектуалну својину других лица.

**Потпис докторанда**

У Београду, 22. Новембра 2017. године



**Прилог 2.**

**Изјава о истоветности штампане и електронске верзије докторског рада**

Име и презиме аутора Mohamed Mohamed Abudabbus

Број индекса ДС - 2013/4049

Студијски програм Хемија

Наслов рада

**Elektrohemijska sinteza i karakterizacija nanokompozita polivinil-alkohola i nanočestica srebra**

**(Electrochemical synthesis and characterization of poly(vinyl alcohol) nanocomposites with silver nanoparticles)**

Ментор др Весна Мишковић-Станковић, редовни професор ТМФ

Потписани Mohamed Mohamed Abudabbus

Изјављујем да је штампана верзија мог докторског рада истоветна електронској верзији коју сам предала за објављивање на порталу **Дигиталног репозиторијума Универзитета у Београду**.

Дозвољавам да се објаве моји лични подаци везани за добијање академског звања доктора наука, као што су име и презиме, година и место рођења и датум одбране рада.

Ови лични подаци могу се објавити на мрежним страницама дигиталне библиотеке, у електронском каталогу и у публикацијама Универзитета у Београду.

**Потпис докторанда**

У Београду, 22. Новембра 2017. године



### Прилог 3.

#### Изјава о коришћењу

Овлашћујем Универзитетску библиотеку „Светозар Марковић“ да у Дигитални репозиторијум Универзитета у Београду унесе моју докторску дисертацију под насловом:

**Elektrohemijska sinteza i karakterizacija nanokompozita polivinil-alkohola i nanočestica srebra**  
**(Electrochemical synthesis and characterization of poly(vinyl alcohol) nanocomposites with silver nanoparticles)**

која је моје ауторско дело.

Дисертацију са свим прилозима предала сам у електронском формату погодном за трајно архивирање.

Моју докторску дисертацију похрањену у Дигитални репозиторијум Универзитета у Београду могу да користе сви који поштују одредбе садржане у одабраном типу лиценце Креативне заједнице (Creative Commons) за коју сам се одлучила.

1. Ауторство
2. Ауторство - некомерцијално
- 3. Ауторство – некомерцијално – без прераде**
4. Ауторство – некомерцијално – делити под истим условима
5. Ауторство – без прераде
6. Ауторство – делити под истим условима

Потпис докторанда

У Београду, 22. Новембра 2017. године



1. Ауторство - Дозвољавате умножавање, дистрибуцију и јавно саопштавање дела, и прераде, ако се наведе име аутора на начин одређен од стране аутора или даваоца лиценце, чак и у комерцијалне сврхе. Ово је најслободнија од свих лиценци.
2. Ауторство – некомерцијално. Дозвољавате умножавање, дистрибуцију и јавно саопштавање дела, и прераде, ако се наведе име аутора на начин одређен од стране аутора или даваоца лиценце. Ова лиценца не дозвољава комерцијалну употребу дела.
3. Ауторство - некомерцијално – без прераде. Дозвољавате умножавање, дистрибуцију и јавно саопштавање дела, без промена, преобликовања или употребе дела у свом делу, ако се наведе име аутора на начин одређен од стране аутора или даваоца лиценце. Ова лиценца не дозвољава комерцијалну употребу дела. У односу на све остале лиценце, овом лиценцом се ограничава највећи обим права коришћења дела.
4. Ауторство - некомерцијално – делити под истим условима. Дозвољавате умножавање, дистрибуцију и јавно саопштавање дела, и прераде, ако се наведе име аутора на начин одређен од стране аутора или даваоца лиценце и ако се прерада дистрибуира под истом или сличном лиценцом. Ова лиценца не дозвољава комерцијалну употребу дела и прерада.
5. Ауторство – без прераде. Дозвољавате умножавање, дистрибуцију и јавно саопштавање дела, без промена, преобликовања или употребе дела у свом делу, ако се наведе име аутора на начин одређен од стране аутора или даваоца лиценце. Ова лиценца дозвољава комерцијалну употребу дела.
6. Ауторство - делити под истим условима. Дозвољавате умножавање, дистрибуцију и јавно саопштавање дела, и прераде, ако се наведе име аутора на начин одређен од стране аутора или даваоца лиценце и ако се прерада дистрибуира под истом или сличном лиценцом. Ова лиценца дозвољава комерцијалну употребу дела и прерада. Слична је софтверским лиценцама, односно лиценцама отвореног кода.